REPUBLIC OF TURKEY

ACIBADEM MEHMET ALI AYDINLAR UNIVERSITY

INSTITUTE OF HEALTH SCIENCES

HOMOGENEOUS TIME RESOLVED FLUORESCENCE ASSAY WITH *CANDIDA AURIS* BDF1 FOR INHIBITOR SCREENING

YORDAN HAYAT

MASTER THESIS

DEPARTMENT OF MEDICAL BIOTECHNOLOGY

SUPERVISOR

Asst. Prof. Dr. Zeynep KANLIDERE

COSUPERVISOR

Dr. Dimitrios SKOUFIAS

ISTANBUL - 2021

REPUBLIC OF TURKEY

ACIBADEM MEHMET ALI AYDINLAR UNIVERSITY

INSTITUTE OF HEALTH SCIENCES

HOMOGENEOUS TIME RESOLVED FLUORESCENCE ASSAY WITH *CANDIDA AURIS* BDF1 FOR INHIBITOR SCREENING

YORDAN HAYAT

MASTER THESIS

DEPARTMENT OF MEDICAL BIOTECHNOLOGY

SUPERVISOR

Asst. Prof. Dr. Zeynep KANLIDERE

COSUPERVISOR

Dr. Dimitrios SKOUFIAS

ISTANBUL - 2021

DECLARATION

I declare that this thesis is my own work and that there have not been any unethical behaviour at all stages from planning to writing. All informations were obtained within academic and ethical rules, and those which were not obtained through this thesis were cited and included in the references. Additionally I declare that I did not violate patents and copyrights during the study and writing of this thesis.

20 / 05 / 2021

Yordan Hayat

ACKNOWLEDGMENT

I would like to express my sincere gratitudes towards my spiritual Father Senior Metropolitan Constantine of Nicea who followed my studies closely throughout my life and has always been a constant support in each step of it. I had the blessing to discuss the progress of my experiments till the last moment.

I could never thank you enough.

May your Memory be Eternal.

TABLE OF CONTENTS

LIST OF ABBREVIATIONS AND SYMBOLS

BD: Bromodomain

Bdf1: Bromodomain factor 1

BET: Bromodomain and ExtraTerminal

CEA: French Atomic Energy Commission

DMF: *N*,*N*-Dimethylformamide

DMSO: Dimethyl Sulfoxide

ESI-MS: Electrospray Ionization Mass Spectrometry

FMOC: Fluorenylmethyloxycarbonyl

FRET: Förster Resonance Energy Transfer

HPLC: High Performance Liquid Chromatography

HTRF: Homogeneous Time Resolved Fluorescence

IBS: Structural Biology Institute

MALDI-TOF MS: Matrix-Assisted Laser Desorption Ionization-Time Of Flight Mass Spectrometry

MEG: Monoethylene Glycol

PCR: Polymerase Chain Reaction

PTM: Post Translational Modifications

VIC: Viral Infection and Cancer

LIST OF FIGURES

LIST OF TABLES

SUMMARY

Candida auris, a newly emerging *Candida* species, has put the healthcare professionals on alert because of the endonosocomial outbreaks it causes and its high mortality rate with immune compromised patients. To date, *Candida auris* is resistant to all known classes of available antifungal drugs. This work is based on a novel epigenetic strategy targeting *Candida auris* Bdf1 bromodomain containing protein, a DNA modulator protein and has its main goal to develop the necessary tools for high throughput screening of compounds against it. In that goal *C. auris* putative Bdf1 bromodomains were specifically expressed, purified and optimized for homogeneous time resolved fluorescence assays. Additionally modified histone tail peptides bearing acetyl and butyryl to be used in the assay were synthesized. The results have shown that the reagents prepared can be used for high throughput screening of inhibitors against *C. auris* bromodomains. As a preliminary study *C. glabrata* Bdf1 inhibitor compound 409 was tested. Only one bromodomain of *C. auris* Bdf1 seemed sensitive to compound 409. Furthermore bromodomain affinity to post-translational modifications other than acetyl will be monitored for fungal species for the first time that will help select more specific antifungal compounds to be assessed for later *in vitro* and *in vivo* assays.

Keywords: Antifungal, Bromodomain, *Candida auris*, Histone, HTRF

ÖZET

Inhibitör Taraması Için *Candida auris* Bdf1 Ile Homojen Zaman Çözümlü Floresans Deneyi

Yeni ortaya çıkan bir *Candida* türü olan *Candida auris*, sebep olduğu hastane içi salgınlar ve bağışıklık sistemi zayıflamış hastalarda yüksek ölüm oranı nedeniyle sağlık uzmanlarını alarma geçirdi. *Candida auris*, günümüzde bilinen tüm antifungal ilaç sınıflarına dirençlidir. Bu çalışma, bir DNA modülatörü olan bromodomain içeren protein Bdf1'i hedefleyen yeni bir epigenetik stratejiye dayanmaktadır. Çalışmanın temel amacı bu proteine karşı bileşiklerin bulunması için yüksek verimli taramaya gerekli araçları geliştirmektir. Bu hedef doğrultusunda, *C. auris* varsayılan Bdf1 bromodomainleri spesifik olarak ifade edildi, saflaştırıldı ve homojen zamanla çözümlenmiş floresan deneyleri için optimize edildi. Ek olarak testte kullanılacak asetil ve butiril içeren modifiye histon kuyruk peptidleri sentezlendi. Elde edilen sonuçlar, *C. auris* bromodomainlerine karşı inhibitörlerin bulunması için hazırlanan reaktiflerin yüksek verimli tarama ile kullanılabileceğini göstermiştir. Bir ön çalışma olarak, *C. glabrata* Bdf1 inhibitörü olan 409 isimli bileşiğin etkisi test edildi. *C. auris* Bdf1'in yalnızca bir bromodomainin 409 bileşiğine duyarlı olduğu görüldü. Bu çalışma ile ayrıca, asetil dışındaki translasyon sonrası modifikasyonlara bromodomain afinitesi, ilk kez mantar türleri üzerinde değerlendirilecek ve ilerideki *in vitro* ve *in vivo* deneylerde mantarlara karşı daha spesifik bileşiklerin seçilmesine yardımcı olacaktır.

Anahtar Sözcükler: Antifungal, Bromodomain, *Candida auris*, Histone, HTRF

1. BACKGROUND AND AIM OF THE STUDY

Candidiasis is a global health concern causing severe diseases from meningitis to vulvovaginitis and balanitis (1). In case of an invasive candidiasis where the infection reaches the bloodstream the mortality can go up to 38% (2) and is especially critical for patients with predisposing conditions (3, 4). The illness appears upon infection from eukaryotic organisms of the Fungi kingdom, more specifically yeasts that belong to the class of Saccharomycetes and form the *Candida* genus (5). To date, the most commonly studied species has been *Candida albicans*, an emergence in non *albicans* species is a global trend (6). Among them, a new species, *Candida auris*, named after the latin word for ear, has been reported in 2009 from a patient in Japan suffering with ear infection (7). *Candida auris* has been responsible for multiple outbreaks in hospitals as it spreads easily and can survive on non-living materials (8). Furthermore it is ranked now as one of the major nosocomial infections (9). More dramatically *Candida auris* is an exception among its genus with resistance to all classes of antifungal drugs present on the pharmaceutical market (10, 11) making the infection a hard challenge for the healthcare professionals to cure (12). In this context the identification of novel antifungal compounds targeting novel targets is of great medical interest. Recently, the Petosa group proposed a novel antifungal strategy based on the identification of specific inhibitors targeting the epigenetic reader called Bromodomain factor 1 (Bdf1) (13). Within this context a novel compound was identified, compound 409, targeting the bromodomains of *C. glabrata*. Additionally some molecules can inhibit specifically fungal Bdf1 versus its human analogue (14). The goal of the present work was to develop biochemical assays and the necessary reagents to be used for the high throughput screening targeting the two bromodomains of the human pathogen *Candida auris*. The identified small molecules will then be used to verify the hypothesis that Bdf1 can be an efficient antifungal target against *Candida auris* as well. The objectives of the present work was to bacterially express and then purify *Candida auris* Bdf1 bromodomain 1 (BD1) and bromodomain 2 (BD2) domains separately to be used in *in vitro* biochemical assays enabling the quantitative measurements of the

bromodomain ability to bind post-translationally modified histones. The *in vitro* biochemical assay of choice for the bromodomain-histone interaction is based on the generation of fluorescence signal when two chromophores are brought in vicinity named homogenous time resolved fluorescence (HTRF) assay. However, the HTRF assay requires specific optimization for the two *C. auris* bromodomains. A prerequisite for the HTRF assay is the use of modified histone peptides carrying post-translational modifications (PTM) on lysines. Therefore, a second aspect of the work was the synthesis of histone peptide carrying PTMs that is read by the bromodomains of *C. auris*. This novel strategy has the advantage to be target specific. In other words it prevents the unwanted side effects of actual antifungal drugs like amphotericin B which is highly toxic to human cells (15). Above all, this work aims to bring hope in the treatment of *Candida auris* infection that has no particular solution up to date.

2. INTRODUCTION

2.1. Emerging Drug Resistant Pathogen

2.1.1. Human pathogen fungi

Fungi represent a distinct kingdom in Eukarya domain. New molecular sequencing techniques allowed the identification of new species and recently the number of estimated species increased rapidly. In 2017 total fungal species were estimated to be between 1.5 to 3.8 million (16) whereas in 2019 this estimation was updated to 12 million (17). Even though the majority of them is beneficial to the ecosystem (18) and has helped human civilization develop (19), this cannot be said for the whole kingdom as some of them are pathogenic to humans (20). Until now approximately 300 fungal species have been identified as dangerous towards human health (21).

In order for any fungal species to infect healthy Humans it must be first of all resistant to body heat, precisely to 37°C and above. Then, it must be capable of crossing tissue barriers. When it does so, it must as well be able to absorb and digest cell components. Last but not least the fungus must overcome the human immune system. The lineages of fungi that possess those four criteria are the Zygomycota, Entomophthorales, Ascomycota and Basidiomycota (22).

Although the most common fungal infections are superficial and affect skin and nails (23) *Candida* genus infections (candidiasis) have high mortality rates (24). In context with the thesis research field the prevalence of candidiasis caused by *Candida* genus infection has been found. The most encountered clinical species are *Candida albicans*, which represent 65% of diagnosis results, and *Candida glabrata*,

less seen (11%). The remaining 14% are mainly attributed to *Candida tropicalis*, *Candida parapsilosis* and *Candida krusei* (25). There is an urgent need to find effective medicaments as almost half of patients die following the month of infection (26).

2.1.2. Drugs used for fungal infection treatment

Existing antifungals drugs are categorized in four according to their targets (27). Polyenes bind to the fungal membrane and form pores aiming to alter its permeability. Pyrimidine analogs interfere with DNA synthesis. Azoles inhibit the conversion of lanosterol to ergosterol, a crucial membrane component whereas echinocandins prevent synthesis of β-1,3 glucans, another crucial component but of the fungal cell wall this time.

Although resistance to those antifungal drugs (28) is a limiting factor to efficient therapy, cytotoxicity caused by those molecules is an additional obstacle (29).

In addition to the already available drugs in the market, immunotherapy techniques are being investigated (30) for fungal infections but none has been approved by any regulatory agency yet (31).

Most importantly, the newly emerged species, *Candida auris*, has raised many concerns as resistance to all current antifungal drugs has been reported for some strains (32). Therefore, even if *Candida auris* is not mentioned as the most abundantly observed clinical species, it must be studied thoroughly to prevent a crisis in the health system (33).

2.1.3. *Candida auris*

Candida auris first isolated in 2009 (7) has already been noticed in more than 40 countries spread across three continents (34).

C. auris has been classified phylogenetically in the Metschnikowiaceae family (35). It has been identified as a haploid fungus, containing seven chromosomes coding for over five thousand genes (36). Furthermore it was found that it translates CTG codon to serine instead of leucine which makes it a member of CTG clade (37).

Contrary to other *Candida* species, *C. auris* tolerates temperatures up to 42°C (38) and forms white, pink or purple colonies when grown at those temperatures (39) but could lead to wrong laboratory diagnostic. Accurate identification of *C. auris* can be achieved with Matrix-assisted laser desorption ionization-time of flight mass spectrometry (MALDI-TOF MS) (40) and polymerase chain reaction (PCR) (41).

Even if its name tends to consider it as an infection occurring exclusively in the ear, it has been isolated so far from different part of the body such as urine, bile, blood, wounds, the nares, the axilla, the skin, and the rectum (42).

C. auris has been seen to develop three distinct phenotypic forms named as typical yeast, filamentation competent yeast and filamentous form (43).

2.2. New Epigenetic Target as Treatment Strategy

2.2.1. Chromatin structure

Eukaryotic cells contain all of their genetic information in their DNA which is tightly stored within their nucleus. Taking into consideration its length, DNA must be in a compact form to fit within the nucleus of the cell (44). The smallest compacted unit of DNA is called nucleosome (Figure 1). DNA of 146 base pairs is wrapped around an octamer of core histone proteins composed of dimers of H2A, H2B, H3 and H4 (45). Additionally each core histone protein has a characteristic N-terminal tail extending from the core structure.

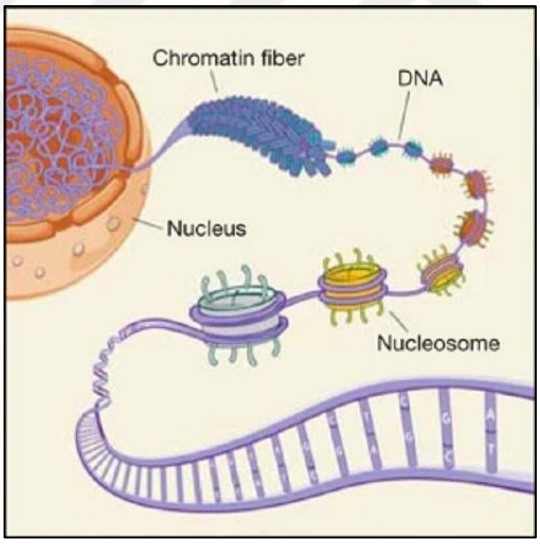

Figure 1. Schematic representation of nucleosome and chromatin

Compaction levels of DNA from double strand to chromosome as stored in the nucleus (46) are reported in figure 1.

Several post-translational modifications have been identified on those histone N-terminal tails playing a role in chromatin modelling (47). Such modifications are

referred as epigenetic determinants. To date modifications occurring on four residues have been identified. Lysine residues can have acetyl, methyl, ubiquitin, butyryl, propionyl, crotonyl groups added. Arginines were detected to have methyl, ribosyl and citrullin groups added. Serine and threonine residues could have phosphoryl or glycosyl groups added (48).

Those groups serve as recognition sites for proteins to bind to DNA. There are three types of proteins that recognize the PTMs on histone tails known as writers, erasers and readers (Figure 2). The writers catalyze the addition of PTMs, and the erasers remove them. The third class such as bromodomain containing proteins, bind to modified histone tails and mediate the formation of large protein complexes which enable gene transcription or DNA recombination (49).

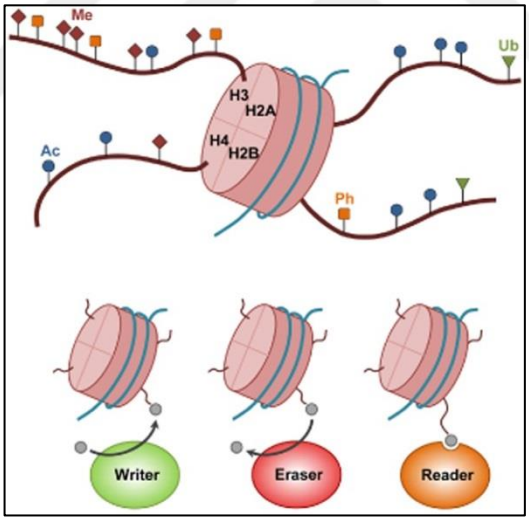

Figure 2. Schematic illustration of three classes of enzymes involved with histone post translation modifications

Writer enzymes add PTMs such as methyl, acetyl, ubiquitin, phosphoryl on histone tails. Eraser enzymes remove them. Reader enzymes recognize those PTMs and take a mediator role in gene transcription (50).

2.2.2. Brd4

Brd4 belongs to the bromodomain and extraterminal protein (BET) family of bromodomain containing proteins which contains 2 bromodomains (BD) recognizing post-translational modifications (PTM) on histone tails, more precisely acetylated lysine residues (51). Brd4 affinity to histone peptides with bulkier than acetyl PTM groups have been studied as well recently and it was demonstrated that Brd4 and other human bromodomains can bind to such histone peptides (52).

All bromodomains have a conserved structure composed of four α-helices named Z, A, B and C (53). Two loops in the structure help the recognition and binding of acetyl lysines. A large loop between α_Z and α_A and a smaller one between α_B and α_C (54). Brd4 plays a crucial role in gene expression by recruiting positive transcriptional elongation factor b (P-TEFb) to chromatin (Figure 3). Therefore Brd4 inhibition has been studied to stop the translation of oncogenic (55) or inflammation (56) responsible genes. Brd4 inhibition as a potential therapy for cardiovascular diseases (57) has been a studied as well. The success of these findings has brought the idea to Petosa group to develop inhibitors for the fungal BET protein (13).

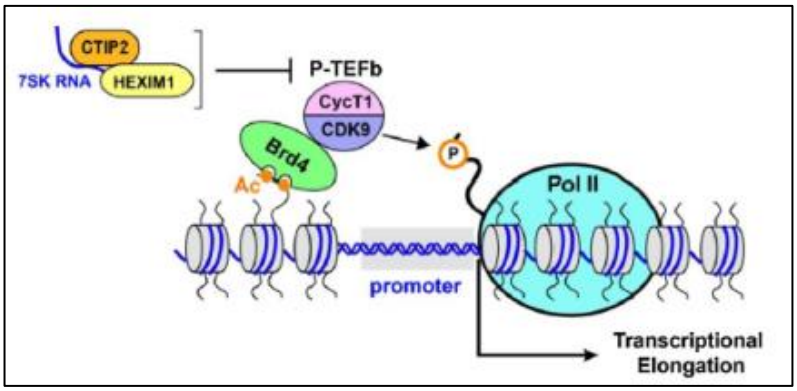

Figure 3. Schematic illustration of Brd4 role in gene transcription

Upon binding to acetylated histone tails Brd4 recruits a protein complex P-TEFb which on its turn activates RNA polymerase II by phosphorylating its C-terminal domain (58).

2.2.3. Bdf1

Bdf1 is the fungal analog of Brd4. Its two bromodomains recognize as well acetylated histone tails. It has been proven on the yeast model organism *Saccharomyces cerevisiae* that Bdf1 is essential for growth. Its bromodomains on the other hand are necessary for meiosis to progress and for spores to reach maturity (59).

2.3. Fluorescence Detected Binding Assays

In order to measure the binding affinity of each bromodomain to histone peptides and more importantly to measure the effect of an inhibitor on that affinity, binding assays must be performed. There are several options when choosing assays to monitor the interaction of a protein to its ligand. Fluorescent ligand binding assays

have the advantage of being relatively cheap and more practical in high throughput screening campaigns.

2.3.1. HTRF

Homogeneous Time Resolved Fluorescence (HTRF) is a fluorometric detection method quantifying the emitted wavelength of a fluorophore joined to an antibody. That fluorophore is first excited by another fluorophore's emission wavelength when in close proximity (Figure 4). Additionally to a Förster Resonance Energy Transfer (FRET) HTRF has a difference in the timing between excitation and emission. In HTRF the fluorescent molecules used are called lanthanide chelate labels. They permit the detection of the emitted light after excitation took place, whereas in FRET excitation and emission are concurrent. This difference in time for emission detection limits background signals thus permits more intense specific readings. Furthermore HTRF does not require washing steps (60).

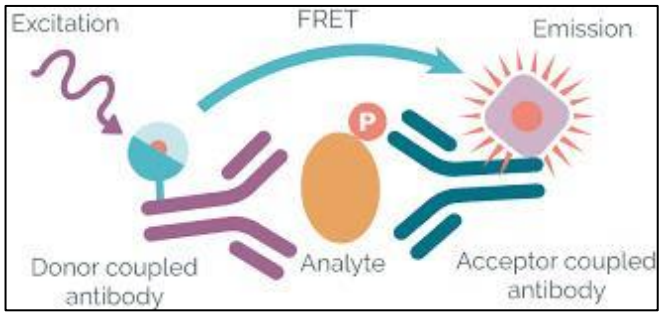

Figure 4. Schematic illustration of FRET mediated fluorescent detection of protein ligand binding

Fluorescent signal emission from a fluorophore coupled antibody when in close proximity with another antibody coupled with a donor fluorophore.

3. MATERIALS AND METHODS

The first part of the experiments dedicated to protein purification and HTRF assays were conducted from February 2020 to August 2020 in the group of Carlo Petosa (Viral Infection and Cancer group, VIC), at the Structural Biology Institute (IBS), affiliated to the University Grenoble Alpes (UGA), the National Center for Scientific Research (CNRS) and the French Atomic Commission (CEA) and located within the European Photon & Neutron Science Campus (EPN) Grenoble, France. The second part comprised peptide synthesis at Acıbadem Mehmet Ali University, Istanbul, Turkey from December 2020 to May 2021.

The methods used have been based on previous experiments conducted on *Candida glabrata* by Petosa group (61, unpublished data, PhD thesis).

The hypothesis of the work was to verify if *Candida auris* putative bromodomains can be developed and optimized for high throughput screening of inhibitors against it.

3.1. Protein 3D Structure Modelling

3.1.1. Swiss Model

The structures of the putative bromodomains BD1 and BD2 were predicted in silico and bound to identified inhibitors to *Candida glabrata* bromodomains by Swiss Modelling (62). The target sequence was filled with the 110 and 119 amino acids of *C. auris* BD1 and BD2 (Appendix 1) respectively. *Candida glabrata* BD1 and BD2 crystal structures were used as the template file for each construct

respectively. QMEAN Z and global model quality estimation (GMQE) statistics were checked for each bromodomain model.

3.1.2. PyMOL

Candida auris Bdf1 3D model predictions obtained by Swiss Modelling were visualized via PyMOL software (63). *Candida glabrata* BD1 and BD2 crystal structures were superimposed with the predicted models of *Candida auris* BDs.

3.2. Cloning

3.2.1. Sequence design

The sequences of *C. glabrata* and *C. auris* were aligned on Serial Cloner (64) and the adequate amino acid for the beginning and the end of the wanted sequence were noted.

3.2.2. Secondary structure prediction

Once the sequences were determined a predictive secondary structure analysis of the proteins was conducted with Phyre 2 (65).

3.2.3. Primers

Forward and reverse oligonucleotide primers were designed targeting different sequences of the BD1 and BD2 domains of *C. auris* Bdf1 and synthesised

commercially by Eurofins Genomics Company (Table 1). The primers were designed so they carry BamH1 and Xho1 restrictions sites for further sub cloning purposes.

Table 1. *Candida auris* bromodomain constructs primers sequences

	Bdf 1 nucleotide sequence interval	Forward primer sequence	Reverse primer sequence
C. auris BD1	346 – 738	CCGCGTGGATCCCCTGCACCTAAGCCACCT	CGGCCGCTCGAGTTAGGCAGCAAGAACCTTGGG
	346 – 771	CCGCGTGGATCCCCTGCACCTAAGCCACCT	CGGCCGCTCGAGTTACGATGCAGCACCAGTGTT
	367 - 738	CCGCGTGGATCCGAACCAGACATGACGAATCTCC	CGGCCGCTCGAGTTAGGCAGCAAGAACCTTGGG
	367 - 771	CCGCGTGGATCCGAACCAGACATGACGAATCTCC	CGGCCGCTCGAGTTACGATGCAGCACCAGTGTT
	385 - 738	CCGCGTGGATCCCTCCCTGCGGACCCTATC	CGGCCGCTCGAGTTAGGCAGCAAGAACCTTGGG
	385 - 771	CCGCGTGGATCCCTCCCTGCGGACCCTATC	CGGCCGCTCGAGTTACGATGCAGCACCAGTGTT
C. auris BD2	820 - 1224	CCGCGTGGATCCGCTGCTCATAGGCCAAAGAG	CGGCCGCTCGAGTTACTTTTGAGCCCATTTCTTGTCG
	859 - 1224	CCGCGTGGATCCTCAAAGGAATTGCCATATGATGTGA	CGGCCGCTCGAGTTACTTTTGAGCCCATTTCTTGTCG
	859 - 1227	CCGCGTGGATCCTCAAAGGAATTGCCATATGATGTGA	CGGCCGCTCGAGTTAAGGCTTTTGAGCCCATTTCTTG
	859 - 1239	CCGCGTGGATCCTCAAAGGAATTGCCATATGATGTGA	CGGCCGCTCGAGTTAAGGTTGTGGGACAGGCTT
	859 - 1248	CCGCGTGGATCCTCAAAGGAATTGCCATATGATGTGA	CGGCCGCTCGAGTTAAGGAGGCGAAGGTTGTGG
	859 - 1272	CCGCGTGGATCCTCAAAGGAATTGCCATATGATGTGA	CGGCCGCTCGAGTTAACTATCGTACTCGCCATCA

3.2.4. PCR

PCR was performed in Biometra T personal machine. Forward and reverse primers were mixed at 0.5 μM with 200 ng of the plasmid including the full length *C. auris Bdf1* gene in 1X Phusion High Fidelity PCR Master Mix (NewEngland Biolabs, USA). Programmed thermocycling conditions are reported in Table 2. Steps 2 to 4 were repeated for 35 cycles before proceeding to steps 5 and 6.

PCR products were run in a 1% Agarose gel with 1 X Tris acetate EDTA (TAE) buffer. DNA was visualised through GelGreen® nucleic acid gel stain. Images were captured with ChemiDoc™ MP imaging system.

Table 2. Thermocycling conditions for PCR

Step	Temperature	Time
1	98°C	30 seconds
2	98°C	10 seconds
3	60°C	30 seconds
4	72°C	10 seconds
5	72°C	600 seconds
6	14°C	∞

3.2.5. Ligation into pJET

Once the PCR was accomplished, the reaction products were ligated into pJET carrier cloning vector with T4 DNA ligase according to the manufacturer's protocol (Thermo Fisher Scientific). The reaction mixture was let half an hour at 22°C.

3.2.6. *E.coli* transformation

Briefly the cells were left in ice with the plasmid for 30 minutes. Then they were incubated at 42°C for three quarters of a minute only and put again on ice. The reaction tube content was poured on a LB petri dish protected with ampicilin and let for overnight incubation at 37°C.

3.2.7. Plasmid isolation

The day following transformation, colonies were amplified in LB ampicillin overnight culture. The day after a miniprep plasmid isolation kit (Macherey-Nagel™ Kit NucleoSpin Plasmid QuickPure™) was used to isolate the different plasmids.

3.2.8. Restriction enzyme digestion

The isolated pJET plasmids (1µg) and the GST incorporated pGEX plasmid (1µg) were both digested with BamH1 and Xho1 according to the manufacturer's protocol (New England Biolabs, USA) and then run on an agarose gel as mentioned above.

3.2.9. Ligation into pGEX

The ligation of the bromodomain inserts into the plasmid pGEX occurred at 16°C overnight with the help of T4 DNA ligase according to the manufacturer's protocol (New England Biolabs, USA).

3.2.10. Sequencing

Following pGEX plasmid purification plasmids were sent to GENEWIZ® for sequence verification using 3GEX primers.

3.3. Purification

3.3.1. Inducing gene promoter

Pre-culture solution's OD was measured at 595 nm and diluted to 0.05 in 50 mL. The culture was kept at 37°C until OD_{595} reaches 0.5. At this point the plasmids were induced by adding 1 mM isopropyl β-D-1-thiogalactopyranoside (IPTG) and left at 16°C overnight.

3.3.2. Centrifugation

The pellet was recovered by centrifuging at 4200 rpm during 10 minutes.

3.3.3. Cell lysis

The cell walls were broken with 20 second sonication in 800 µL lyse buffer (Table 3).

3.3.4. Affinity chromatography

Cellular lysates for each bromodomain constructs were incubated separately with 150 µL agarose glutathione resin during 2 hours with rotation at 4°C. Proteins that did not adhere to the resin were withdrawn after spinning the mixture at 3000 rpm. The resin was washed afterwards with the adequate buffer (Table 3) before carrying on to elution. Proteins that adhered to the resin were retrieved with reduced glutathione (GSH) enclosed in elution buffer (Table 3). The buffer was left in contact with the resin in ice then GST tag proteins were taken aside in the supernatant after centrifuging at 3000 rpm.

Table 3. Buffers used for GST tag protein purification

Buffers used during purification	
Lyse	Tris-HCl pH 7.4 50 mM; NaCl 150 mM DTT 1 mM; PMSF
Wash	Tris-HCl pH 7.4 50 mM ; NaCl 500 mM NP-40 1%; DTT 1 mM; PMSF
Elution without GSH	Tris-HCl pH 7.4 50 mM ; NaCl 150 mM NP-40: 0,5%; Glycerol 10 %; DTT 1 mM PMSF
Elution with GSH	Elution without GSH; pH 7.5; GSH 50 mM

3.3.5. Protein concentration determination

Protein concentration was verified by Bradford assay.

3.3.6. Protein parameters

Extinction coefficient (ε) and molecular weight values essential for concentration calculation were procured from Swiss Institute of Bioinformatics website's ExPASy ProtParam tool (66).

3.4. Homogeneous Time Resolved Fluorescence (HTRF) Assay

Incubation with GST-tagged bromodomains and biotinylated tetra acetylated histone 4 tail peptides (H4ac4) brings the donor and acceptor into close proximity and allows FRET. The non-biotinylated H4ac4 peptide competes for binding and was used as a positive control for inhibition.

3.4.1. HTRF reagents and concentrations

GST-tagged proteins in 25mM Hepes pH 7.5, 150mM NaCl, 0.5mM DTT were diluted in EPIgeneous Binding Domain Diluent buffer from Cisbio and assayed at 5 nM final concentration. Biotinylated H4ac4 peptides were diluted in EPIgeneous Binding Domain Diluent buffer and used at a final concentration of 2, 6, 16, 40, 102, 256, 640, 1600, 4000 nM in assays involving optimization of *C. auris* Bdf1 BD1 and BD2, *C. glabrata* Bdf1 BD1 and BD2, *C. albicans* Bdf1 BD1 and BD2, Brd4 BD1 and BD2. The antibody-conjugated donor was diluted in EPIgeneous Binding Domain Detection buffer and used at 0.5nM. The streptavidin-conjugated acceptor

was diluted in EPIgeneous Binding Domain Detection buffer #2 from Cisbio and used at 1/8 of the H4ac4 peptide concentration.

3.4.2. HTRF signal interpretation

Experiments were performed in 384-well white plates (Greiner 781080) in a volume of 16 ml and analyzed in a ClarioStar plate reader (BMG LABTECH). Excitation was at 330 nm and emission intensities were measured at 620 and 665 nm (corresponding to the donor and acceptor emission peaks, respectively; the 665/620 ratio is used to calculate the specific HTRF signal) with an integration delay of 60 μs, an integration time of 400 μs, a number of flashes of 200 and a gain of 2400.

3.5. Peptide Synthesis

3.5.1. Peptide synthesis materials

Automated solid phase peptide synthesis was conducted on a CEM Liberty peptide synthesizer equipped with a CEM Discover microwave reaction cavity. All reactions were conducted microwave-assisted and under nitrogen. All reagents used were of analytical grade and obtained from Sigma-Aldrich. Protected and modified amino acids, resins and coupling reagents were purchased from CEM, Bachem, and Nova Biochem.

3.5.2. Peptide synthesis cycle

At the beginning, the Rink Amid resin was swollen in *N*,*N*-dimethylformamide (DMF) for at least 1 h and then the following synthesis cycle was applied for each amino acid of the sequence. The cycle started with a deprotection step using 20%

piperidine in DMF (2 x 3 mL) then the resin was washed with DMF (2 x 3 mL). The respective fluorenylmethyloxycarbonyl (Fmoc) protected amino acid (0.2 M in DMF) and Oxyma/DIC (0.5 M in DMF) were added into reaction vessel for coupling. All amino acids except arginine (double coupling) and histidine (coupling 50°C, 10 min) were coupled with this method. After the coupling, the resin was washed again with DMF (4 x 3 mL). At the end of the cycle, the terminal Fmoc group of last amino acid was deprotected. The resin was taken into a syringe with filter and washed with DMF (3 x 5 mL). After washing, cleavage coctail (trifluoroacetic acid/H_2O/triisopropylsilane, 95:2.5:2.5, 5 mL) was added and suspended for 30 min at 37°C. The solution was collected and taken up in cold diethyl ether (10 mL) and centrifuged (5000 rpm, 5 min). Diethyl ether was drained and the product peptide was precipitated. Removal of protective groups on side chains were achieved simultaneously during cleavage step.

3.5.3. Peptide purification

Purification of peptides by high performance liquid chromatography (HPLC) was performed on Agilent systems. All runs were conducted with a linear gradient of eluent A (H_2O, 0.1% trifluoroacetic acid) to B (acetonitrile/H_2O/trifluoroacetic acid (80:20:0.1)) in 30 min. UV absorption was detected at 214 nm, 254 nm and 280 nm. A semi-preparative Agilent C18 column was used. Flow-rates were 4 mL/min. All samples were dissolved in ultrapure water and filtered before injection.

3.5.4. Peptide lyophilisation

After purification peptides frozen at -80°C were freeze-dried from aqueous solutions containing minimal amounts of acetonitrile using a Labconco FreeZone 6L lyophilizer attached to a high vacuum pump.

3.5.5. Peptide mass determination

Molecular weights were examined on ThermoFischer Orbitrap Exploris 120 Mass Spectrometer. Peptides' chemical formulas were drawn on ChemDraw (67) to calculate their exact mass.

4. RESULTS

4.1. Bromodomain 3D Structure Modelling

The cDNA coding for the *C. auris* Bdf1 was amplified previously in the Petosa lab from a *C. auris* cDNA library based on sequence similarity to *Candida glabrata Bdf1*. In order to have a preliminary idea concerning the identification of *C. auris* Bdf1 the structures of the putative bromodomains BD1 and BD2 were predicted.

First 3D models of both *Candida auris* BD1 and BD2 shown in Figure 5 were visualized. *Candida glabrata* BD1 and BD2 crystal structures were superimposed with those of *Candida auris* to verify structure similarity (Appendix 2). Both *C. auris* putative BD1 and BD2 manifest the four α-helices conserved among all bromodomains.

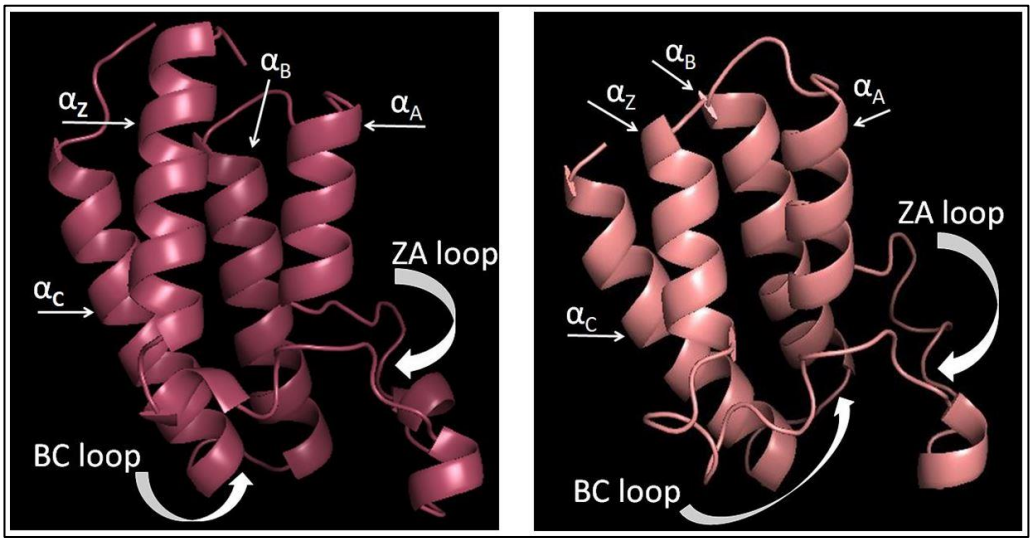

Figure 5. 3D models of *Candida auris* BD1 (left) and BD2 (right)

3D model reliability was verified with QMEAN Z, QMQE statistics (Table 4).

Table 4. 3D model prediction statistics for *C. auris* BDs

	C. auris BD1	*C. auris* BD2
QMEAN Z	- 0.32	- 0.51
QMQE	0.89	0.77

QMEAN Z-score indicates whether the QMEAN score of the model is comparable to what one would expect from experimental structures of similar size. QMEAN Z-scores nearby zero reflect good agreement between the model structure and experimental structures of similar size. Scores of -4.0 or below are an indication of models with low quality. As QMEAN Z-scores are almost equal to 0 both *C. auris* BD1 and BD2 predicted 3D models have high quality.

GMQE is a marker taking into consideration target-template alignment and target structure. The result can between 0 and 1 with figures close to 1 reflecting more reliability. Thus both *C. auris* BD1 and BD2 predicted 3D models are estimated reliable.

Later, the compound that showed significant inhibition for both *C. glabrata* BDs was added to the model to predict its interaction with *C. auris* bromodomain pockets. The way compound 409 could be positioned in *C. auris* BD1 is exhibited in Figure 6.

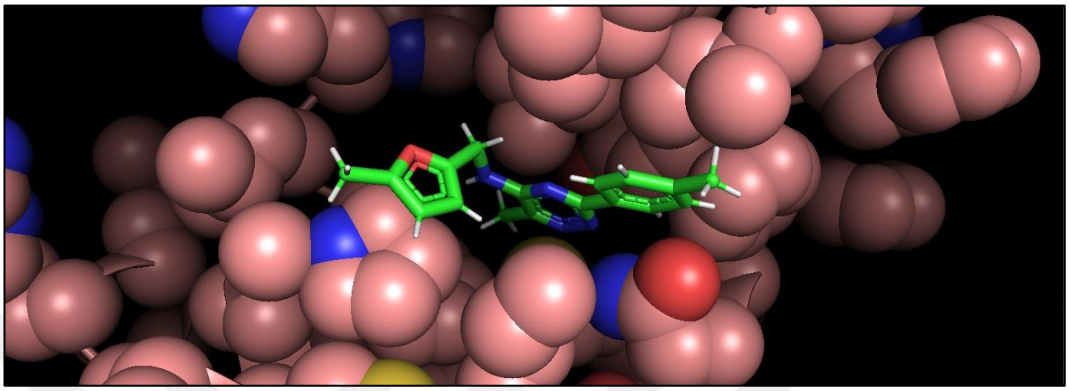

Figure 6. *Candida auris* BD1 3D model with compound 409

Compound 409 fits easily in *C. auris* bromodomain loop and not steric clash has been seen.

On the other hand the way compound 409 could be positioned in *C. auris* BD2 is exhibited in Figure 7.The steric clash that might occur while compound 409 tries to fit in *C. auris* BD2 is pointed out.

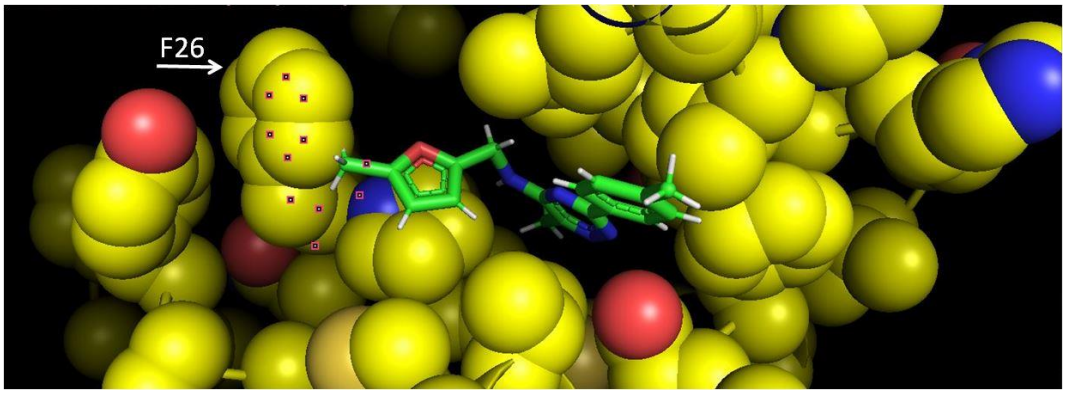

Figure 7. *Candida auris* BD2 3D model with compound 409

C. auris BD2 phenylalanine 26 blocks compound 409 from fully penetrating its pocket. This predicts that compound 409 would not have interactions to the bromodomain pocket.

4.2. Design of *Candida auris* Bdf1 BD1 and BD2 GST-Fusion Proteins

In order to carry out *C. auris* BD1 and BD2 HTRF assays each bromodomain needed to be used in frame with the C-terminus of GST so that a fluorophore labelled anti-GST antibody would be able to bind. Based from previous experiences the Petosa group made evident that the length of the individual bromodomain fused to GST from either *C. albicans* or *C. glabrata* plays an important role in obtaining an optimal signal in the HTRF assay. Therefore twelve *C. auris* bromodomain constructs of different amino acid length, six for BD1 and six for BD2 were designed. Their lengths were designed based on similarities with the bromodomain constructs of *C. glabrata* (Appendix 3 to 5) used previously in HTRF. Based on secondary structure predictions of *C. glabrata* (Appendix 6 and 7) and *C. auris* (Appendix 8 and 9) bromodomains the constructs that were designed for *C. auris* include the characteristic α-helices. The desired amino acid sequences for the 12 different *C. auris* proteins are reported in Figure 8. The sequences themselves are stated in Appendix 10.

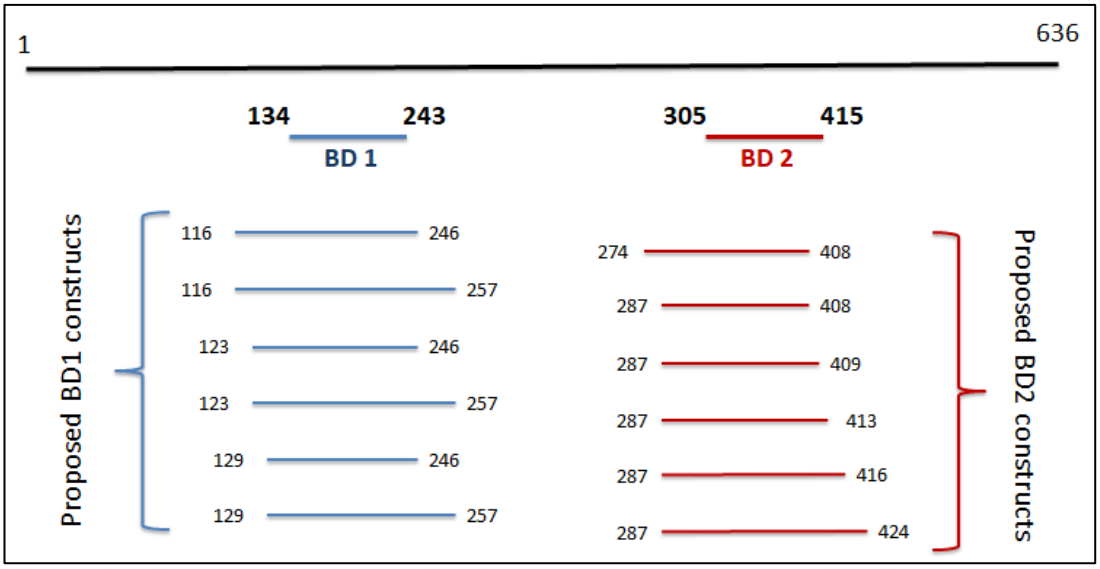

Figure 8. Schematic illustration showing designed construct lengths and bromodomain locations for *Candida auris* Bdf1

Finally, *C. auris Bdf1* nucleotide sequence (Appendix 11) was used to identify and design the primers for each bromodomain construct.

The different steps used for constructing the different BD1 and BD2 GST fusion proteins are presented in Figure 9.

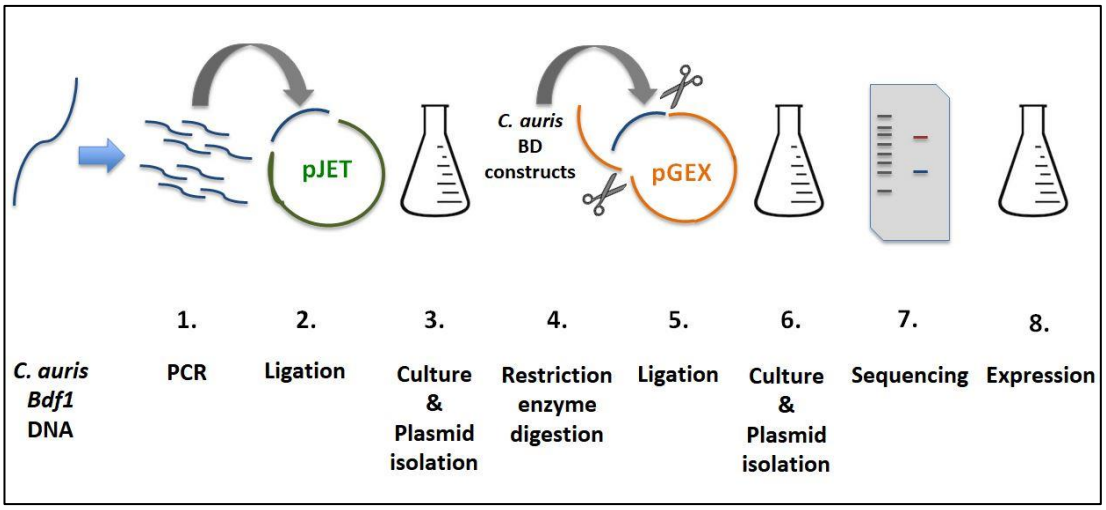

Figure 9. Experimental steps for BD1 and BD2 GST fusion protein expression

Briefly, sequence specific oligonucleotide primers were used to amplify the cDNA of the desired length coding for the *C. auris* bromodomain. PCR products of the correct predicted length were subcloned in the pJET carrier vector (Appendix 12). Following colony amplification for plasmid purification, the different plasmids were digested with BamHI and XhoI restriction enzymes and the excised DNA fragments were ligated in the similarly digested pGEX vector (Appendix 13). Following colony amplification and plasmid purification the correct reading frame and protein sequence was confirmed before bacterial expression by induction with IPTG. The *C. auris* bromodomain constructs that were found to be fused in frame to GST (Appendix 14) are A, B, C, D, E, F, G, H, K, J, and L. Their sequencing result and validation by alignment are issued in Appendices 15 to 25. Consequently purification and thus HTRF assays will be pursued with those 11 constructs.

4.2.1. Purification of the GST BD1 and BD2 fusion proteins

Following sequence confirmation of the different pGEX fusion proteins carrying either BD1 or BD2 experiments were proceeded to GST based protein affinity.

Figure 10 displays an overview of the stages taken to separate the GST fused bromodomains from other cellular proteins.

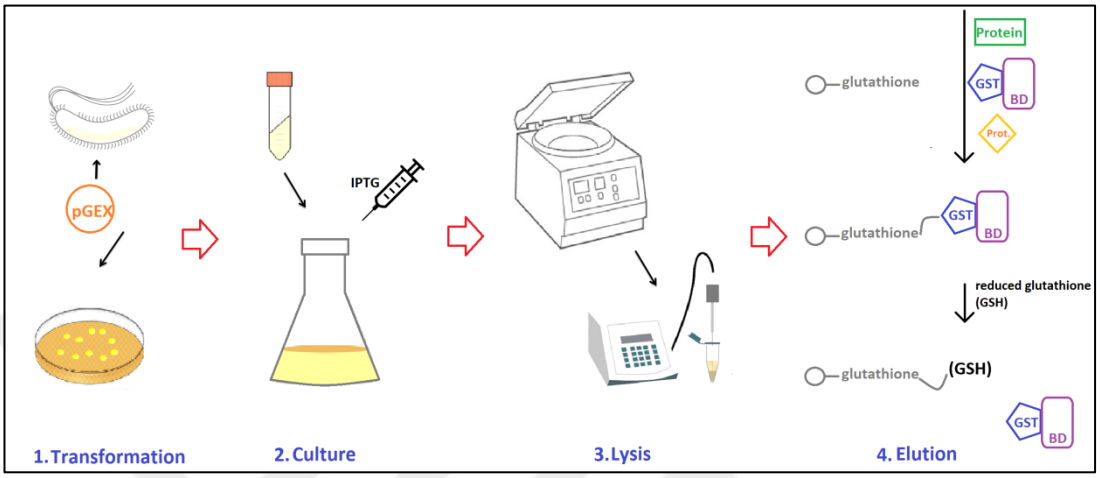

Figure 10. Experimental steps for GST tag affinity protein purification

1. Plasmids containing *C. auris* bromodomain and GST sequences used to transform bacterial cells. 2. Liquid culture to amplify cells and protein production. 3. Bacterial cell lysis. 4. GST tag bromodomains purified on glutathione resin.

Plasmids that contained the designed *C. auris* bromodomain of different sequence length were transformed in *E.coli* cells for protein expression. Expression of purified GST tag proteins was confirmed by visualisation of a band on SDS gel (Figure 11 and 12). Samples entitled “lysa” corresponds to the samples retrieved from the lysate obtained after cell sanitation whereas “FT” indicates the flow through molecules that did not bound to the resin and “Elu” points to the target proteins that were eluted from the resin following washing.

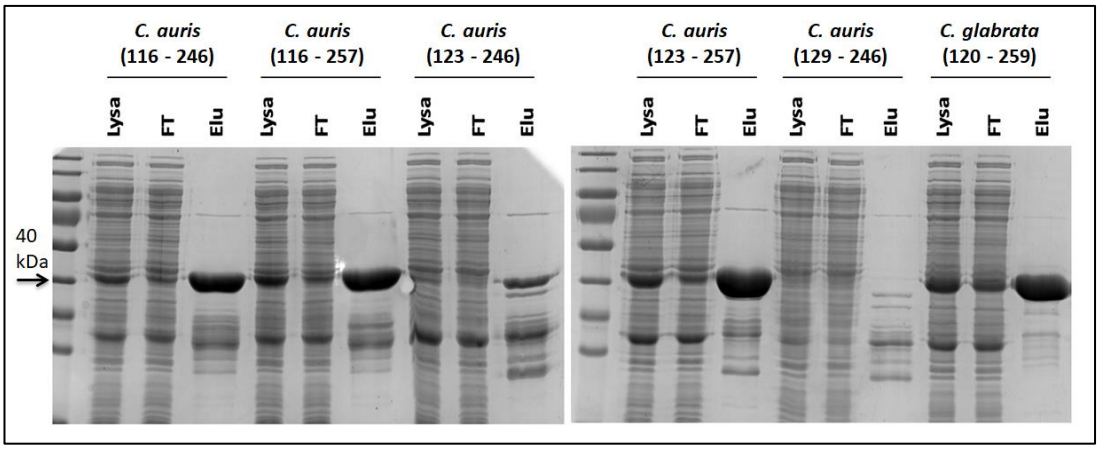

Figure 11. SDS gel of samples taken during *C. auris* BD1 purification

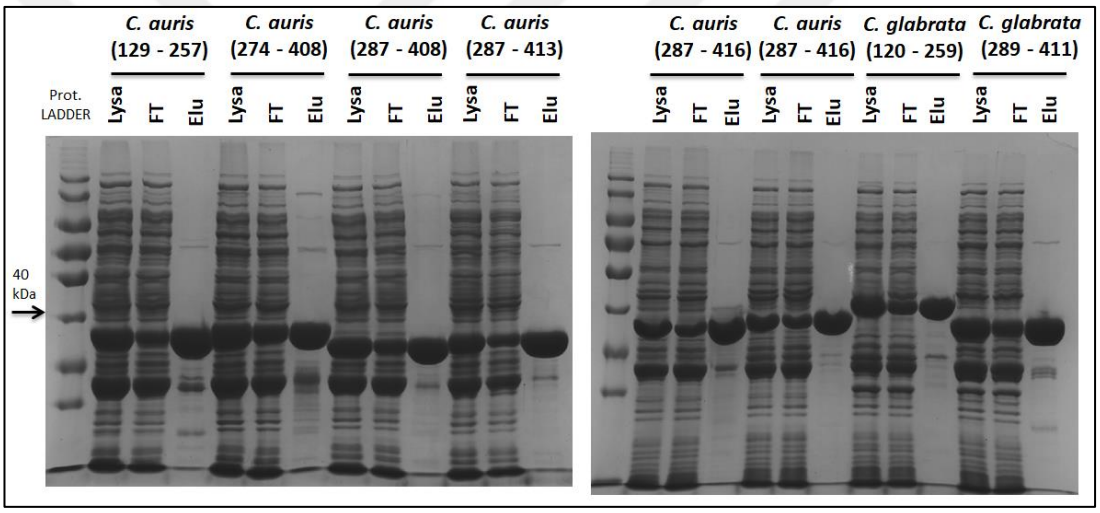

Figure 12. SDS gel of samples taken during *C. auris* BD2 purification

All 11 *C. auris* constructs listed A to L and one construct for each *C. glabrata* BD were successfully purified according to gel results where a thick band is visible under eluted samples. The concentration of each purified protein is shown in Table 5.

Table 5. *C. auris* BD1 and BD2 purification yield

Protein	**ε (M^{-1} cm^{-1})**	**Mean of OD_{595}**	**Concentration (mg/mL)**	**Size (kDa)**	**Concentration (µM)**
A2	47580	0.084	1.129	41.11	27.46
B3	47580	0.11	1.471	42.09	34.95
C1	47580	0.049	0.653	40.42	16.16
D2	47580	0.153	2.04	41.41	49.37
E2	47580	0.015	0.2	39.74	5.03
F11	47330	0.565	7.53	40.722	184.9
G3	57300	0.537	7.16	42.011	170.4
H5	57300	0.535	7.13	40.52	175.9
J1	57300	0.575	7.66	41.039	186.6
K6	57300	0.625	8.33	41.32	201.6
L3	58790	0.469	6.25	42.202	148.1
Cg BD1 (120-259)	45840	0.44	5.86	42.094	139.2
Cg BD2 (289-411)	65780	0.597	7.96	40.766	195.2

4.3. HTRF Assay of C*andida auris* Bdf1

As mentioned in the introduction, in order to evaluate and quantitate the ability of the GST-fused BD1 and BD2 bromodomains of the *C. auris* to bind acetylated Histone 4 tails HTRF assay had to be optimized based on previous protocols established with *C. albicans* and *C. galbrata* Bdf1 bromodomains.

Briefly the GST-fused bromodomains recognize and bind to acetylated lysines on histone tail peptide that carries a biotinylated lysine at its C-terminus. The fluorophore labelled anti-GST antibody that recognizes GST serves as donor to the acceptor fluorophore which is bound to streptavidin that binds to the biotinylated peptide. When the bromodomain is bound to the peptide the two fluorophores come in close proximity and there is FRET (Figure 13a). In the presence of a bromodomain binding inhibitor the donor and acceptor fluorophores move away and FRET signal decreases (Figure 13b).

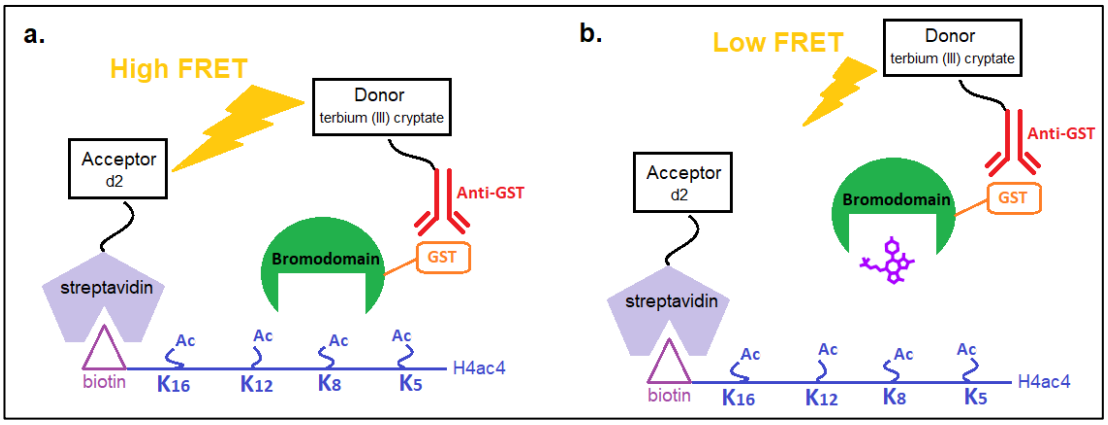

Figure 13. Bromodomain inhibition detection by HTRF

In order to adapt the HTRF assay for screening for inhibitors of *C. auris* bromodomains some preliminary experimental steps were followed. First different

bromodomain constructs of different amino acid lengths had to be tested to choose the one that gives the highest signal.

4.3.1. Optimum construct

The different purified GST tagged bromodomains of *C. auris* were then used to identify the particular bromodomain constructs that would give the best HTRF signal and were compared with human bromodomain Brd4 and *C. glabrata* BDs. Bromodomains that were assessed to have a protein signal/background ratio superior to 3 were chosen for further inhibition studies in presence of competitive peptides and/or compounds (Figure 14 and 15).

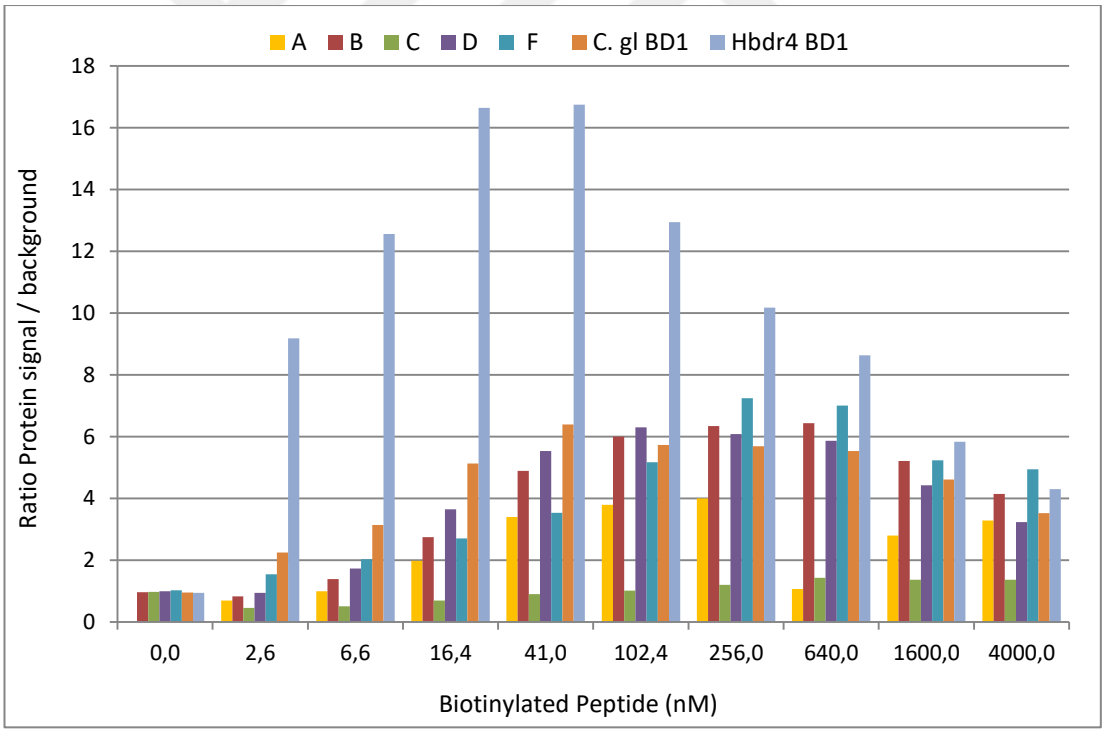

Figure 14. *C. auris* BD1 constructs HTRF assay

Construct D (*C. auris* 123–257) and F (*C. auris* 129–257) were selected to advance HTRF study for BD1.

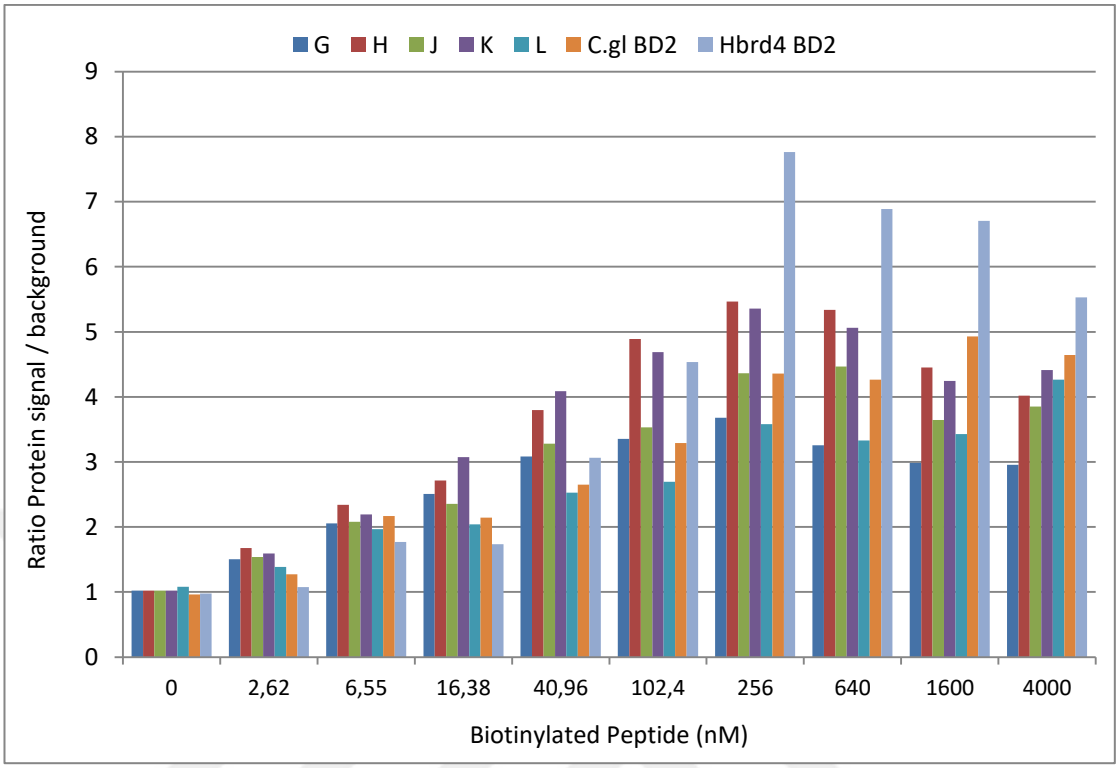

Figure 15. *C. auris* BD2 constructs HTRF assay

Constructs H (*C. auris* 287–408) and K (*C. auris* 287–416) were privileged to continue BD2 HTRF assays.

4.3.2. Effect of solvents

Once constructs with high HTRF signals were determined the effect of 0.2% DMSO and 1% MEG (Figure 16 and 17) on the signal was controlled because inhibitor compounds are dissolved in such solvents and they might decrease the fluorescence values during inhibiton assays. Hence inhibition experiments have been directed with these two solvents.

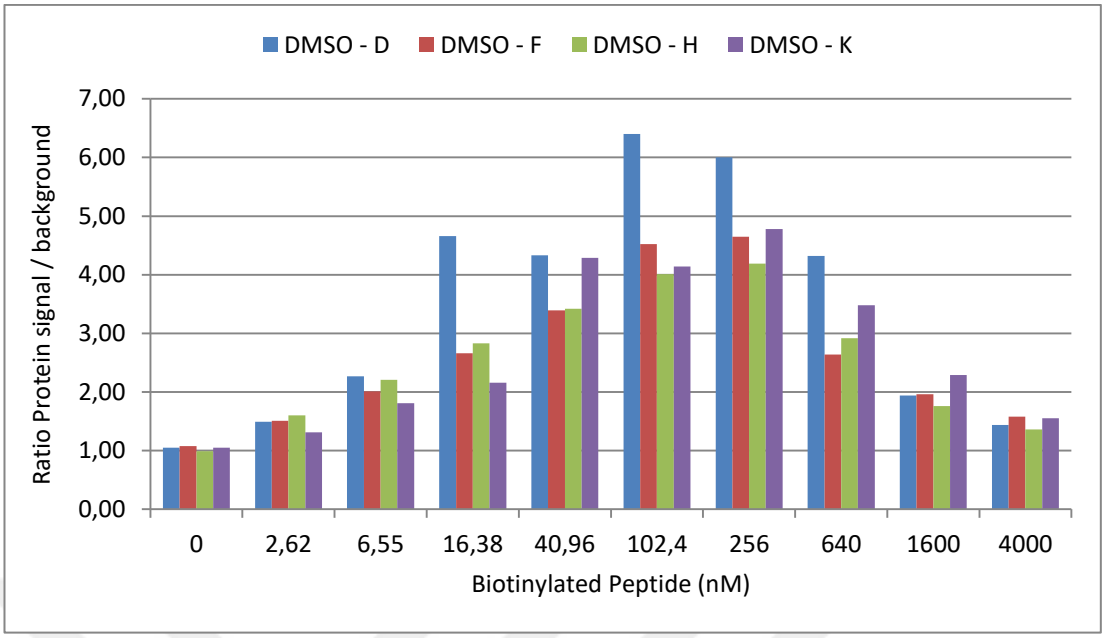

Figure 16. HTRF of *C. auris* bromodomain constructs in 0.2% DMSO

Among BD1 constructs D (*C. auris* 123–257) has the highest signal in presence of 0.2% DMSO. Concerning BD2 constructs K (*C. auris* 287–416) is less sensitive to DMSO.

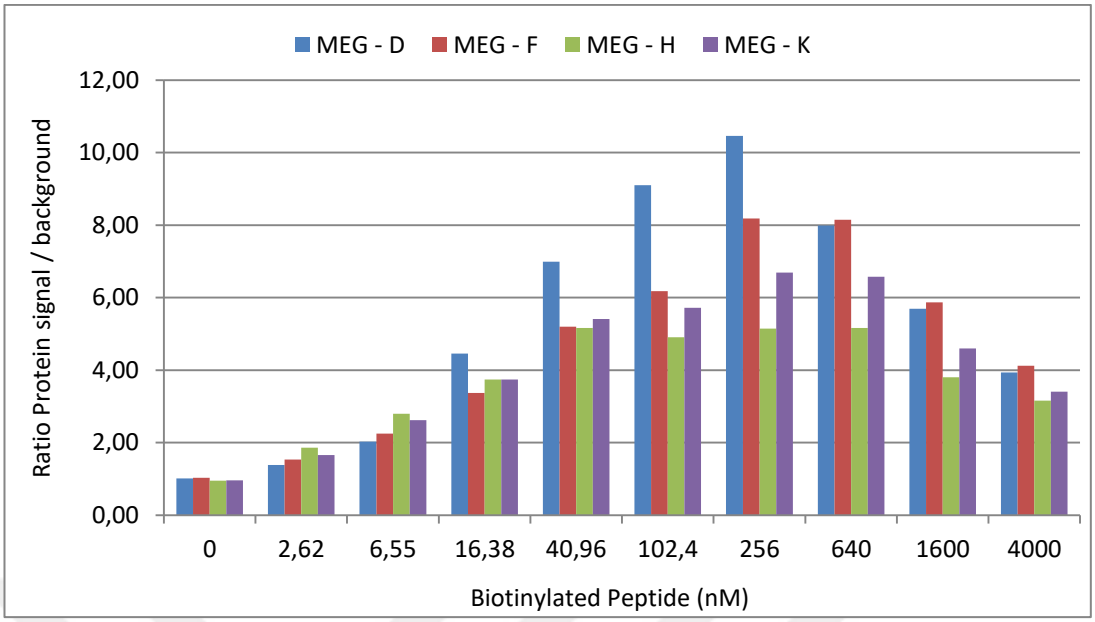

Figure 17. HTRF of *C. auris* bromodomain constructs in 1% MEG

The constructs that gave the highest signal in 1% MEG were D (*C. auris* 123–257) for BD1 and K (*C. auris* 287–416) for BD2.

Overall, the most resistant constructs for both solvent conditions have been found to be D (*C. auris* 123–257) for BD1 and K (*C. auris* 287–416) for BD2.

4.3.3. EC50

For the purpose of optimizing the future inhibition experiments the concentration of biotinylated peptide which gives half of the maximum HTRF signal (EC50) was then determined (Figure 18). When biotinylated peptide concentrations are conditioned to EC50 values a significant bromodomain inhibition would result in a sharp decrease of the signal. On the contrary if there are too many biotinylated peptides in the medium then even if some bromodomains are inhibited the signal would remain elevated.

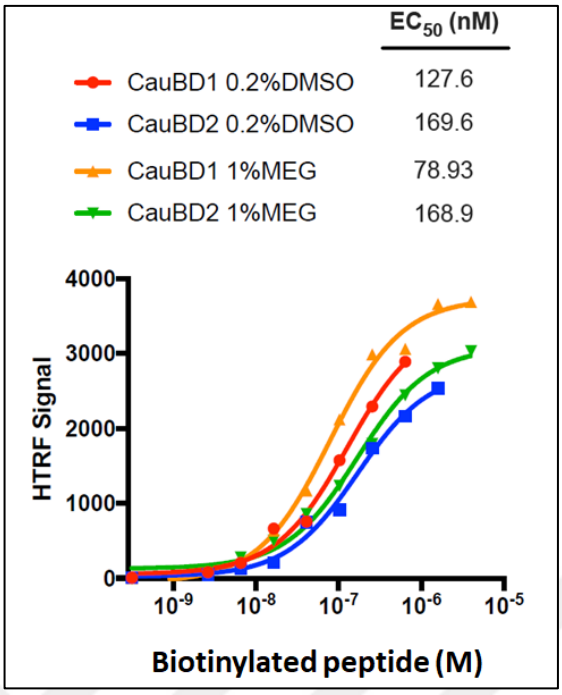

Figure 18. Determination of biotinylated peptide concentration for *C. auris* HTRF inhibition assays

EC50 values for 0.2% DMSO has been kept because inhibitor compound 409 dissolved better in that solvent. Following experiments are set to be conditioned at fixed 130 nM biotinylated peptide for *C. auris* BD1 and 170 nM for *C. auris* BD2.

4.3.4. Competitive inhibition

In order to evaluate the capacity of bromodomains to be inhibited the HTRF signal profile when increasing non-biotinylated peptide is dispensed over the reaction is communicated in Figure 19.

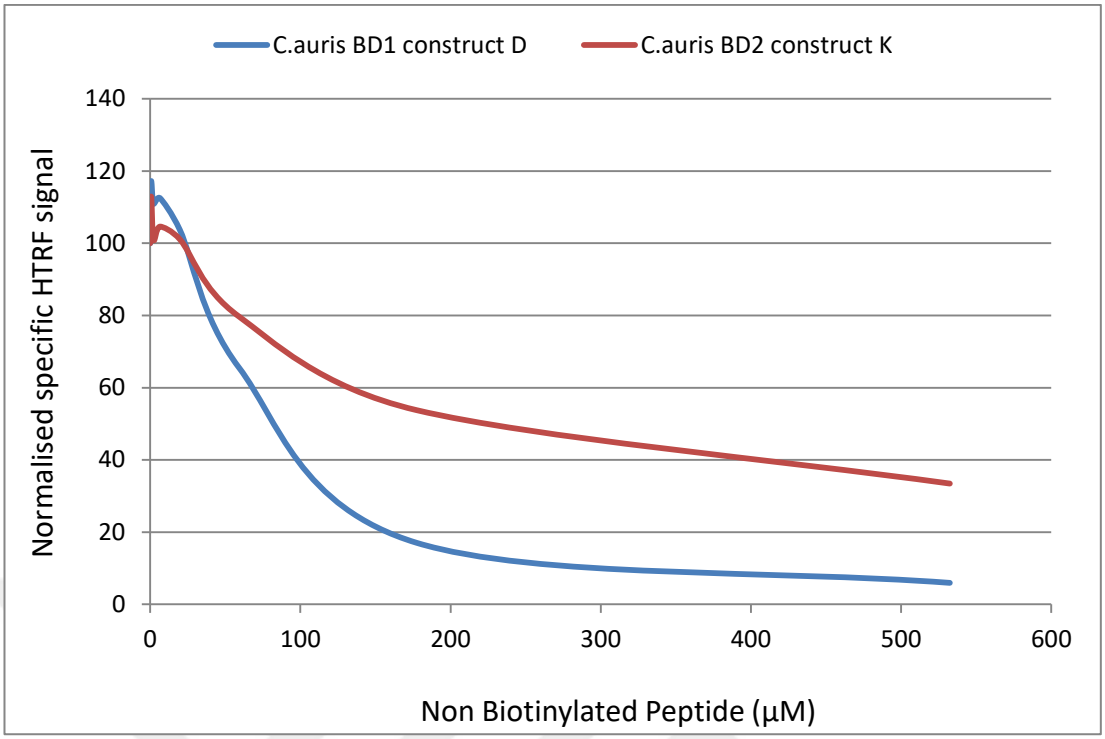

Figure 19. HTRF competitive inhibition with non-biotinylated peptide

At first glance *C. auris* BD1 inhibition susceptibility over *C. auris* BD2 was evident.

4.3.5. IC50

Following the previous acquired data IC_{50} values were determined (Figure 20) to quantify the inhibition susceptibility.

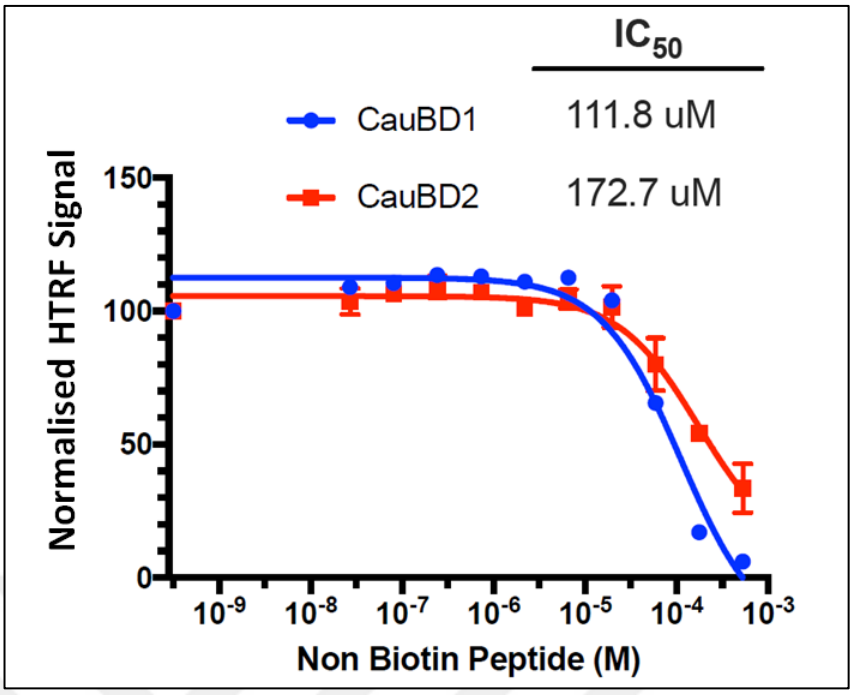

Figure 20. IC50 for *C. auris* bromodomains

A smaller concentration of biotinylated peptide can decrease the maximum signal of *C. auris* BD1 by half. Indeed *C. auris* BD1 was found to be more sensitive to competitive inhibitors rather than *C. auris* BD2.

4.3.6. Preliminary evaluation of *C. auris* inhibition

Finally as a proof of concept preliminary inhibition HTRF assays for *C. auris* Bdf1 (Figure 21) were carried out using the previously identified inhibitor of *C. glabatra* Bdf1 protein.

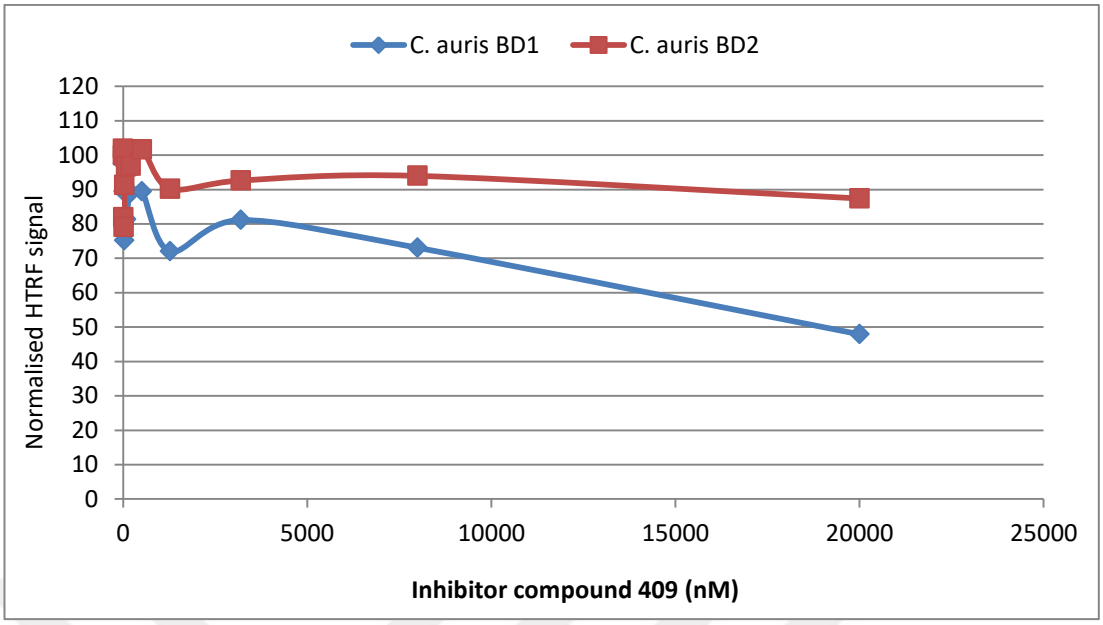

Figure 21. *C. auris* HTRF inhibition assay with compound 409

Using the HTRF assay optimised for the *C. auris* BD1 and BD2 the results showed that the *C. auris* BD1 is 50% inhibited at 20 µM inhibitor. However, the *C. auris* BD2 appears not be inhibited by the compound. This profile was similar to the results witnessed with compound 409 against *C. albicans* bromodomains (Appendix 26). Positive control rerun of HTRF assay with *C. glabrata* in presence of compound 409 (Appendix 26) validated the results as same performance of the inhibitor for both BDs was noted as discovered previously (61).

4.4. Peptide Synthesis

4.4.1. Peptide sequences

Histone 4 tail peptide and three derivatives were synthesized (Table 6). The first peptide has the native lysine in the sequence without any modification. The second peptide has an acetyl group on all four lysines. The third and fourth peptides have one acetyl and one butyryl group on two lysines.

Table 6. Synthesized peptides sequences*

aa#	1	2	3	4	5	6	7	8	9	10	11	12	13	14	15	16	17	18	19	20	21	22	23
aa	S	G	R	G	K	G	G	K	G	L	G	K	G	G	A	K	R	H	G	S	G	S	Y
Peptide 1					-			-				-				-							
Peptide 2					**A**			**A**				**A**				**A**							
Peptide 3					**A**			**B**				-				-							
Peptide 4					**B**			**A**				-				-							

*Amino acids are designed with their one letter code. For peptides 2 to 4 the letter A in the sequence designates the presence of an acetyl group at that amino acid position whereas the letter B designates the butyryl group.

4.4.2. Peptide purification

Crude peptides cleaved from the resin were purified from impurities by reverse phase high performance liquid chromatography (RP-HPLC). The impurities may consist of deletion/insertion sequences, incomplete deprotection and byproducts during the automated synthesis or the final cleavage. Peptides are monitored at 214 nm where the peptide bond absorbs. However, simultaneous detection of aromatic residues at other wavelengths such as 254 nm and 280 nm, has been used.

Purification profile obtained by HPLC is given in Figure 20 and Appendix 27. For each peptide the first chromatogram on top corresponds to readings at 214 nm. The chromatogram in the middle shows readings at 254 nm. Lastly readings at 280 nm can be visualized at the bottom.

The purity of synthesized peptides can be quantified by the peak area of the desired peptide in comparison to the total area of all peaks detected within the

chromatogram. The purity of peptides after synthesizer was calculated as high as 95%.

For peptide 1, fractions at retention time 12.1 to 12.9 minutes (Figure 22) were collected and lyophilized. Likewise, the peaks with retention times from 14.1 to 14.4, 13.2 to 13.8 and 13.2 to 13.4 minutes were collected for peptides 2, 3, and 4 respectively (Appendix 27).

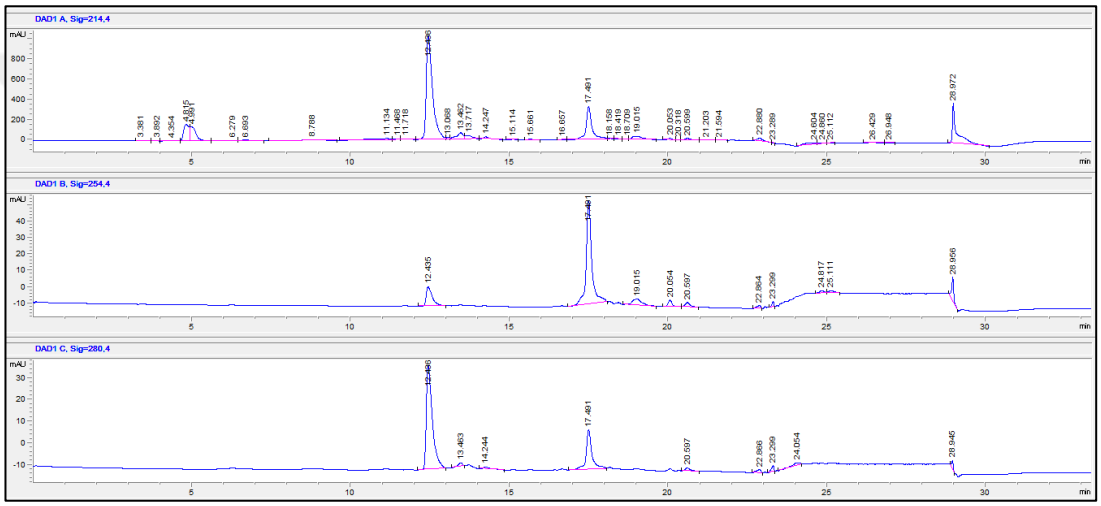

Figure 22. HPLC profile of peptide 1

Purification profile of crude peptide 1 after solid phase synthesis and HPLC at 214 nm, 254 nm and 280 nm. Solvent system A (H_2O, 0.1% trifluoroacetic acid) and B (acetonitrile/H_2O/trifluoroacetic acid (80:20:0.1)). Gradient 10 - 40 % B in 30 min.

4.4.3. Peptide mass verification

Peptides chemical formulas and exact mass (Table 7) were used to verify the MS results (Figure 23 and Appendix 28). For every synthesized and purified peptide its MS profile announces exactly the fragments counted with a 10^{-2} precision.

Table 7. Peptides chemical formula and exact mass

Peptide	Chemical formula	Theoretical Exact mass (Da)	Found mass $[M+2H]^{2+}$	Found mass $[M+3H]^{3+}$	Found mass $[M+4H]^{4+}$
Peptide 1	$C_{89}H_{152}N_{36}O_{27}$	2157.16	1080.08	720.39	540.54
Peptide 2	$C_{97}H_{160}N_{36}O_{31}$	2325.21	1163.60	776.07	582.30
Peptide 3	$C_{95}H_{160}N_{36}O_{29}$	2269.22	1135.61	757.41	568.31
Peptide 4	$C_{95}H_{160}N_{36}O_{29}$	2269.22	1135.61	757.41	568.30

For peptide 1, signals for mass/charge (Figure 23) at 1080 (z=2); 720 (z=3) and 540 (z=4) justify the synthesis of the wanted sequence which weights 2157.16 Da. Mass spectrum with similar signal results at expected fragments are given in Appendix 28.

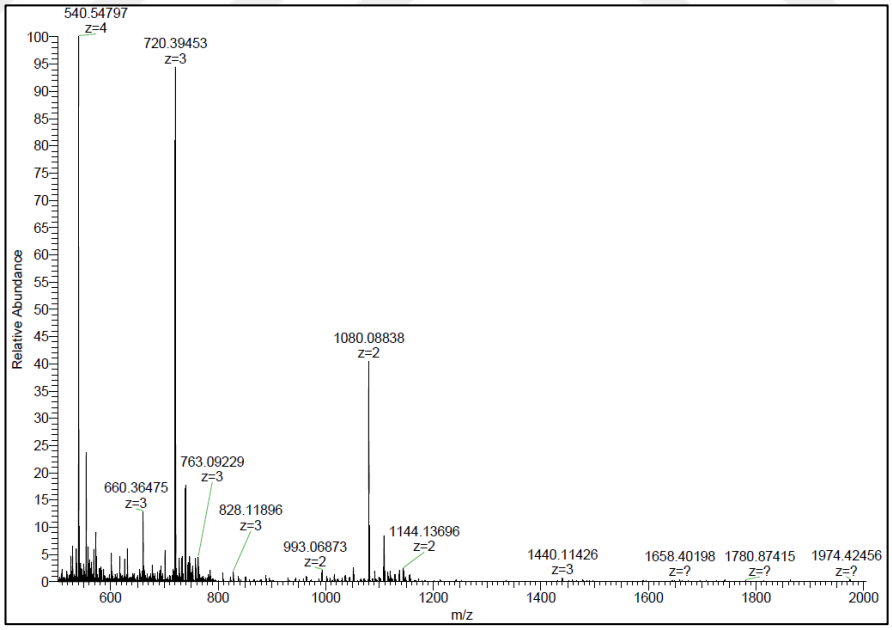

Figure 23. ESI-MS result for peptide 1

5. DISCUSSION AND CONCLUSION

The main goal of the present thesis was to develop the necessary tools for high throughput screening of compounds targeting *Candida auris* Bdf1 bromodomain containing protein, an epigenetic DNA binding protein which based on previous studies from other *Candida* species bind post-translationally modified histone tails. Based on sequence similarity to other *Candida* species the putative *C. auris* bromodomains were cloned using a cDNA coding for the open reading frame of the *C. auris* Bdf1 available in the Petosa lab. 3D model prediction studies demonstrate that indeed the two putative bromodomains of *C. auris* Bdf1 have structural similarities with the well-known bromodomains of other Candida species as well as human analogs. This observation supports the hypothesis that indeed the cloned *C. auris* Bdf1 is the right orthologue.

Furthermore, based on structural comparison of the BD H4 tail binding pockets compared to the human the yeast pocket BD1 and BD2 domains contain amino acid with shorter side chains and therefore could accommodate larger ligands. The observed larger bromodomain pockets in yeasts may explain why some of the current inhibitors targeting human bromodomain may not be efficient inhibitors for yeast. Furthermore, it suggests that inhibitors to yeast bromodomain may be highly specific since they cannot be accommodated within the smaller ligand binding sites of human bromodomains. Finally, the yeast bromodomains may have higher binding affinities to Histone tails having lysine modified with groups that are bulkier than the acetyl groups such as butyric and crotonyl groups.

For HTRF screening assay optimization, different lengths of *C. auris* bromodomains were successfully expressed and purified. Among those constructs tested *C. auris* BD1 (123-257), BD1 (129-257), BD2 (287-408), BD2 (287-416) gave good HTRF signal and were found to be optimal for further use for inhibition screening purposes. Using the identified constructs EC50 values of biotinylated

peptide were determined as 130 nM for *C. auris* BD1 and 170 nM for BD2. These results will be very useful for high throughput screening of inhibitors because at that concentration of biotinylated peptide the HTRF signal representing bromodomain affinity is very sensitive and bromodomain inhibition is easily detectable. As a preliminary study compound 409 that was able to inhibit both *C. glabrata* bromodomains showed significant inhibition for *C. auris* BD1 but not for BD2. Further, 3D model *in silico* prediction studies demonstrated that there is a steric clash with *C. auris* BD2 phenylalanine 26 when compound 409 was modelled to fit the BD2 domain. That means compound 409 cannot fit inside the bromodomain pocket and thus it is unable to compete with PTMs bearing histones. This result was in accordance with the ones obtained against *C. albicans* for which compound 409 showed significant inhibition only against its BD1.

The Petosa group had previously demonstrated that deletion of both bromodomains of *Bdf1* at the same time resulted in a viability loss for *C. albicans* whereas inhibition of only one bromodomain permits the fungus to survive. Inhibition of both bromodomains might be necessary as well for *C. auris*. Nevertheless, because of lack of molecular tools to manipulate *C. auris* genetics such experiments could not be conducted. Therefore there is a need to gain more knowledge about *C. auris* genetic manipulation in order to carry out gene knockout experiments. Only then the necessity of both *C. auris* Bdf1 bromodomains for viability could be determined. Supposingly there is a need to develop compounds that would inhibit both *C. auris* bromodomains at the same time. Having a mixture of inhibitors that would target separetely the bromodomains would make the formulation difficult and the therapy less efficient. In that sense further crystallization studies for *C. auris* bromodomains would elucidate their exact structure and therefore compounds that would fit perfectly the bromodomain pocket could be designed. Once compounds that inhibit both bromodomains could be found *in vitro,* minimum inhibitory concentration assays should be performed to verify their effect on fungal cell growth.

Another important development in current research is the determination of affinity for some human bromodomains to bind better to other PTM groups rather the studied acetyl-lysine. Some other group examples are propionyl, butyryl and crotonyl added to lysine in a post translational manner as well. Such affinity assays with fungal bromodomains have not been studied yet. Thus, the synthesis of histone tail peptides carrying butyryl and/or crotonyl groups added to the lysine of histone tail will be of great interest to pursue for future affinity binding studies. This achievement promises to bring insights into fungal bromodomain affinity with PTMs. As a future prospective other PTM groups could be added as well on histone peptides in that purpose.

6. REFERENCES

1. Pappas PG, Kauffman CA, Andes D, Benjamin DK, Calandra TF, Edwards JE, et al. Clinical practice guidelines for the management of candidiasis: 2009 update by the Infectious Diseases Society of America. Clin Infect Dis. 2009 Mar 1;48(5):503–35.

2. Koehler P, Stecher M, Cornely OA, Koehler D, Vehreschild MJGT, Bohlius J, et al. Morbidity and mortality of candidaemia in Europe: an epidemiologic meta-analysis. Clin Microbiol Infect. 2019 Oct;25(10):1200–12.

3. Rodrigues CF, Rodrigues ME, Henriques M. Candida sp. Infections in Patients with Diabetes Mellitus. Journal of Clinical Medicine. 2019 Jan;8(1):76.

4. José P, Alvarez-Lerma F, Maseda E, Olaechea P, Pemán J, Soriano C, et al. Invasive fungal infection in crtically ill patients: hurdles and next challenges. J Chemother. 2019 Apr;31(2):64–73.

5. https://www.ncbi.nlm.nih.gov/Taxonomy/Browser/wwwtax.cgi?mode=Undefandid=1540022&lvl=3&keep=1&srchmode=1&unlock (Accessed 03.2020)

6. Lamoth F, Lockhart SR, Berkow EL, Calandra T. Changes in the epidemiological landscape of invasive candidiasis. J Antimicrob Chemother. 2018 01;73(suppl_1):i4–13.

7. Satoh K, Makimura K, Hasumi Y, Nishiyama Y, Uchida K, Yamaguchi H. Candida auris sp. nov., a novel ascomycetous yeast isolated from the external ear canal of an inpatient in a Japanese hospital. Microbiol Immunol. 2009 Jan;53(1):41–4.

8. Walits E, Patel G, Lavache S, Faotto R-M, Pobliner A, Wilson S, et al. Management of Candida auris in an inpatient acute rehabilitation setting. American Journal of Infection Control. 2020 Feb 1;48(2):222–3.

9. Rhodes J, Fisher MC. Global epidemiology of emerging Candida auris. Curr Opin Microbiol. 2019 Dec;52:84–9.

10. Ostrowsky B, Greenko J, Adams E, Quinn M, O'Brien B, Chaturvedi V, et al. Candida auris Isolates Resistant to Three Classes of Antifungal Medications — New York, 2019. MMWR Morb Mortal Wkly Rep. 2020 Jan 10;69(1):6–9.

11. Forsberg K, Woodworth K, Walters M, Berkow EL, Jackson B, Chiller T, et al. Candida auris: The recent emergence of a multidrug-resistant fungal pathogen. Med Mycol. 2019 Jan 1;57(1):1–12.

12. de Cássia Orlandi Sardi J, Silva DR, Soares Mendes-Giannini MJ, Rosalen PL. Candida auris: Epidemiology, risk factors, virulence, resistance, and therapeutic options. Microb Pathog. 2018 Dec;125:116–21.

13. Mietton F, Ferri E, Champleboux M, Zala N, Maubon D, Zhou Y, et al. Selective BET bromodomain inhibition as an antifungal therapeutic strategy. Nat Commun. 2017 18;8:15482.

14. Dupper NJ, Zhou Y, Govin J, McKenna CE. Bromodomain Inhibition and Its Application to Human Disease. Pharmacoepigenetics. 2019 Jan 1;475–92.

15. Grela E, Piet M, Luchowski R, Grudzinski W, Paduch R, Gruszecki WI. Imaging of human cells exposed to an antifungal antibiotic amphotericin B reveals the mechanisms associated with the drug toxicity and cell defence. Sci Rep. 2018 14;8(1):14067.

16. Hawksworth DL, Lücking R. Fungal Diversity Revisited: 2.2 to 3.8 Million Species. Microbiol Spectr. 2017 Jul;5(4).

17. Wu B, Hussain M, Zhang W, Stadler M, Liu X, Xiang M. Current insights into fungal species diversity and perspective on naming the environmental DNA sequences of fungi. Mycology. 2019;10(3):127–40.

18. Rodriguez R, Redman R. More than 400 million years of evolution and some plants still can't make it on their own: plant stress tolerance via fungal symbiosis. Journal of Experimental Botany. 2008 Mar 1;59(5):1109–14.

19. Fungi in the Ancient World: How Mushrooms, Mildews, Molds, and Yeast Shaped the Early Civilizations of Europe, the Mediterranean, and the Near East.

20. Köhler JR, Casadevall A, Perfect J. The spectrum of fungi that infects humans. Cold Spring Harb Perspect Med. 2014 Nov 3;5(1):a019273.

21. Perfect JR. The antifungal pipeline: a reality check. Nat Rev Drug Discov. 2017 Sep;16(9):603–16.

22. Köhler JR, Hube B, Puccia R, Casadevall A, Perfect JR. Fungi that Infect Humans. Microbiol Spectr. 2017 Jun;5(3).

23. Havlickova B, Czaika VA, Friedrich M. Epidemiological trends in skin mycoses worldwide. Mycoses. 2008 Sep;51 Suppl 4:2–15.

24. Brown GD, Denning DW, Gow NAR, Levitz SM, Netea MG, White TC. Hidden Killers: Human Fungal Infections. Science Translational Medicine. 2012;4(165):165rv13-165rv13.

25. Pfaller MA, Castanheira M, Messer SA, Moet GJ, Jones RN. Variation in Candida spp. distribution and antifungal resistance rates among bloodstream infection isolates by patient age: report from the SENTRY Antimicrobial Surveillance Program (2008-2009). Diagn Microbiol Infect Dis. 2010 Nov;68(3):278–83.

26. Muderris T, Kaya S, Ormen B, Aksoy Gokmen A, Varer Akpinar C, Yurtsever Gul S. Mortality and risk factor analysis for Candida blood stream infection: A three-year retrospective study. Journal de Mycologie Médicale. 2020 Sep 1;30(3):101008.

27. Di Mambro T, Guerriero I, Aurisicchio L, Magnani M, Marra E. The Yin and Yang of Current Antifungal Therapeutic Strategies: How Can We Harness Our Natural Defenses? Front Pharmacol. 2019;10:80.

28. Doğan Ö, Yeşilkaya A, Menekşe Ş, Güler Ö, Karakoç Ç, Çınar G, et al. Effect of initial antifungal therapy on mortality among patients with bloodstream infections with different Candida species and resistance to antifungal agents: A multicentre observational study by the Turkish Fungal Infections Study Group. International Journal of Antimicrobial Agents. 2020 Jul 1;56(1):105992.

29. Benitez LL, Carver PL. Adverse Effects Associated with Long-Term Administration of Azole Antifungal Agents. Drugs. 2019 Jun;79(8):833–53.

30. Ulrich S, Ebel F. Monoclonal Antibodies as Tools to Combat Fungal Infections. J Fungi (Basel). 2020 Feb 4;6(1).

31. Boniche C, Rossi SA, Kischkel B, Vieira Barbalho F, Nogueira D'Aurea Moura Á, Nosanchuk JD, et al. Immunotherapy against Systemic Fungal Infections Based on Monoclonal Antibodies. J Fungi (Basel) [Internet]. 2020 Feb 29 [cited 2021 May 11];6(1). Available from: https://www.ncbi.nlm.nih.gov/pmc/articles/PMC7151209/

32. Lockhart SR, Etienne KA, Vallabhaneni S, Farooqi J, Chowdhary A, Govender NP, et al. Simultaneous Emergence of Multidrug-Resistant Candida auris on 3 Continents Confirmed by Whole-Genome Sequencing and Epidemiological Analyses. Clin Infect Dis. 2017 Jan 15;64(2):134–40.

33. Schelenz S, Hagen F, Rhodes JL, Abdolrasouli A, Chowdhary A, Hall A, et al. First hospital outbreak of the globally emerging Candida auris in a European hospital. Antimicrob Resist Infect Control. 2016;5:35.

34. Lockhart SR, Etienne KA, Vallabhaneni S, Farooqi J, Chowdhary A, Govender NP, et al. Simultaneous Emergence of Multidrug-Resistant Candida auris on 3 Continents Confirmed by Whole-Genome Sequencing and Epidemiological Analyses. Clin Infect Dis. 2017 Jan 15;64(2):134–40.

35. Chatterjee S, Alampalli SV, Nageshan RK, Chettiar ST, Joshi S, Tatu US. Draft genome of a commonly misdiagnosed multidrug resistant pathogen Candida auris. BMC Genomics. 2015 Sep 7;16:686.

36. Muñoz JF, Gade L, Chow NA, Loparev VN, Juieng P, Berkow EL, et al. Genomic insights into multidrug-resistance, mating and virulence in Candida auris and related emerging species. Nature Communications. 2018 Dec 17;9(1):5346.

37. Santos MAS, Gomes AC, Santos MC, Carreto LC, Moura GR. The genetic code of the fungal CTG clade. Comptes Rendus Biologies. 2011 Aug 1;334(8):607–11.

38. Casadevall A, Kontoyiannis DP, Robert V. On the Emergence of Candida auris: Climate Change, Azoles, Swamps, and Birds. mBio. 2019 Jul 23;10(4).

39. Kumar A, Sachu A, Mohan K, Vinod V, Dinesh K, Karim S. Simple low cost differentiation of Candida auris from Candida haemulonii complex using CHROMagar Candida medium supplemented with Pal's medium. Rev Iberoam Micol. 2017 Jun;34(2):109–11.

40. Kathuria S, Singh PK, Sharma C, Prakash A, Masih A, Kumar A, et al. Multidrug-Resistant Candida auris Misidentified as Candida haemulonii: Characterization by Matrix-Assisted Laser Desorption Ionization–Time of Flight Mass Spectrometry and DNA Sequencing and Its Antifungal Susceptibility Profile Variability by Vitek 2, C…. Warnock DW, editor. Journal of Clinical Microbiology. 2015;53(6):1823–30.

41. Ruiz-Gaitán AC, Fernández-Pereira J, Valentin E, Tormo-Mas MA, Eraso E, Pemán J, et al. Molecular identification of Candida auris by PCR amplification of species-specific GPI protein-encoding genes. International Journal of Medical Microbiology. 2018; 308(7):812–8.

42. Osei Sekyere J. Candida auris: A systematic review and meta-analysis of current updates on an emerging multidrug-resistant pathogen. Microbiologyopen. 2018 Jan 18;7(4).

43. Yue H, Bing J, Zheng Q, Zhang Y, Hu T, Du H, et al. Filamentation in Candida auris, an emerging fungal pathogen of humans: passage through the mammalian body induces a heritable phenotypic switch. Emerging Microbes & Infections. 2018 Dec 1;7(1):1–13.

44. Bednar J, Horowitz RA, Grigoryev SA, Carruthers LM, Hansen JC, Koster AJ, et al. Nucleosomes, linker DNA, and linker histone form a unique structural motif that directs the higher-order folding and compaction of chromatin. PNAS. 1998 Nov 24;95(24):14173–8.

45. Luger K, Mäder AW, Richmond RK, Sargent DF, Richmond TJ. Crystal structure of the nucleosome core particle at 2.8 Å resolution. Nature. 1997 Sep;389(6648):251–60.

46. Baker M. Making sense of chromatin states. Nature Methods. 2011 Sep;8(9):717–22.

47. Allahverdi A, Yang R, Korolev N, Fan Y, Davey CA, Liu C-F, et al. The effects of histone H4 tail acetylations on cation-induced chromatin folding and self-association. Nucleic Acids Research. 2011 Mar 1;39(5):1680–91.

48. Zhang G, Pradhan S. Mammalian epigenetic mechanisms. IUBMB Life. 2014 Apr;66(4):240–56.

49. Musselman CA, Lalonde M-E, Côté J, Kutateladze TG. Perceiving the epigenetic landscape through histone readers. Nat Struct Mol Biol. 2012 Dec;19(12):1218–27.

50. L S-R, M E. Targeting the histone orthography of cancer: drugs for writers, erasers and readers. Br J Pharmacol. 2014 Sep 5;172(11):2716–32.

51. Ferri E, Petosa C, McKenna CE. Bromodomains: Structure, function and pharmacology of inhibition. Biochem Pharmacol. 2016 Apr 15;106:1–18.

52. Flynn EM, Huang OW, Poy F, Oppikofer M, Bellon SF, Tang Y, et al. A Subset of Human Bromodomains Recognizes Butyryllysine and Crotonyllysine Histone Peptide Modifications. Structure. 2015 Oct 6;23(10):1801–14.

53. Dhalluin C, Carlson JE, Zeng L, He C, Aggarwal AK, Zhou M-M, et al. Structure and ligand of a histone acetyltransferase bromodomain. Nature. 1999 Jun;399(6735):491–6.

54. Filippakopoulos P, Picaud S, Mangos M, Keates T, Lambert J-P, Barsyte-Lovejoy D, et al. Histone recognition and large-scale structural analysis of the human bromodomain family. Cell. 2012 Mar 30;149(1):214–31.

55. Chaidos A, Caputo V, Karadimitris A. Inhibition of bromodomain and extra-terminal proteins (BET) as a potential therapeutic approach in haematological malignancies: emerging preclinical and clinical evidence. Ther Adv Hematol. 2015 Jun;6(3):128–41.

56. Xiao Y, Liang L, Huang M, Qiu Q, Zeng S, Shi M, et al. Bromodomain and extra-terminal domain bromodomain inhibition prevents synovial inflammation via blocking IκB kinase-dependent NF-κB activation in rheumatoid fibroblast-like synoviocytes. Rheumatology (Oxford). 2016 Jan;55(1):173–84.

57. 1. Nicholls SJ, Puri R, Wolski K, Ballantyne CM, Barter PJ, Brewer HB, et al. Effect of the BET Protein Inhibitor, RVX-208, on Progression of Coronary Atherosclerosis: Results of the Phase 2b, Randomized, Double-Blind, Multicenter, ASSURE Trial. Am J Cardiovasc Drugs. 2016 Feb;16(1):55–65.

58. 1. Junwei S, Vakoc CR. The mechanisms behind the therapeutic activity of BET bromodomain inhibition. Mol Cell. 2014 Jun 5;54(5):728–36.

59. García-Oliver E, Ramus C, Perot J, Arlotto M, Champleboux M, Mietton F, et al. Bdf1 Bromodomains Are Essential for Meiosis and the Expression of Meiotic-Specific Genes. PLoS Genet . 2017 Jan 9 ;13(1).

60. Handl HL, Gillies RJ. Lanthanide-based luminescent assays for ligand-receptor interactions. Life Sci. 2005 Jun 10;77(4):361–71.

61. Wei K. Développement D'Une Nouvelle Stratégie Antifongique Ciblant Un Domaine De Lecture Epigénétique U.G.A Ecole Doctorale Chimie Science Du Vivant, PhD Thesis, Grenoble, 2020 (Advisors : Petosa C, Govin J). Available from: http://www.theses.fr/2020GRALV013/document

62. Waterhouse A, Bertoni M, Bienert S, Studer G, Tauriello G, Gumienny R, et al. SWISS-MODEL: homology modelling of protein structures and complexes. Nucleic Acids Research. 2018 Jul 2;46(W1):W296–303.

63. The PyMOL Molecular Graphics System, Version 2.0 Schrödinger, LLC. 2018

64. SerialCloner 2.6.1, SerialBasics, Franck Perez, 2013

65. Kelley LA, Mezulis S, Yates CM, Wass MN, Sternberg MJE. The Phyre2 web portal for protein modeling, prediction and analysis. Nature Protocols. 2015 Jun;10(6):845–58.

66. Gasteiger E, Hoogland C, Gattiker A, Duvaud S, Wilkins MR, Appel RD, et al. Protein Identification and Analysis Tools on the ExPASy Server. In: Walker JM, editor. The Proteomics Protocols Handbook. Totowa, NJ: Humana Press; 2005. p. 571–607. (Springer Protocols Handbooks)

67. ChemDraw Ultra 9.0. CambridgeSoft, 100 CambridgePark Drive, Cambridge, MA 02140. 2005

7. APPENDICES

Appendix 1. *Candida auris* bromodomains amino acid sequences

C. auris BD1 amino acid sequence	*C. auris* BD2 amino acid sequence
IPKHQNKFALNTIKAIKRLKDAGPF LHPVDIVKLNIPFYYNFIKRPMDLS TIERKLTVNAYEDPLQIVDDFNLM VDNCIKFNGESAGISRMAKNIQAQ FEKHMLNIPPKV	KYAAELRFCNQVLKELTSKKLYSI NFPFLQPVDPVALNIPHYFDVVKN PMDLGTIQSNLANNKYENADDVE RDVRLVFSNCYLFNPEGTDVNTM GHRLESVFDKKWAQKPVPQPSPPQ S

Appendix 2. *Candida auris* bromodomains predicted 3D models superimposed on *Candida glabrata* crystal structures

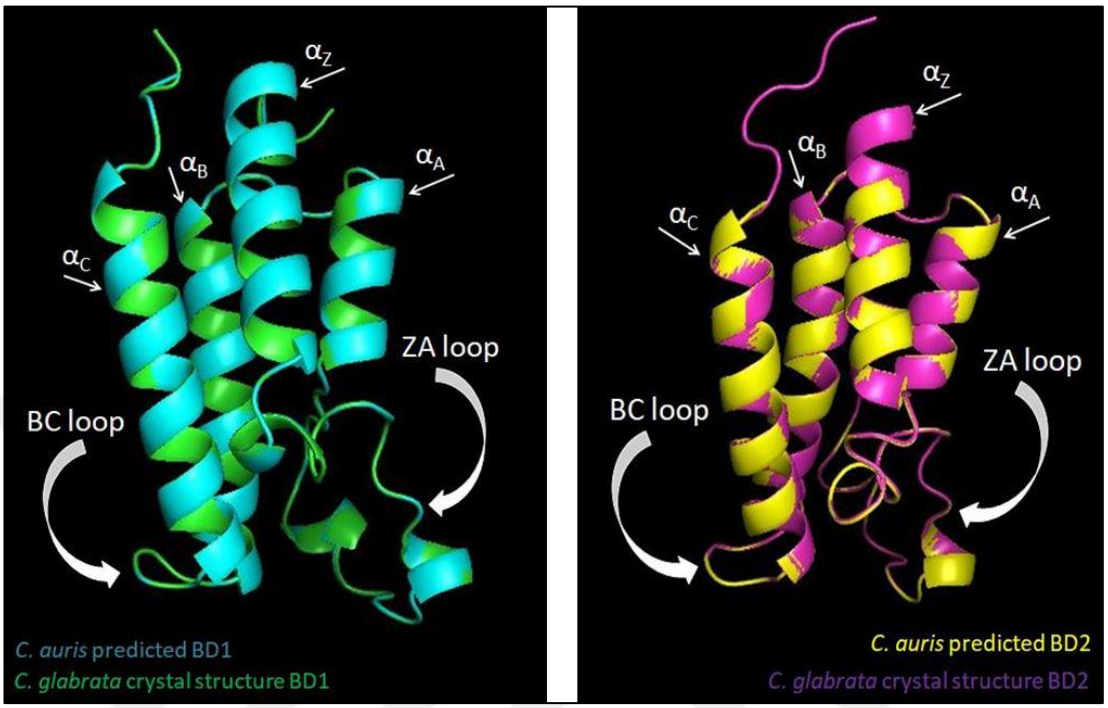

Appendix 3. *Candida glabrata Bdf1* gene amino acid sequence

Candida glabrata Bdf1 amino acid sequence
MNVELPPSPPAQEELKRSFDMVEDAVDTHEDKKLKVEESATPTSQTEEHAH TDKVIEEEKSESKVSEDKEGKEEGKEESKEAEAAEDKSEDKSEDAAETKNVV DTSNMTPAPAPPQEPDMDNLPANPIPQHQQKHALMAIKAVKRLKDARPFLQ PVDPVALNIPLYFNFIKRPMDLQTIERKLNANAYETPEQITEDFNLMVENSAK FNGPTAVITQMGRNIQAAFEKHMLNMPAKDLPQRDPLPGTKATTGRGKKKT TDSDTPVVIRRAQTHNGRPKREIHPPKSKDIYPYEMNSKPKSKSLQRAMKFC QGVVRELMSKKYASFNYPFLEPVDPVALNCPTYFDYVKEPMDLGTVSKKLS NWEYENLDQAEHDIRLIFQNCYAFNPDGTIVNMMGHRLEDIFNTKWADRPL YSDVESEEAESAYDDEESDESDVEIDETSITNPAIQYLEDQLERMKVELQQLK KQELEKIRKERRLARGPKKTRGRRGRKKGSTKAKTGRGKKKLKSVVTYDM KKIITENINDLPTAKLEKVIEIIKKSMPNIGDDEEVELDLDTLDNNTILTLYNTF FRQFEAPANDSGNDNQSVSPTNGLGRRKRSKNLSREEQSKQIEKIRNKLALL DGASPLSQNGSPVTPASFASNIQNGYSSSSSDDDSSESEEE

Appendix 4. *Candida glabrata* bromodomain constructs used for HTRF

	Construct number	*Bdf 1* amino acid sequence interval	Amino acid sequence
C. glabrata BD 1	1	111 – 248	APAPPQEPDMDNLPANPIPQHQQKHALMAIKAVKRLKDARPFLQPV DPVALNIPLYFNFIKRPMDLQTIERKLNANAYETPEQITEDFNLMVEN SAKFNGPTAVITQMGRNIQAAFEKHMLNMPAKDLPQRDPLPGTK
	2	111 – 259	APAPPQEPDMDNLPANPIPQHQQKHALMAIKAVKRLKDARPFLQPV DPVALNIPLYFNFIKRPMDLQTIERKLNANAYETPEQITEDFNLMVEN SAKFNGPTAVITQMGRNIQAAFEKHMLNMPAKDLPQRDPLPGTKAT TGRGKKKTT
	3	120 – 248	MDNLPANPIPQHQQKHALMAIKAVKRLKDARPFLQPVDPVALNIPL YFNFIKRPMDLQTIERKLNANAYETPEQITEDFNLMVENSAKFNGPT AVITQMGRNIQAAFEKHMLNMPAKDLPQRDPLPGTK
	4	120 – 259	MDNLPANPIPQHQQKHALMAIKAVKRLKDARPFLQPVDPVALNIPL YFNFIKRPMDLQTIERKLNANAYETPEQITEDFNLMVENSAKFNGPT AVITQMGRNIQAAFEKHMLNMPAKDLPQRDPLPGTKATTGRGKKK TT
	5	128 – 248	IPQHQQKHALMAIKAVKRLKDARPFLQPVDPVALNIPLYFNFIKRPM DLQTIERKLNANAYETPEQITEDFNLMVENSAKFNGPTAVITQMGRN IQAAFEKHMLNMPAKDLPQRDPLPGTK
	6	128 – 259	IPQHQQKHALMAIKAVKRLKDARPFLQPVDPVALNIPLYFNFIKRPM DLQTIERKLNANAYETPEQITEDFNLMVENSAKFNGPTAVITQMGRN IQAAFEKHMLNMPAKDLPQRDPLPGTKATTGRGKKKTT
C. glabrata BD 2	7	276 – 410	RPKREIHPPKSKDIYPYEMNSKPKSKSLQRAMKFCQGVVRELMSKK YASFNYPFLEPVDPVALNCPTYFDYVKEPMDLGTVSKKLSNWEYEN LDQAEHDIRLIFQNCYAFNPDGTIVNMMGHRLEDIFNTKWADR
	8	276 – 426	RPKREIHPPKSKDIYPYEMNSKPKSKSLQRAMKFCQGVVRELMSKK YASFNYPFLEPVDPVALNCPTYFDYVKEPMDLGTVSKKLSNWEYEN LDQAEHDIRLIFQNCYAFNPDGTIVNMMGHRLEDIFNTKWADRPLYS DVESEEAESAYD
	9	289 – 410	IYPYEMNSKPKSKSLQRAMKFCQGVVRELMSKKYASFNYPFLEPVD PVALNCPTYFDYVKEPMDLGTVSKKLSNWEYENLDQAEHDIRLIFQ NCYAFNPDGTIVNMMGHRLEDIFNTKWADR
	10	289 – 411	IYPYEMNSKPKSKSLQRAMKFCQGVVRELMSKKYASFNYPFLEPVD PVALNCPTYFDYVKEPMDLGTVSKKLSNWEYENLDQAEHDIRLIFQ NCYAFNPDGTIVNMMGHRLEDIFNTKWADRP
	11	289 – 415	IYPYEMNSKPKSKSLQRAMKFCQGVVRELMSKKYASFNYPFLEPVD PVALNCPTYFDYVKEPMDLGTVSKKLSNWEYENLDQAEHDIRLIFQ NCYAFNPDGTIVNMMGHRLEDIFNTKWADRPLYSD
	12	289 – 418	IYPYEMNSKPKSKSLQRAMKFCQGVVRELMSKKYASFNYPFLEPVD PVALNCPTYFDYVKEPMDLGTVSKKLSNWEYENLDQAEHDIRLIFQ NCYAFNPDGTIVNMMGHRLEDIFNTKWADRPLYSDVES

Appendix 5. *Candida auris* and *Candida glabrata* Bdf1 alignement

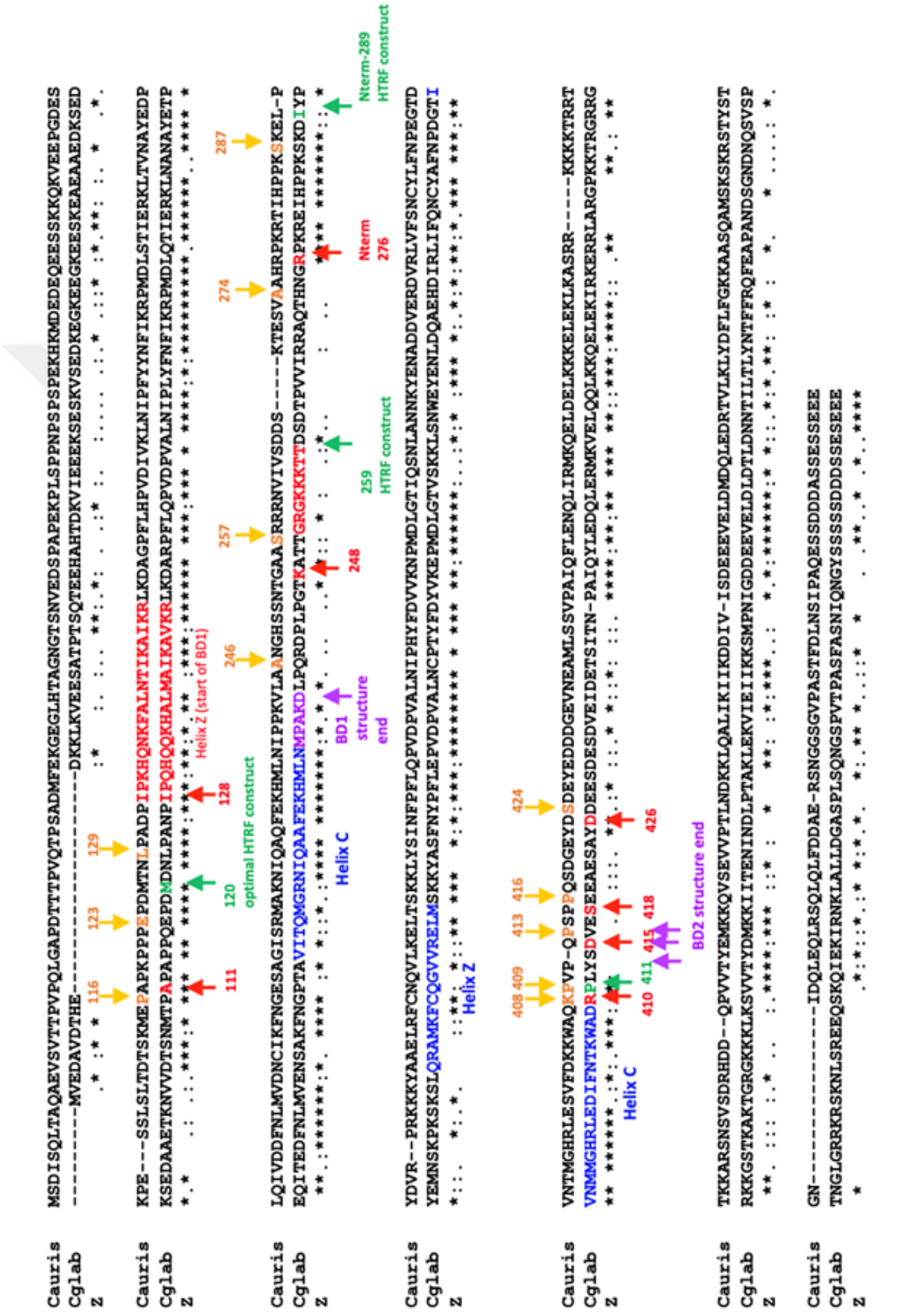

Appendix 6. *Candida glabrata* BD1 secondary structure prediction

Appendix 7. *Candida glabrata* BD2 secondary structure prediction

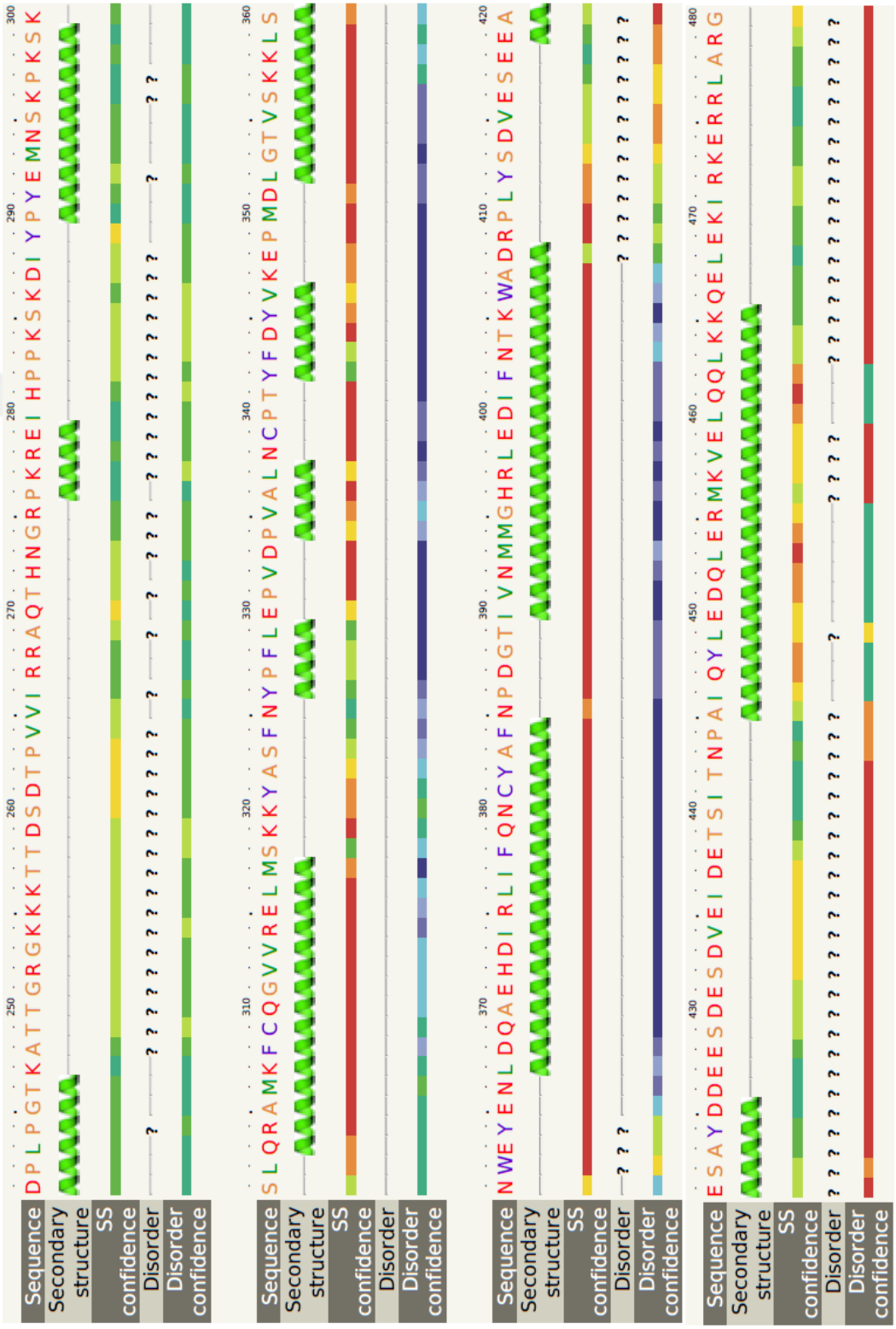

Appendix 8. *Candida auris* BD1 secondary structure prediction

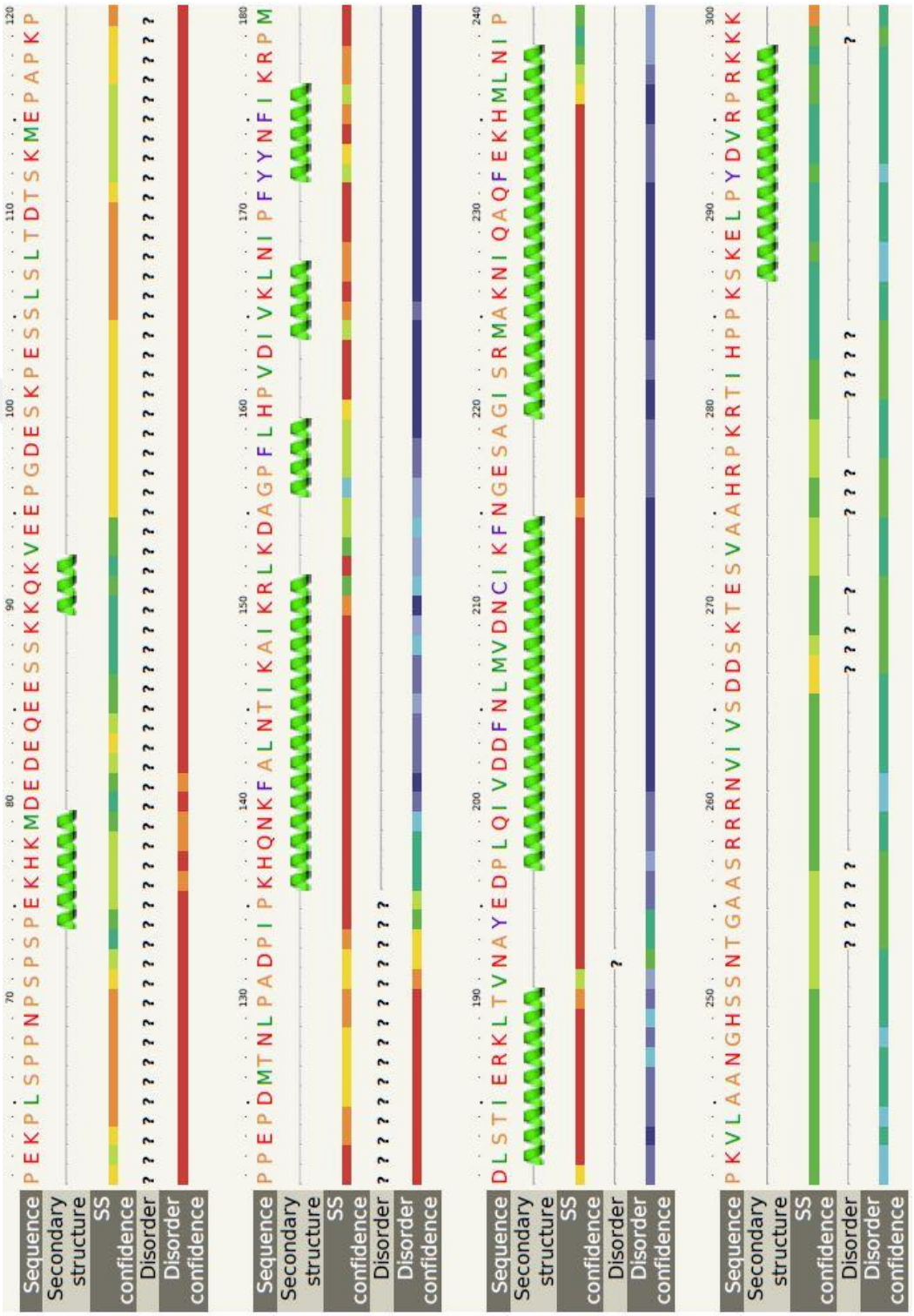

Appendix 9. *Candida auris* BD2 secondary structure prediction

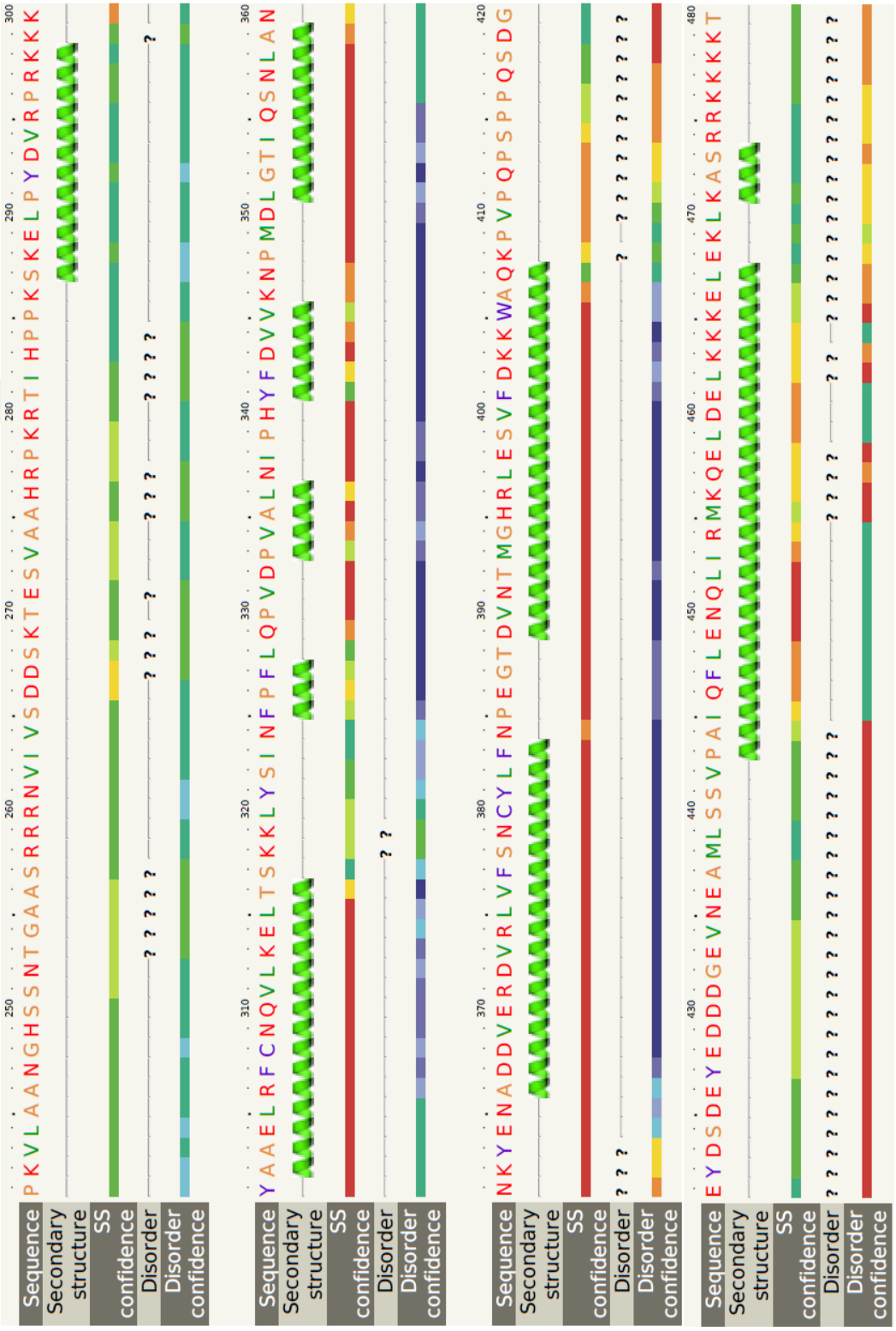

Appendix 10. *Candida auris* bromodomain constructs amino acid sequences

	1 letter pseudo code	*Bdf 1* amino acid sequence interval	Amino acid sequence
C. auris BD1	A	116 – 246	PAPKPPPEPDMTNLPADPIPKHQNKFALNTIKAIKRLKDAGPFLHP VDIVKLNIPFYYNFIKRPMDLSTIERKLTVNAYEDPLQIVDDFNLM VDNCIKFNGESAGISRMAKNIQAQFEKHMLNIPPKVLAA
	B	116 – 257	PAPKPPPEPDMTNLPADPIPKHQNKFALNTIKAIKRLKDAGPFLHP VDIVKLNIPFYYNFIKRPMDLSTIERKLTVNAYEDPLQIVDDFNLM VDNCIKFNGESAGISRMAKNIQAQFEKHMLNIPPKVLAANGHSSN TGAAS
	C	123 – 246	EPDMTNLPADPIPKHQNKFALNTIKAIKRLKDAGPFLHPVDIVKL NIPFYYNFIKRPMDLSTIERKLTVNAYEDPLQIVDDFNLMVDNCIK FNGESAGISRMAKNIQAQFEKHMLNIPPKVLAA
	D	123 – 257	EPDMTNLPADPIPKHQNKFALNTIKAIKRLKDAGPFLHPVDIVKL NIPFYYNFIKRPMDLSTIERKLTVNAYEDPLQIVDDFNLMVDNCIK FNGESAGISRMAKNIQAQFEKHMLNIPPKVLAANGHSSNTGAAS
	E	129 – 246	LPADPIPKHQNKFALNTIKAIKRLKDAGPFLHPVDIVKLNIPFYYN FIKRPMDLSTIERKLTVNAYEDPLQIVDDFNLMVDNCIKFNGESA GISRMAKNIQAQFEKHMLNIPPKVLAA
	F	129 – 257	LPADPIPKHQNKFALNTIKAIKRLKDAGPFLHPVDIVKLNIPFYYN FIKRPMDLSTIERKLTVNAYEDPLQIVDDFNLMVDNCIKFNGESA GISRMAKNIQAQFEKHMLNIPPKVLAANGHSSNTGAAS
	G	274 – 408	AAHRPKRTIHPPKSKELPYDVRPRKKKYAAELRFCNQVLKELTS KKLYSINFPFLQPVDPVALNIPHYFDVVKNPMDLGTIQSNLANNK YENADDVERDVRLVFSNCYLFNPEGTDVNTMGHRLESVFDKKW AQK
	H	287 – 408	SKELPYDVRPRKKKYAAELRFCNQVLKELTSKKLYSINFPFLQPV DPVALNIPHYFDVVKNPMDLGTIQSNLANNKYENADDVERDVR LVFSNCYLFNPEGTDVNTMGHRLESVFDKKWAQK
	I	287 – 409	SKELPYDVRPRKKKYAAELRFCNQVLKELTSKKLYSINFPFLQPV DPVALNIPHYFDVVKNPMDLGTIQSNLANNKYENADDVERDVR LVFSNCYLFNPEGTDVNTMGHRLESVFDKKWAQKP
	J	287 – 413	SKELPYDVRPRKKKYAAELRFCNQVLKELTSKKLYSINFPFLQPV DPVALNIPHYFDVVKNPMDLGTIQSNLANNKYENADDVERDVR LVFSNCYLFNPEGTDVNTMGHRLESVFDKKWAQKPVPQP
	K	287 – 416	SKELPYDVRPRKKKYAAELRFCNQVLKELTSKKLYSINFPFLQPV DPVALNIPHYFDVVKNPMDLGTIQSNLANNKYENADDVERDVR LVFSNCYLFNPEGTDVNTMGHRLESVFDKKWAQKPVPQPSPP
	L	287 – 424	SKELPYDVRPRKKKYAAELRFCNQVLKELTSKKLYSINFPFLQPV DPVALNIPHYFDVVKNPMDLGTIQSNLANNKYENADDVERDVR LVFSNCYLFNPEGTDVNTMGHRLESVFDKKWAQKPVPQPSPPQS DGEYDS

Appendix 11. *Candida auris Bdf1* nucleotide sequence

Candida auris Bdf1 nucleotide sequence
ATGTCTGACATTTCTCAACTGACTGCTCAAGCTGAAGTGTCTGTGACGACGCCAG
TTCCACAGCTGGGAGCTCCGGATACCACGACGCCGGTGCAAACACCGTCGGCAG
ATATGTTTGAGAAGGGAGAAGGACTGCACACCGCTGGAAACGGCACCTCAAAT
GTCGAAGATTCTCCCGCTCCTGAAAAGCCTTTGTCCCCACCAAACCCCTCCCCTT
CCCCCGAGAAGCACAAGATGGATGAGGATGAACAGGAAGAGAGCTCAAAAAAG
CAAAAGGTTGAAGAACCTGGAGATGAGTCCAAGCCAGAGTCTAGCTTATCCCTG
ACGGATACGTCGAAGATGGAACCTGCACCTAAGCCACCTCCAGAACCAGACATG
ACGAATCTCCCTGCGGACCCTATCCCTAAGCACCAGAACAAGTTTGCTCTCAATA
CGATCAAGGCTATCAAGCGTTTAAAGGATGCCGGCCCATTTCTCCATCCAGTCG
ACATCGTGAAGTTGAACATCCCTTTTTATTACAACTTCATTAAGAGACCAATGGA
CCTTTCCACCATTGAGAGGAAACTCACAGTTAACGCATACGAAGACCCTCTGCA
AATTGTTGACGACTTCAACCTCATGGTTGACAACTGCATTAAGTTCAACGGTGAA
TCAGCTGGTATATCCAGAATGGCAAAAAATATCCAGGCCCAGTTTGAGAAGCAT
ATGTTGAACATACCTCCCAAGGTTCTTGCTGCCAATGGGCACTCTTCGAACACTG
GTGCTGCATCGAGAAGACGCAATGTTATTGTGAGTGATGACTCGAAGACTGAAT
CTGTGGCTGCTCATAGGCCAAAGAGAACGATCCACCCACCAAAGTCAAAGGAAT
TGCCATATGATGTGAGGCCAAGAAAGAAGAAGTATGCAGCTGAGTTGCGCTTCT
GCAACCAGGTACTTAAAGAGTTGACATCCAAAAAGCTTTACAGCATCAACTTCC
CCTTCTTACAACCAGTTGATCCAGTTGCATTGAACATTCCTCACTACTTCGATGT
GGTGAAGAACCCAATGGATCTCGGGACTATTCAATCCAATCTTGCAAACAACAA
GTATGAGAATGCTGATGATGTTGAGCGAGACGTGAGATTGGTGTTCTCAAACTG
TTACTTGTTTAACCCAGAAGGTACTGATGTTAACACTATGGGACACCGCCTTGAA
AGTGTGTTCGACAAGAAATGGGCTCAAAAGCCTGTCCCACAACCTTCGCCTCCT
CAGTCTGATGGCGAGTACGATAGTGACGAGTACGAGGATGATGATGGTGAGGTC
AATGAAGCCATGTTGTCCAGTGTTCCAGCTATCCAGTTTTTGGAGAATCAGCTCA
TCAGAATGAAGCAGGAGCTCGATGAGTTGAAAAAGAAGGAACTTGAGAAGTTG
AAGGCCTCTCGCAGAAAGAAGAAGAAGACAAGGAGAACAACAAAGAAGGCCA
GATCTAACTCCGTCTCGGATCGTCATGACGATCAGCCTGTTGTGACGTACGAGAT
GAAAAAACAGGTGAGTGAGGTTGTTCCTACGTTGAATGACAAGAAGTTGCAAGC
ATTAATCAAAATCATCAAGGATGATATTGTCATCAGCGATGAAGAAGAAGTTGA
GCTCGATATGGATCAGCTTGAAGACCGTACCGTGTTGAAGCTTTACGATTTCTTG
TTTGGTAAGAAGGCTGCGTCGCAAGCGATGAGCAAGAGCAAGAGATCCACTTAT
TCTACCGGCAATATTGACCAGCTCGAGCAGTTAAGATCACAACTCCAGTTGTTTG
ATGACGCTGAAAGATCAAACGGAGGTTCGGGTGTTCCCGCCTCCACGTTCGACC
TCAATAGTATTCCTGCACAGGAGTCGTCTGACGATGATGCATCTTCAGAGTCCTC
GGAGGAGGAATAG

Appendix 12. *Candida auris* bromodomain constructs amplified by PCR and cloned into pJET

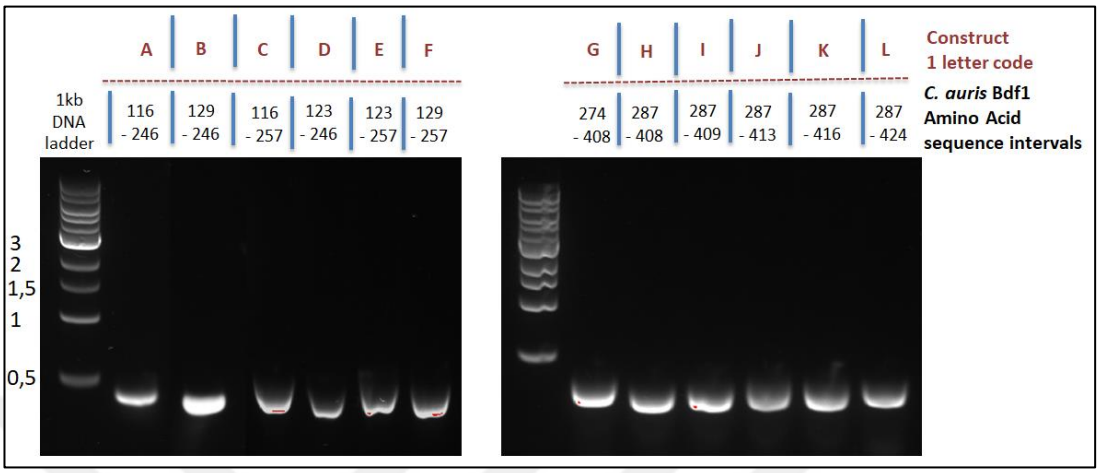

Figure 24. *C. auris* BD1 and BD2 constructs amplified with PCR

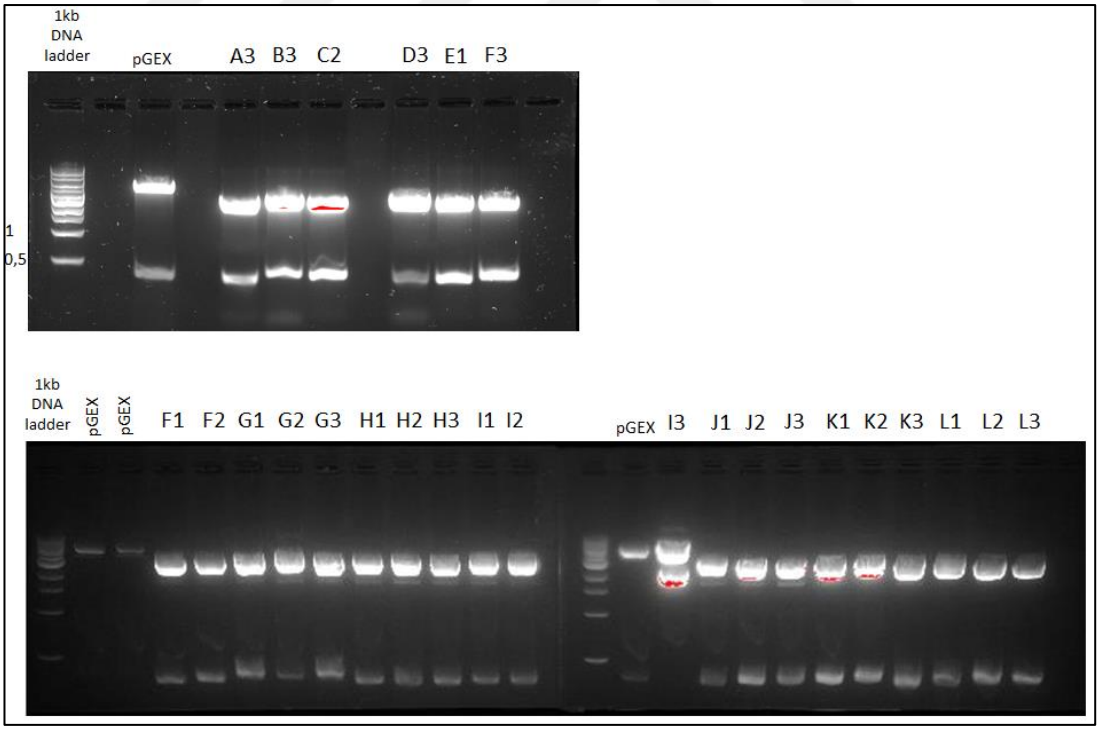

Figure 25. *C. auris* BD constructs isolated and digested from pJET then run on agarose gel

Appendix 13. *Candida auris* bromodomain constructs cloned and digested from pGEX

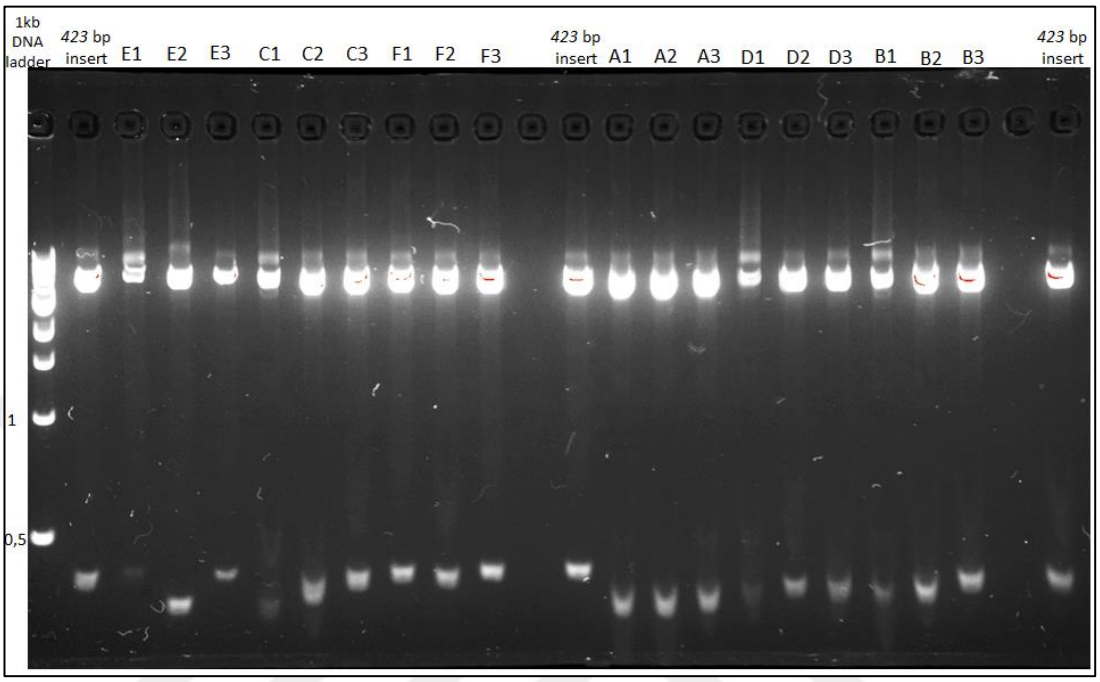

Figure 26. *C. auris* BD1 constructs isolated and digested from pGEX

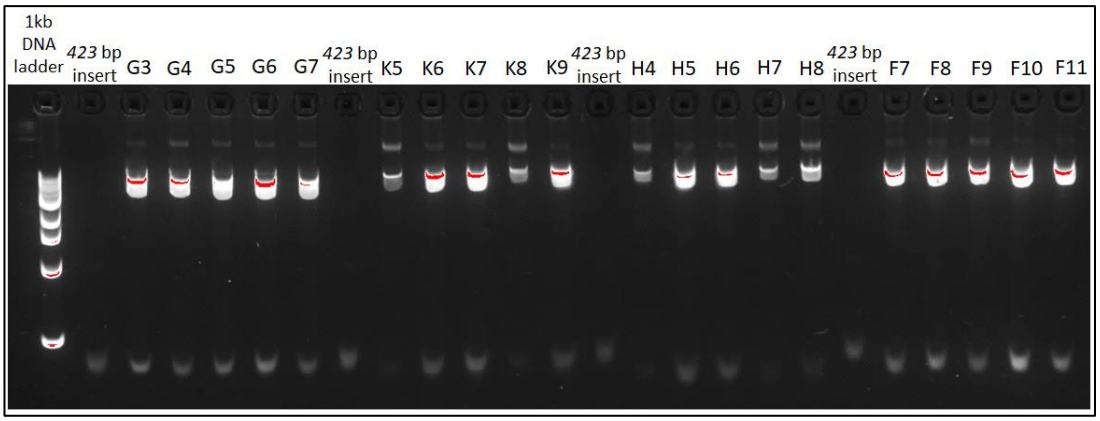

Figure 27. *C. auris* BD2 constructs isolated and digested from pGEX

Appendix 14. GST nucleotide sequence

GST nucleotide sequence
ATGTCCCCTATACTAGGTTATTGGAAAATTAAGGGCCTTGTGCAACCCAC TCGACTTCTTTTGGAATATCTTGAAGAAAAATATGAAGAGCATTTGTATG AGCGCGATGAAGGTGATAAATGGCGAAACAAAAAGTTTGAATTGGGTTT GGAGTTTCCCAATCTTCCTTATTATATTGATGGTGATGTTAAATTAACACA GTCTATGGCCATCATACGTTATATAGCTGACAAGCACAACATGTTGGGTG GTTGTCCAAAAGAGCGTGCAGAGATTTCAATGCTTGAAGGAGCGGTTTTG GATATTAGATACGGTGTTTCGAGAATTGCATATAGTAAAGACTTTGAAAC TCTCAAAGTTGATTTTCTTAGCAAGCTACCTGAAATGCTGAAAATGTTCG AAGATCGTTTATGTCATAAAACATATTTAAATGGTGATCATGTAACCCAT CCTGACTTCATGTTGTATGACGCTCTTGATGTTGTTTTATACATGGACCCA ATGTGCCTGGATGCGTTCCCAAAATTAGTTTGTTTTAAAAAACGTATTGA AGCTATCCCACAAATTGATAAGTACTTGAAATCCAGCAAGTATATAGCAT GGCCTTTGCAGGGCTGGCAAGCCACGTTTGGTGGTGGCGACCATCCTCCA AAA

Appendix 15. *Candida auris* BD1 construct (116-246) sequencing result

Sequence of *C. auris* bromodomain construct A
NNNCGGAATCCTCAAATCGGATCTGGTTCCGCGTGGATCCCCTGCACCTAAGCCACCTCCAGAACC AGACATGACGAATCTCCCTGCGGACCCTATCCCTAAGCACCAGAACAAGTTTGCTCTCAATACGATC AAGGCTATCAAGCGTTTAAAGGATGCCGGCCCATTTCTCCATCCAGTCGACATCGTGAAGTTGAACA TCCCTTTTTATTACAACTTCATTAAGAGACCAATGGACCTTTCCACCATTGAGAGGAAACTCACAGT TAACGCATACGAAGACCCTCTGCAAATTGTTGACGACTTCAACCTCATGGTTGACAACTGCATTAAG TTCAACGGTGAATCAGCTGGTATATCCAGAATGGCAAAAAATATCCAGGCCCAGTTTGAGAAGCAT ATGTTGAACATACCTCCCAAGGTTCTTGCTGCCTAACTCGAGCGGCCGCATCGCGACTGACTGACGA TCTGCCTCGCGCGTTTCGGTGATGACGGTGAAAACCTCTGACACATGCAGCTCCCGGAGACGGTCA CAGCTTGTCTGTAAGCGGATGCCGGGAGCAGACAAGCCCGTCAGGGCGCGTCAGCGGGTGTTGGCG GGTGTCGGGGCGCAGCCATGACCCAGTCACGTAGCGATAGCGGAGTGTATAATTCTTGAAGACGAA AGGGCCTCGTGATACGCCTATTTTTATAGGTTAATGTCATGATAATAATGGTTTCTTAGACGTCAGG TGGCACTTTTCGGGGAAATGTGCGCGGAACCCCTATTTGTTTATTTTTCTAAATACATTCAAATATGT ATCCGCTCATGAGACAATAACCCTGATAAATGCTTCAATAATATTGAAAAAGGAAGAGTATGAGTA TTCAACATTTCCGTGTCGCCCTTATTCCCTTTTTTGCGGCATTTTGCCTTCCTGTTTTTGCTCACCCAG AAACGCTGGTGAAAGTAAAAGATGCTGAAGATCAGTTGGGTGCACGAGTGGGTTACATCGAACTGG ATCTCAACAGCGGTAAGATCCTTGAGAGTTTTCGCCCCGAAGAACGTTTTCCAATGATGAGCACTTT TAAAGTTCTGCTATGTGGCGCGGTATTATCCCGTGTTGACGCCGGGCAAGAGCAACTCGGTCGCCGC ATACACTATTCTCAGAATGACTTGGTTGAGTACTCACCAGTCACAGAAAAGCATCTTACGGATGGCA TGACAGTAAGAGAATTATGCAGGGCTGCCTAACCATGAATGAAAACCTGCGGCCACTTACTTTTGA ACACGATCGGAGGACCAAAGGAACTAACCNNTTTTTTTCCCNNNNAGGGGGAATCNTAANNCCCTT TTTTTTTGGGAAACGGAATTAAGAAAANCTCAAAANNNGAGGGGACCCCCNGCCCGGNAGGGAAA CNGTGGCGANNNTATGGGGAAAATTTTCTCTTCCCGAAAAAAANNNAAGGGGGGNNANAAAATAA NNNACCCCTCCCCCCCCCNNNGGNNNGNTTTANAAAAAAAGGCNNGGNGGGGCCCCTTTTTCCGGGG GAGAANNCNCCCTNNATTAAAGGGANNGAGAA

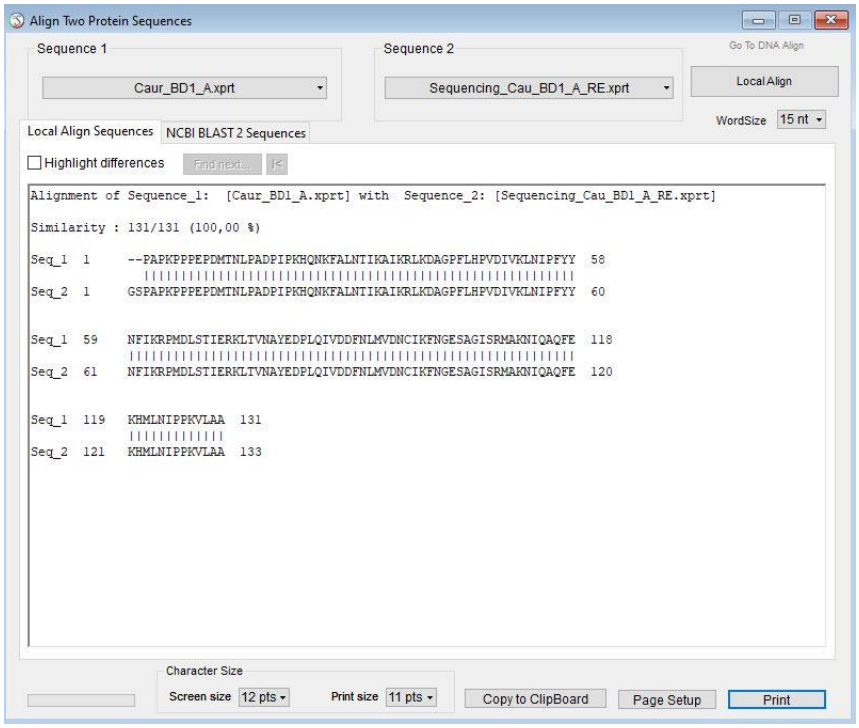

Appendix 16. *Candida auris* BD1 construct (116-257) sequencing result

Sequence of *C. auris* bromodomain construct B

NNNNNNATCTCAAATCGGATCTGGTTCCGCGTGGATCCCCTGCACCTAAGCCACCTCCAGAACCAG
ACATGACGAATCTCCCTGCGGACCCTATCCCTAAGCACCAGAACAAGTTTGCTCTCAATACGATCAA
GGCTATCAAGCGTTTAAAGGATGCCGGCCCATTTCTCCATCCAGTCGACATCGTGAAGTTGAACATC
CCTTTTTATTACAACTTCATTAAGAGACCAATGGACCTTTCCACCATTGAGAGGAAACTCACAGTTA
ACGCATACGAAGACCCTCTGCAAATTGTTGACGACTTCAACCTCATGGTTGACAACTGCATTAAGTT
CAACGGTGAATCAGCTGGTATATCCAGAATGGCAAAAAATATCCAGGCCCAGTTTGAGAAGCATAT
GTTGAACATACCTCCCAAGGTTCTTGCTGCCAATGGGCACTCTTCGAACACTGGTGCTGCATCGTAA
CTCGAGCGGCCGCATCGCGACTGACTGACGATCTGCCTCGCGCGTTTCGGTGATGACGGTGAAAAC
CTCTGACACATGCAGCTCCCGGAGACGGTCACAGCTTGTCTGTAAGCGGATGCCGGGAGCAGACAA
GCCCGTCAGGGCGCGTCAGCGGGTGTTGGCGGGTGTCGGGGCGCAGCCATGACCCAGTCACGTAGC
GATAGCGGAGTGTATAATTCTTGAAGACGAAAGGGCCTCGTGATACGCCTATTTTTATAGGTTAATG
TCATGATAATAATGGTTTCTTAGACGTCAGGTGGCACTTTTCGGGGAAATGTGCGCGGAACCCCTAT
TTGTTTATTTTTCTAAATACATTCAAATATGTATCCGCTCATGAGACAATAACCCTGATAAATGCTTC
AATAATATTGAAAAAGGAAGAGTATGAGTATTCAACATTTCCGTGTCGCCCTTATTCCCTTTTTTGC
GGCATTTTGCCTTCCTGTTTTTGCTCACCCAGAAACGCTGGTGAAAGTAAAAGATGCTGAAGATCAG
TTGGGTGCACGAGTGGGTTACATCGAACTGGATCTCAACAGCGGTAAGATCCTTGAGAGTTTTCGCC
CCGAAGAACGTTTTCCAATGATGAGCACTTTTAAAGTTCTGCTATGTGGCGCGGTATTATCCCGGGT
TGACGCCGGGCAAGAGCAACTCGGTCGCCGCATACCCAATTCTCAGAATGACTTGGTTGAGTACTC
ACCAGTCCCAGAAAAACTTCTTACGGAGGNANGAAAAAAAAAAAATTTGGCGGGGCGNCCAAANA
GGGNGAAAACCNGGGGCAATTNNNTTGAAAAAAATGGGGGAAAAAAAAAACAACCCTTTTTTTAA
AAAGGGGGAAATTNNNNCCCCTTTTTTTGGGAACGAAGAAAAAAAAACCAAAAAAAAAAGGGACC
CCGGTGGGAAGGGAAATTTCCAAATAAGGGGAACTTTCTTCCCNNNAAAAAAAANNGGGGAAAAA
AGANACCCCCCCCCCCCCGGGGTTTTAAAAAAAAGGGGGGGGTCCTTTATGC

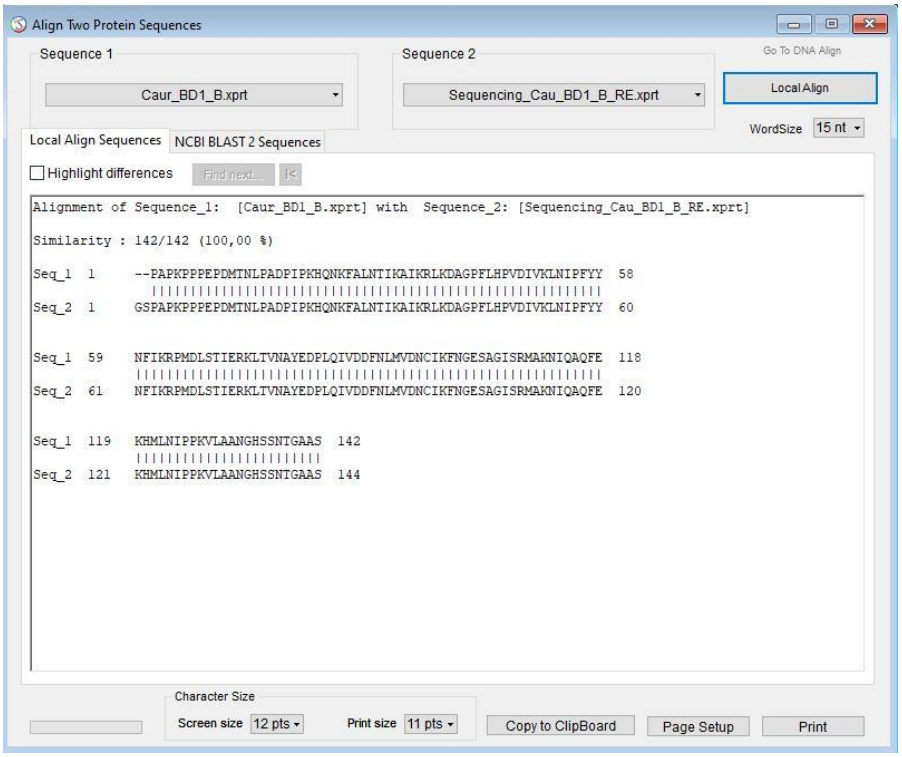

Appendix 17. *Candida auris* BD1 construct (123-246) sequencing result

Sequence of *C. auris* bromodomain construct C
NNNNGCATCCTCAAATCGGATCTGGTTCCGCGTGGATCCGAACCAGACATGACGAATCTCCCTGCG GACCCTATCCCTAAGCACCAGAACAAGTTTGCTCTCAATACGATCAAGGCTATCAAGCGTTTAAAG GATGCCGGCCCATTTCTCCATCCAGTCGACATCGTGAAGTTGAACATCCCTTTTTATTACAACTTCAT TAAGAGACCAATGGACCTTTCCACCATTGAGAGGAAACTCACAGTTAACGCATACGAAGACCCTCT GCAAATTGTTGACGACTTCAACCTCATGGTTGACAACTGCATTAAGTTCAACGGTGAATCAGCTGGT ATATCCAGAATGGCAAAAAATATCCAGGCCCAGTTTGAGAAGCATATGTTGAACATACCTCCCAAG GTTCTTGCTGCCTAACTCGAGCGGCCGCATCGCGACTGACTGACGATCTGCCTCGCGCGTTTCGGTG ATGACGGTGAAAACCTCTGACACATGCAGCTCCCGGAGACGGTCACAGCTTGTCTGTAAGCGGATG CCGGGAGCAGACAAGCCCGTCAGGGCGCGTCAGCGGGTGTTGGCGGGTGTCGGGGCGCAGCCATG ACCCAGTCACGTAGCGATAGCGGAGTGTATAATTCTTGAAGACGAAAGGGCCTCGTGATACGCCTA TTTTTATAGGTTAATGTCATGATAATAATGGTTTCTTAGACGTCAGGTGGCACTTTTCGGGGAAATG TGCGCGGAACCCCTATTTGTTTATTTTTCTAAATACATTCAAATATGTATCCGCTCATGAGACAATAA CCCTGATAAATGCTTCAATAATATTGAAAAAGGAAGAGTATGAGTATTCAACATTTCCGTGTCGCCC TTATTCCCTTTTTTGCGGCATTTTGCCTTCCTGTTTTTGCTCACCCAGAAACGCTGGTGAAAGTAAAA GATGCTGAAGATCAGTTGGGTGCACGAGTGGGTTACATCGAACTGGATCTCAACAGCGGTAAGATC CTTGAGAGTTTTCGCCCGGAAGAACGTTTTCCAATGATGAGCACTTTTAAAGTTCTGCTATGTGGCG CGGTATTATCCCGTGTTGACGCCGGGCAAGAGCAACTCGGTCGCCGCATACCTATTCTCAGAAGGA CTTGGGTGAGTACTCCCCCGTCNNAGAAAAGCATCTTACGGATGGCNTGACAGTAAGAAAATATGC AGGGNTGCCTAAACCANGAGTGGAAACATGGCGGCCAATTTTTTCTGAAAACATCGGAGGACCCAA AGAAATATACCCCTTTTTGCGATAATGGGGGATANATTAATCCTCTTTTACTT

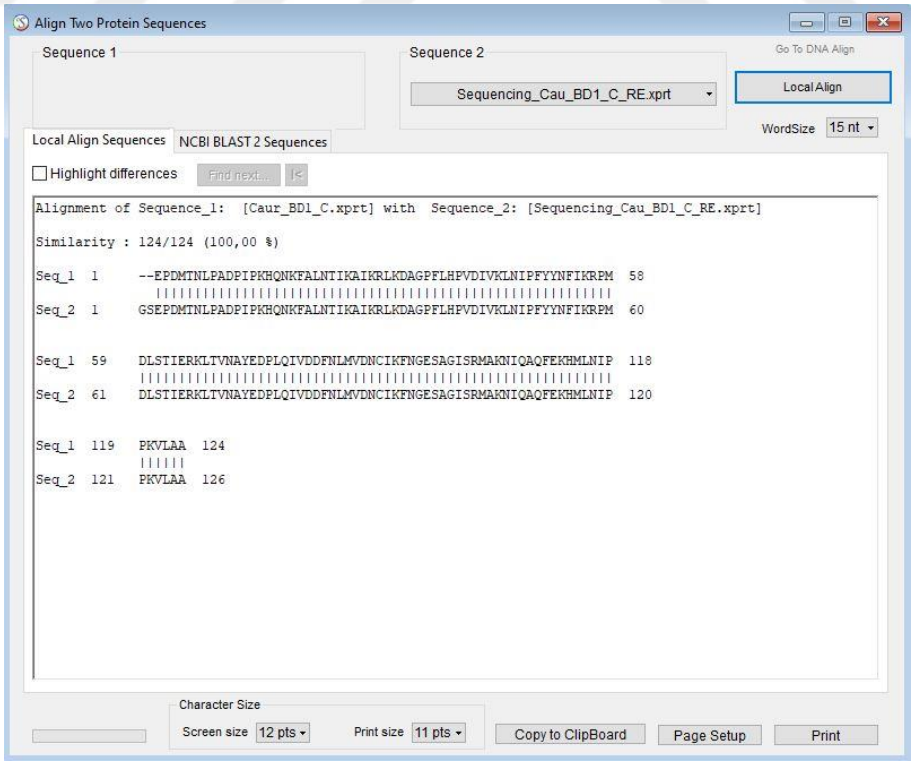

Appendix 18. *Candida auris* BD1 construct (123-257) sequencing result

Sequence of *C. auris* bromodomain construct D

NNNNNNATCTCAAATCGGATCTGGTTCCGCGTGGATCCGAACCAGACATGACGAATCTCCCTGCGG
ACCCTATCCCTAAGCACCAGAACAAGTTTGCTCTCAATACGATCAAGGCTATCAAGCGTTTAAAGG
ATGCCGGCCCATTTCTCCATCCAGTCGACATCGTGAAGTTGAACATCCCTTTTTATTACAACTTCATT
AAGAGACCAATGGACCTTTCCACCATTGAGAGGAAACTCACAGTTAACGCATACGAAGACCCTCTG
CAAATTGTTGACGACTTCAACCTCATGGTTGACAACTGCATTAAGTTCAACGGTGAATCAGCTGGTA
TATCCAGAATGGCAAAAAATATCCAGGCCCAGTTTGAGAAGCATATGTTGAACATACCTCCCAAGG
TTCTTGCTGCCAATGGGCACTCTTCGAACACTGGTGCTGCATCGTAACTCGAGCGGCCGCATCGCGA
CTGACTGACGATCTGCCTCGCGCGTTTCGGTGATGACGGTGAAAACCTCTGACACATGCAGCTCCCG
GAGACGGTCACAGCTTGTCTGTAAGCGGATGCCGGGAGCAGACAAGCCCGTCAGGGCGCGTCAGC
GGGTGTTGGCGGGTGTCGGGGCGCAGCCATGACCCAGTCACGTAGCGATAGCGGAGTGTATAATTC
TTGAAGACGAAAGGGCCTCGTGATACGCCTATTTTTATAGGTTAATGTCATGATAATAATGGTTTCT
TAGACGTCAGGTGGCACTTTTCGGGGAAATGTGCGCGGAACCCCTATTTGTTTATTTTTCTAAATAC
ATTCAAATATGTATCCGCTCATGAGACAATAACCCTGATAAATGCTTCAATAATATTGAAAAAGGA
AGAGTATGAGTATTCAACATTTCCGTGTCGCCCTTATTCCCTTTTTTGCGGCATTTTGCCTTCCTGTTT
TTGCTCACCCAGAAACGCTGGTGAAAGTAAAAGATGCTGAAGATCAGTTGGGTGCACGAGTGGGTT
ACATCGAACTGGATCTCAACAGCGGTAAGATCCTTGAGAGTTTTCGCCCCGAAGAACGTTTTCCAAT
GATGAGCACTTTTAAAGTTCTGCTATGTGGCGCGGTATTATCCCGTGTTGACGCCGGGCAAGAGCAA
CTCGGTCGCCGCATACACTATTCTCAGAATGACTTGGTTGAGTACTCACCAGTCCCGAAAAGCATCT
TACGGATGGCATGACAGTAAGAGAATTTGCAGGGCTGCCAAACCATGNGTGAAAACCTGNGGCCA
ATTNTNTTGAAAACAANCGGGGGACCAAAGGAATCACCTTTTTTTCCAANNGGGGGAATTTAAACC
CCTTTTTTGGGAACGGATAAAAAACCTCCAAAAAAAGGGNACCCCGTCCGGGAGGGGAAANNTGG
AAAAATAATGGGGAAATTTTTTTCCCCCCCCAAAAAAAAAAGGGGGGGGGAGAAAAAAGGACCCC
CCCCCC

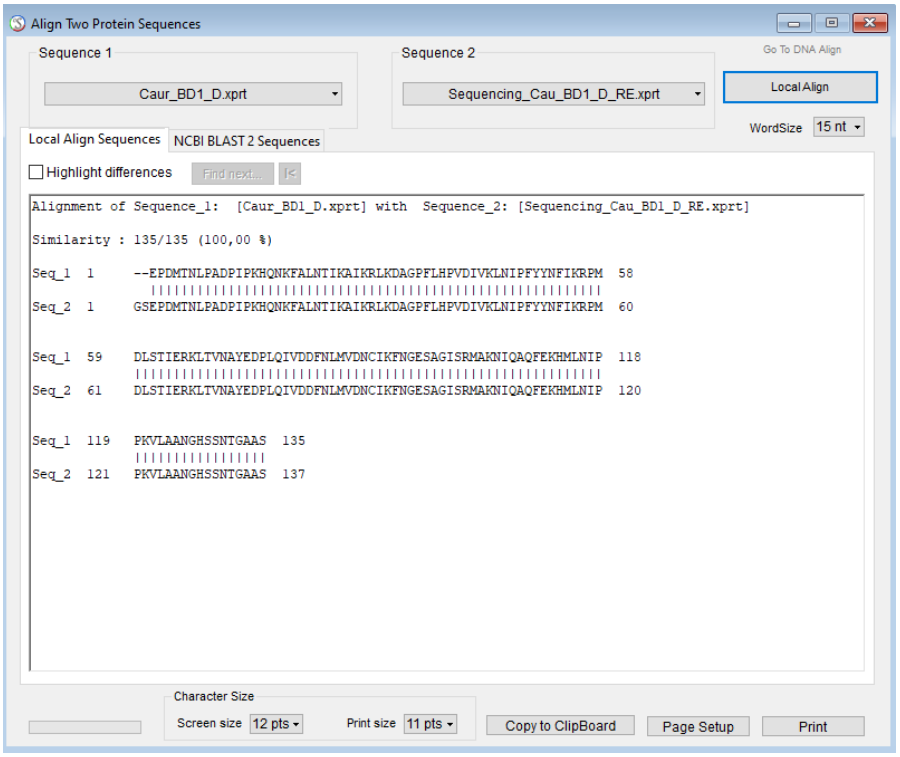

Appendix 19. *Candida auris* BD1 construct (129-246) sequencing result

Sequence of *C. auris* bromodomain construct E

AATCGGGATCTGGGTTCCGCGTGGATCCCTCCCTGCGGACCCTATCCCTAAGCACCAGAACAAGTTT
GCTCTCAATACGATCAAGGCTATCAAGCGTTTAAAGGATGCCGGCCCATTTCTCCATCCAGTCGACA
TCGTGAAGTTGAACATCCCTTTTTATTACAACTTCATTAAGAGACCAATGGACCTTTCCACCATTGA
GAGGAAACTCACAGTTAACGCATACGAAGACCCTCTGCAAATTGTTGACGACTTCAACCTCATGGTT
GACAACTGCATTAAGTTCAACGGTGAATCAGCTGGTATATCCAGAATGGCAAAAAATATCCAGGCC
CAGTTTGAGAAGCATATGTTGAACATACCTCCCAAGGTTCTTGCTGCCTAACTCGAGTTTTTCAGCA
AGATCCGCGTGGATCCCTCCCTGCGGACCCTATCCCTAAGCACCAGAACAAGTTTGCTCTCAATACG
ATCAAGGCTATCAAGCGTTTAAAGGATGCCGGCCCATTTCTCCATCCAGTCGACATCGTGAAGTTGA
ACATCCCTTTTTATTACAACTTCATTAAGAGACCAATGGACCTTTCCACCATTGAGAGGAAACTCAC
AGTTAACGCATACGAAGACCCTCTGCAAATTGTTGACGACTTCAACCTCATGGTTGACAACTGCATT
AAGTTCAACGGTGAATCAGCTGGTATATCCAGAATGGCAAAAAATATCCAGGCCCAGTTTGAGAAG
CATATGTTGAACATACCTCCCAAGGTTCTTGCTGCCTAACTCGAGCGGCCGCATCGCGACTGACTGA
CGATCTGCCTCGCGCGTTTCGGTGATGACGGTGAAAACCTCTGACACATGCAGCTCCCGGAGACGG
TCACAGCTTGTCTGTAAGCGGATGCCGGGAGCAGACAAGCCCGTCAGGGCGCGTCAGCGGGTGTTG
GCGGGTGTCGGGGCGCAGCCATGACCCAGTCACGTAGCGATAGCGGAGTGTATAATTCTTGAAGAC
GAAAGGGCCTCGTGATACGCCTATTTTTATAGGTTAATGTCATGATAATAATGGTTTCTTAGACGTC
AGGTGGCACTTTTCGGGGAAATGTGCGCGGAACCCCTATTTGTTTATTTTTCTAAATACATTCAAAT
ATGTATCCGCTCATGAAACAATAACCCTGATAAATGCTTCAATAATATTGAAAAAGGAAGANTTGA
NTTTTCAAAATTTCCGGGTCGCCCTTATTCCCTTTTTTGCGGCATTTTGCCTTCCTTTTTNNCCCCCCC
AAAACNNGGGGAAAAAAAAAAAGGGGAAAAAANNATTTGGGGGCCAAAGGGGGTAAACCAAGGG
ATTCAAAGGGAAAAATTTTGAAATTTTCCCCCCAAAAAATTTTTAAGAGGAGAATTTTTAATTTTTT
GGGGGGCGGGTAATTCCGGGGGCCCGGCNAAAAACACGCCNGCCAACATTNNNNNAGGTTGNNNA
T

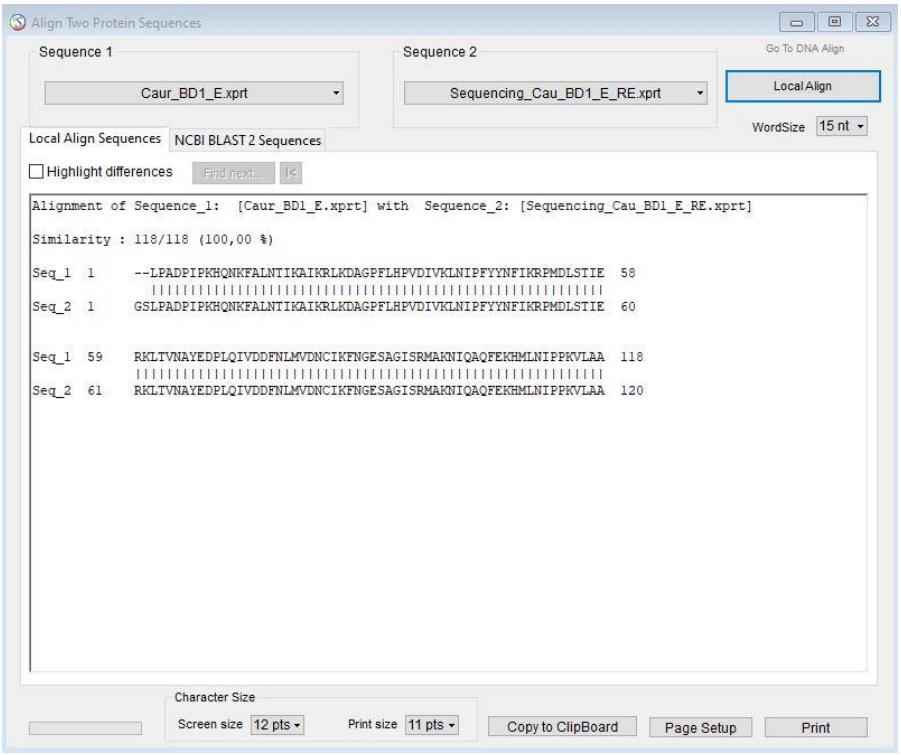

Appendix 20. *Candida auris* BD1 construct (129-257) sequencing result

Sequence of *C. auris* bromodomain construct F

TCCGAAACGCGCGAGGCAGATCGTCAGTCAGTCGCGATGCGGCCGCTCGAGTTACGATGCAGCACC
AGTGTTCGAAGAGTGCCCATTGGCAGCAAGAACCTTGGGAGGTATGTTCAACATATGCTTCTCAAA
CTGGGCCTGGATATTTTTTGCCATTCTGGATATACCAGCTGATTCACCGTTGAACTTAATGCAGTTGT
CAACCATGAGGTTGAAGTCGTCAACAATTTGCAGAGGGTCTTCGTATGCGTTAACTGTGAGTTTCCT
CTCAATGGTGGAAAGGTCCATTGGTCTCTTAATGAAGTTGTAATAAAAAGGGATGTTCAACTTCACG
ATGTCGACTGGATGGAGAAATGGGCCGGCATCCTTTAAACGCTTGATAGCCTTGATCGTATTGAGA
GCAAACTTGTTCTGGTGCTTAGGGATAGGGTCCGCAGGGAGGGATCCACGCGGAACCAGATCCGAT
TTTGGAGGATGGTCGCCACCACCAAACGTGGCTTGCCAGCCCTGCAAAGGCCATGCTATATACTTGC
TGGATTTCAAGTACTTATCAATTTGTGGGATAGCTTCAATACGTTTTTTAAAACAAACTAATTTTGGG
AACGCATCCAGGCACATTGGGTCCATGTATAAAACAACATCAAGAGCGTCATACAACATGAAGTCA
GGATGGGTTACATGATCACCATTTAAATATGTTTTATGACATAAACGATCTTCGAACATTTTCAGCA
TTTCAGGTAGCTTGCTAAGAAAATCAACTTTGAGAGTTTCAAAGTCTTTACTATATGCAATTCTCGA
AACACCGTATCTAATATCCAAAACCGCTCCTTCAAGCATTGAAATCTCTGCACGCTCTTTTGGACAA
CCACCCAACATGTTGTGCTTGTCAGCTATATAACGTATGATGGCCATAGACTGTGTTAATTTAACAT
CACCATCAATATAATAAGGAAGATTGGGAAACTCCAAACCCAATTCAAACTTTTTGTTTCGCCATTT
ATCACCTTCATCGCGCTCATACAAATGCTCTTCATATTTTTCTTCAAGATATTCCAAAAGAAGTCGA
GTGGGTTGCACAAGGCCCTTAATTTTCCAATAACCTAGTATAGGGGACATGAATACTGTTTCCTGTG
TGAAATTGTTATCCGCTCACAATTCCACAATTATACGAGCCGATGATTAATTGTCAACAGCTCATTT
CAGATATTTGCCAGAACCGTTNNGANGTCGGCGNNAAAAACTTTATCCAGAAGGGAATGCCCCTTG
AGCGAACCGAATTTGGCGGGGATTTCAACCTGCCACCCCAACCCANCTTCCCAAGGGGGCCGAGAC
CCCAAAAATTGGGCCCCCGGGGAANNNAAANNNATTCCCACCCCCNNAAAAAANNTCCTTGGCNN
NTNTCTGACCCCGNTTTTTCAAACAAATAAATTGGGACAGGNNNNNACACGNCCATNATATTTC

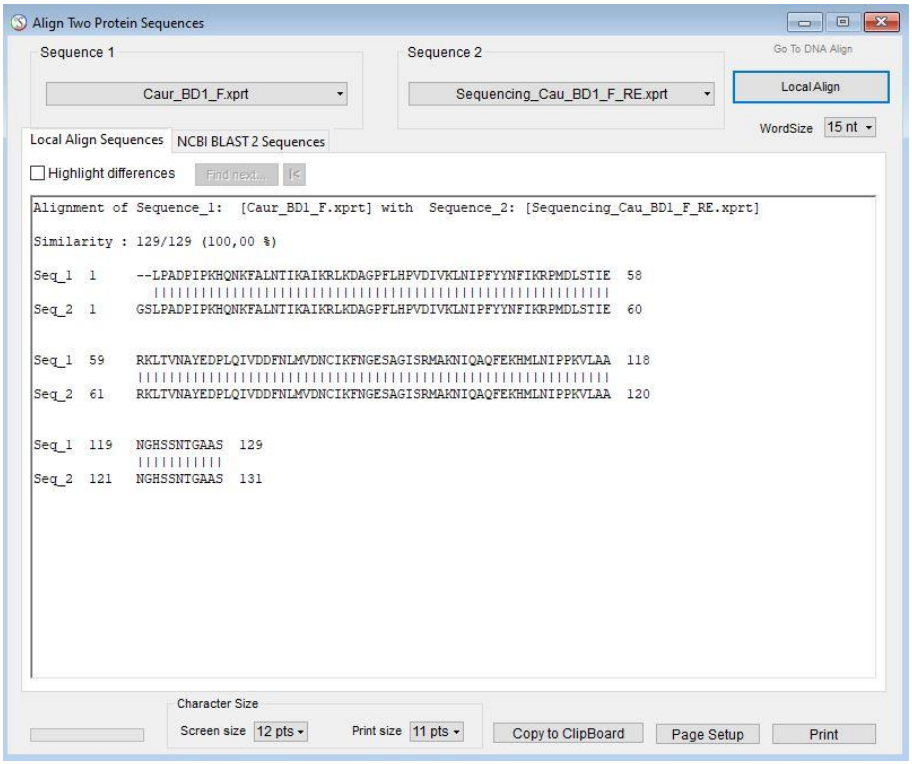

Appendix 21. *Candida auris* BD2 construct (274-408) sequencing result

Sequence of *C. auris* bromodomain construct G
TCCGAACGCGCGAGGCAGATCGTCAGTCAGTCGCGATGCGCGCCGCTCGAGTTACTTTTGAGCCCA TTTCTTGTCGAACACACTTTCAAGGCGGTGTCCCATAGTGTTAACATCAGTACCTTCTGGGTTAAAC AAATAACAGTTTGAGAACACCATTCTCACGTCTCGCTCAACATCATCAGCATTCTCATACTTGTTGTT TGCAAGATTGGATTGAATAGTCCCGAGATCCATTGGGTTCTTCACCACATCGAAGTAGTGAGGAAT GTTCAATGCGACTGGATCAACTGGTTGTAAGAAGGGGAAGTTGATGCTGTAAAGCTTTTTGGATGTC AACTCTTTAAGTACCTGGTTGCAGAAGCGCAACTCAGCTGCATACTTCTTCTTTCTTGGTCTCACATC ATATGGCAATTCCTTTGACTTTGGTGGGTGGATCGTTCTCTTTGGCCTATGAGCAGCGGATCCACGC GGAACCAGATCCGATTTTGGAGGATGGTCGCCACCACCAAACGTGGCTTGCCAGCCCTGCAAAGGC CATGCTATATACTTGCTGGATTTCAAGTACTTATCAATTTGTGGGATAGCTTCAATACGTTTTTTAAA ACAAACTAATTTTGGGAACGCATCCAGGCACATTGGGTCCATGTATAAAACAACATCAAGAGCGTC ATACAACATGAAGTCAGGATGGGTTACATGATCACCATTTAAATATGTTTTATGACATAAACGATCT TCGAACATTTTCAGCATTTCAGGTAGCTTGCTAAGAAAATCAACTTTGAGAGTTTCAAAGTCTTTAC TATATGCAATTCTCGAAACACCGTATCTAATATCCAAAACCGCTCCTTCAAGCATTGAAATCTCTGC ACGCTCTTTTGGACAACCACCCAACATGTTGTGCTTGTCAGCTATATAACGTATGATGGCCATAGAC TGTGTTAATTTAACATCACCATCAATATAATAAGGAAGATTGGGAAACTCCAAACCCAATTCAAACT TTTTGTTTCGCCATTTATCACCTTCATCGCGCTCATACAAATGCTCTTCATATTTTTCTTCAAGATATT CCAAAAGAAGTCGAGTGGGTTGCACAAGGCCCTTAATTTTCCAATAACCTAGTNTAGGGGANATGA ATACTGTTTCCTGGGTGAAATTGTTATCCGCTCNAATTCCCNCATTATACAACCCATGATAATTGCC AACGCTCATTTCAGATATTTGCCAAACCGTTNTGAAGTCGGGNCAAAAACTTTTCCAAAACGGGAT GGCCCTGACCAACCAAATTTGCAGGGATTTCAACCGGCCAGCCNNACCACGTTTCGGGGGGGCCGG ACCNAANAATTTGGGGCCCCGGGGTNCAAAAACNAATTTCCCCACAAAAAAAATTCGCCGGGCCTN GGTCCCCTTTTTCAAAAAGGGGGAAACCCCCCTTTTCCGGGGAAAAGGGATATCTTAGGATAAGAT TT

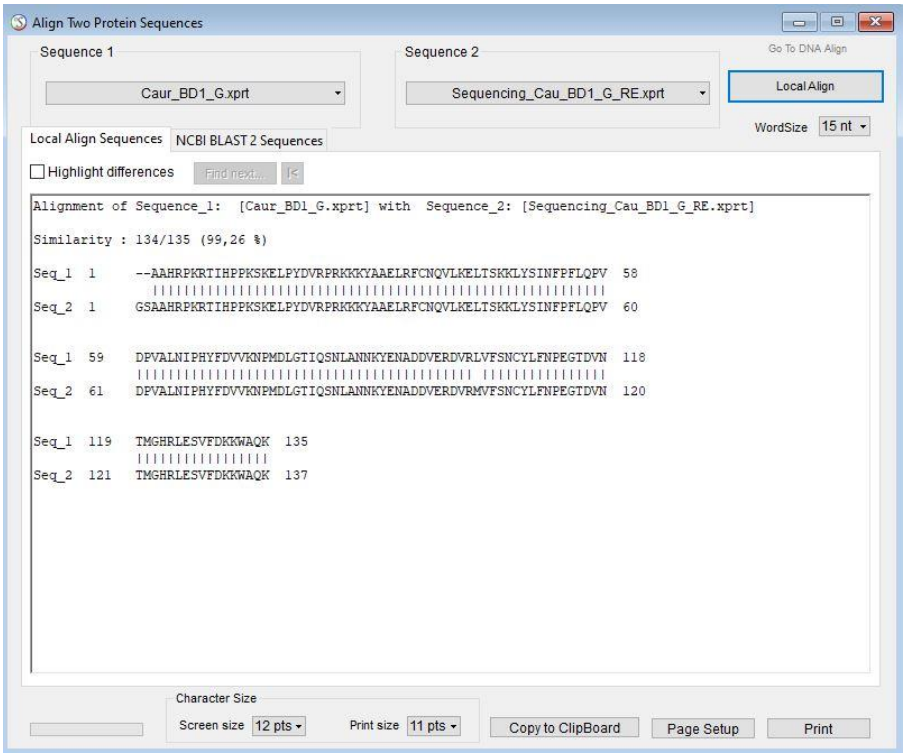

Appendix 22. *Candida auris* BD2 construct (287-408) sequencing result

Sequence of *C. auris* bromodomain construct H

NCCNAACGCGCGAGGCAGATCGTCAGTCAGTCGCGATGCGGCCGCTCGAGTTACTTTTGAGCCCAT
TTCTTGTCGAACACACTTTCAAGGCGGTGTCCCATAGTGTTAACATCAGTACCTTCTGGGTTAAACA
AATAACAGTTTGAGAACACCATTCTCACGTCTCGCTCAACATCATCAGCATTCTCATACTTGTTGTTT
GCAAGATTGGATTGAATAGTCCCGAGATCCATTGGGTTCTTCACCACATCGAAGTAGTGAGGAATG
TTCAATGCGACTGGATCAACTGGTTGTAAGAAGGGGAAGTTGATGCTGTAAAGCTTTTTGGATGTCA
ACTCTTTAAGTACCTGGTTGCAGAAGCGCAACTCAGCTGCATACTTCTTCTTTCTTGGTCTCACATCA
TATGGCAATTCCTTTGAGGATCCACGCGGAACCAGATCCGATTTTGGAGGATGGTCGCCACCACCA
AACGTGGCTTGCCAGCCCTGCAAAGGCCATGCTATATACTTGCTGGATTTCAAGTACTTATCAATTT
GTGGGATAGCTTCAATACGTTTTTTAAAACAAACTAATTTTGGGAACGCATCCAGGCACATTGGGTC
CATGTATAAAACAACATCAAGAGCGTCATACAACATGAAGTCAGGATGGGTTACATGATCACCATT
TAAATATGTTTTATGACATAAACGATCTTCGAACATTTTCAGCATTTCAGGTAGCTTGCTAAGAAAA
TCAACTTTGAGAGTTTCAAAGTCTTTACTATATGCAATTCTCGAAACACCGTATCTAATATCCAAAA
CCGCTCCTTCAAGCATTGAAATCTCTGCACGCTCTTTTGGACAACCACCCAACATGTTGTGCTTGTC
AGCTATATAACGTATGATGGCCATAGACTGTGTTAATTTAACATCACCATCAATATAATAAGGAAG
ATTGGGAAACTCCAAACCCAATTCAAACTTTTTGTTTCGCCATTTATCACCTTCATCGCGCTCATACA
AATGCTCTTCATATTTTTCTTCAAGATATTCCAAAAGAAGTCGAGTGGGTTGCACAAGGCCCTTAAT
TTTCAATAACCTAGTATAGGGGACATGAATACTGTTTCCTGTGTGAAATTGTTATCCGCTCACATTCC
ACACATTATACGAGCCGATGATTATTGTCAAAGCTCATTTCAAATATTTGCCAGACCGTATGATGTC
GCCCAAAAAAATTANCCAGAACGGGAAGGGGCCTGGACGACCGAATTTGCAGGATTTCGACTGCC
AGCCTACCAAGCTTCGAGGGTGCCGGACCCAAAACTTGGGGCCCCGGGAGCAAAAATNATCCCGCC
CCCAAAAATNCCCGGGGCCTCCTNGCNNNTTTCCNANAAAGGGGGAAAAAAACCCCGGTTTCCCGG
GGAAAACGGGGATTCNNNTTGGAAACCCTTTTGTTTAAGGGCCCCCACCCCTCTTCT

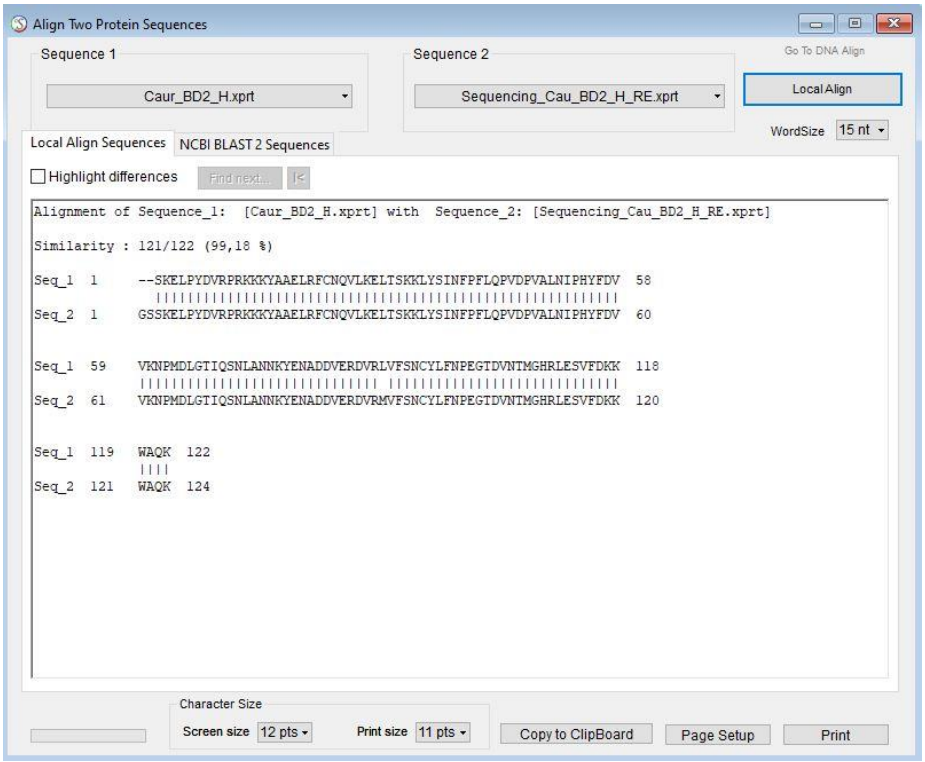

Appendix 23. *Candida auris* BD2 construct (287-413) sequencing result

Sequence of *C. auris* bromodomain construct J

ACATCCTCAAATCGGGATCTGGGTTCCGCGTGGATCCTCAAAGGAATTGCCATATGATGTGAGACC
AAGAAAGAAGAAGTATGCAGCTGAGTTGCGCTTCTGCAACCAGGTACTTAAAGAGTTGACATCCAA
AAAGCTTTACAGCATCAACTTCCCCTTCTTACAACCAGTTGATCCAGTCGCATTGAACATTCCTCAC
TACTTCGATGTGGTGAAGAACCCAATGGATCTCGGGACTATTCAATCCAATCTTGCAAACAACAAGT
ATGAGAATGCTGATGATGTTGAGCGAGACGTGAGAATGGTGTTCTCAAACTGTTATTTGTTTAACCC
AGAAGGTACTGATGTTAACACTATGGGACACCGCCTTGAAAGTGTGTTCGACAAGAAATGGGCTCA
AAAGCCTGTCCCACAACCTTAACTCGAGCGGCCGCATCGCGACTGACTGACGATCTGCCTCGCGCG
TTTCGGTGATGACGGTGAAAACCTCTGACACATGCAGCTCCCGGAGACGGTCACAGCTTGTCTGTAA
GCGGATGCCGGGAGCAGACAAGCCCGTCAGGGCGCGTCAGCGGGTGTTGGCGGGTGTCGGGGCGC
AGCCATGACCCAGTCACGTAGCGATAGCGGAGTGTATAATTCTTGAAGACGAAAGGGCCTCGTGAT
ACGCCTATTTTTATAGGTTAATGTCATGATAATAATGGTTTCTTAGACGTCAGGTGGCACTTTTCGGG
GAAATGTGCGCGGAACCCCTATTTGTTTATTTTTCTAAATACATTCAAATATGTATCCGCTCATGAG
ACAATAACCCTGATAAATGCTTCAATAATATTGAAAAAGGAAGAGTATGAGTATTCAACATTTCCG
TGTCGCCCTTATTCCCTTTTTTGCGGCATTTTGCCTTCCTGTTTTTGCTCACCCAGAAACGCTGGTGA
AAGTAAAAGATGCTGAAGATCAGTTGGGTGCACGAGTGGGTTACATCGAACTGGATCTCAACAGCG
GTAAGATCCTTGAGAGTTTTCGCCCCGAANACGTTTTTCAATGATGACCACTTTTAAAGTTCTGCTAT
GTGGCCGGTATTATCCCGGGTTGANCCGGGCAAGAAAAATTCGGTCCCTCCCTAACCTTANNC

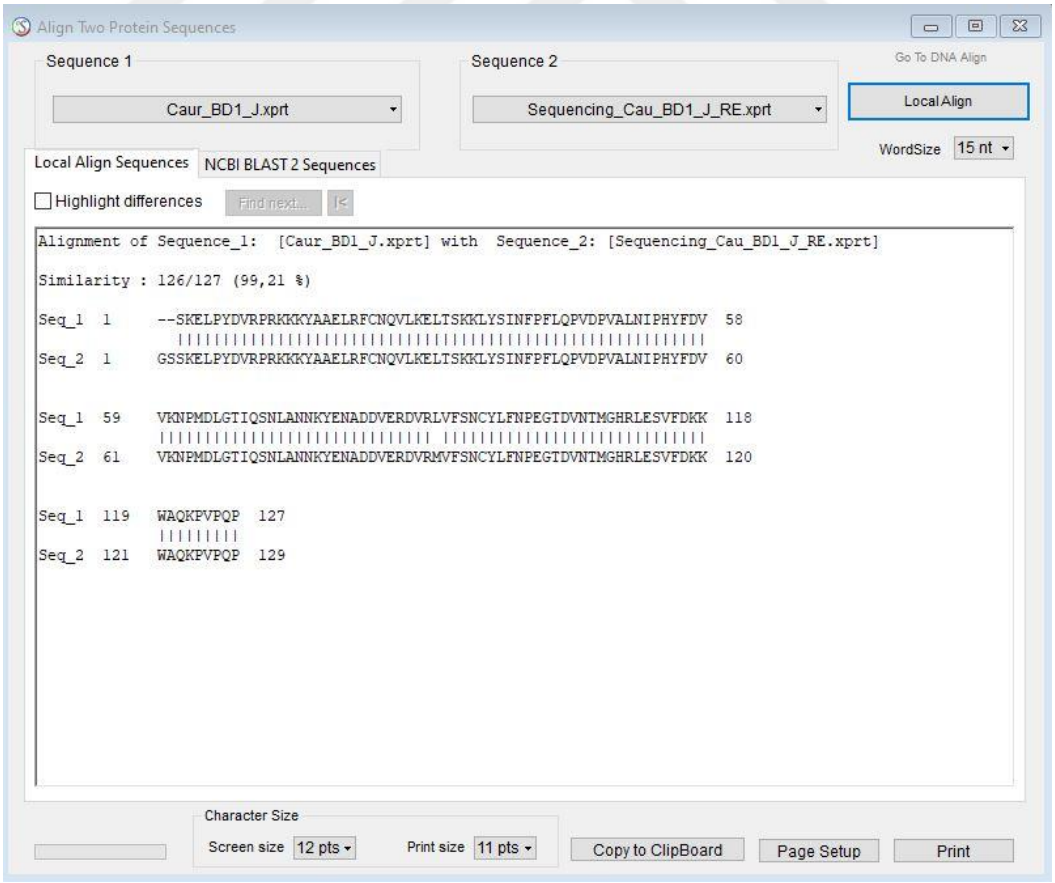

Appendix 24. *Candida auris* BD2 construct (287-416) sequencing result

Sequence of *C. auris* bromodomain construct K
NNNNAACGCGCGAGGCAGTATCGTCAGTCAGTCGCGATGCGGCCGCTCGAGTTAAGGAGGCGAAG GTTGTGGGACAGGCTTTTGAGCCCATTTCTTGTCGAACACACTTTCAAGGCGGTGTCCCATAGTGTT AACATCAGTACCTTCTGGGTTAAACAAATAACAGTTTGAGAACACCATTCTCACGTCTCGCTCAACA TCATCAGCATTCTCATACTTGTTGTTTGCAAGATTGGATTGAATAGTCCCGAGATCCATTGGGTTCTT CACCACATCGAAGTAGTGAGGAATGTTCAATGCGACTGGATCAACTGGTTGTAAGAAGGGGAAGTT GATGCTGTAAAGCTTTTTGGATGTCAACTCTTTAAGTACCTGGTTGCAGAAGCGCAACTCAGCTGCA TACTTCTTCTTTCTTGGTCTCACATCATATGGCAATTCCTTTGAGGATCCACGCGGAACCAGATCCGA TTTTGGAGGATGGTCGCCACCACCAAACGTGGCTTGCCAGCCCTGCAAAGGCCATGCTATATACTTG CTGGATTTCAAGTACTTATCAATTTGTGGGATAGCTTCAATACGTTTTTTAAAACAAACTAATTTTGG GAACGCATCCAGGCACATTGGGTCCATGTATAAAACAACATCAAGAGCGTCATACAACATGAAGTC AGGATGGGTTACATGATCACCATTTAAATATGTTTTATGACATAAACGATCTTCGAACATTTTCAGC ATTTCAGGTAGCTTGCTAAGAAAATCAACTTTGAGAGTTTCAAAGTCTTTACTATATGCAATTCTCG AAACACCGTATCTAATATCCAAAACCGCTCCTTCAAGCATTGAAATCTCTGCACGCTCTTTTGGACA ACCACCCAACATGTTGTGCTTGTCAGCTATATAACGTATGATGGCCATAGACTGTGTTAATTTAACA TCACCATCAATATAATAAGGAAGATTGGGAAACTCCAAACCCAATTCAAACTTTTTGTTTCGCCATT TATCACCTTCATCGCGCTCATACAAATGCTCTTCATATTTTTCTTCAAGATATTCCAAAAGAAGTCGA GTGGGTTGCACAAGGCCCTTAATTTTCCAATAACCTAGTATAGGGGACATGAATACTGTTTCCTGTG TGAAATTGTTATCCGCTCACAATTCCANCATTATACGAGCCGATGATAATTGTCAACAGCTCATTTC AGAANTTTGCCAAACCGTTAGGATGTCGGCCCAAAAAACTTATCCAGAACGGGAGTGNCCTTGNCG ACCCAATTTGGCAGGGATTTCGACCTGCAAACCAACCCAAGCTTCCAGGGGTCCTGGACCCAAAAA ATGGGGGCCCGGGGNNNNAAAAAAATTCCNCCCCCCAAAAAAATCCCGCGGGGCCTCCGGGGCCC CTTTNNCAAAAANNAGGGGGGAAANNACCCNNGGTANTCNNNGGGANNNAGGGGTATACGCGAG GNNNNAAAGTNTNTNGTGTGATAGGNGGCCNCACCGCCGCTCTCCTTTNNGGGAAAAAAAAANNC C

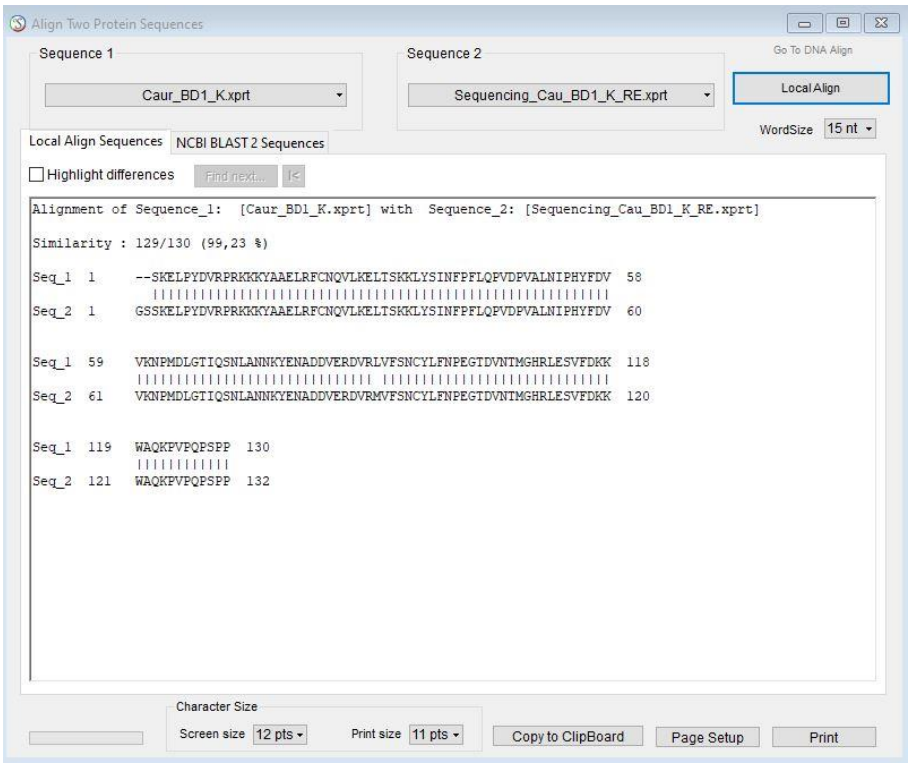

Appendix 25. *Candida auris* BD2 construct (287-424) sequencing result

Sequence of *C. auris* bromodomain construct L

NNNNGCATCCTCAAATCGGATCTGGTTCCGCGTGGATCCTCAAAGGAATTGCCATATGATGTGAGA
CCAAGAAAGAAGAAGTATGCAGCTGAGTTGCGCTTCTGCAACCAGGTACTTAAAGAGTTGACATCC
AAAAAGCTTTACAGCATCAACTTCCCCTTCTTACAACCAGTTGATCCAGTCGCATTGAACATTCCTC
ACTACTTCGATGTGGTGAAGAACCCAATGGATCTCGGGACTATTCAATCCAATCTTGCAAACAACA
AGTATGAGAATGCTGATGATGTTGAGCGAGACGTGAGAATGGTGTTCTCAAACTGTTATTTGTTTAA
CCCAGAAGGTACTGATGTTAACACTATGGGACACCGCCTTGAAAGTGTGTTCGACAAGAAATGGGC
TCAAAAGCCTGTCCCACAACCTTCGCCTCCTCAGTCTGATGGCGAGTACGATAGTTAACTCGAGCGG
CCGCATCGCGACTGACTGACGATCTGCCTCGCGCGTTTCGGTGATGACGGTGAAAACCTCTGACAC
ATGCAGCTCCCGGAGACGGTCACAGCTTGTCTGTAAGCGGATGCCGGGAGCAGACAAGCCCGTCAG
GGCGCGTCAGCGGGTGTTGGCGGGTGTCGGGGCGCAGCCATGACCCAGTCACGTAGCGATAGCGGA
GTGTATAATTCTTGAAGACGAAAGGGCCTCGTGATACGCCTATTTTTATAGGTTAATGTCATGATAA
TAATGGTTTCTTAGACGTCAGGTGGCACTTTTCGGGGAAATGTGCGCGGAACCCCTATTTGTTTATTT
TTCTAAATACATTCAAATATGTATCCGCTCATGAGACAATAACCCTGATAAATGCTTCAATAATATT
GAAAAAGGAAGAGTATGAGTATTCAACATTTCCGTGTCGCCCTTATTCCCTTTTTTGCGGCATTTTGC
CTTCCTGTTTTTGCTCACCCAGAAACGCTGGTGAAAGTAAAAGATGCTGAAGATCAGTTGGGTGCAC
GAGTGGGTTACATCGAACTGGATCTCAACAGCGGTAAGATCCTTGAGAGTTTCGCCCCGAAAAACG
TTTTCCAATGATGAACCATTTTAAAGTTCTGGNNTGTGGGCGGGATTTTCCCGGGTTAGACCGGGCA
AAAGAAAACTCGGCCCCCCAAT

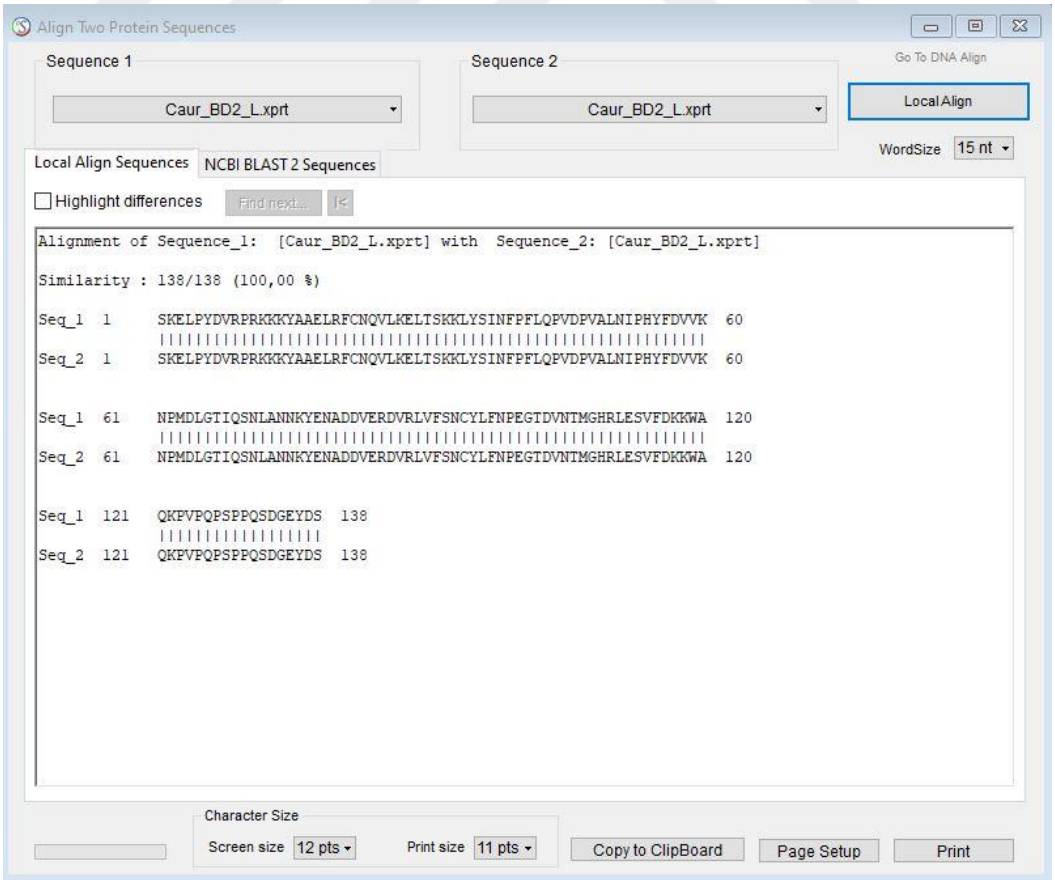

Appendix 26. *Candida glabrata* and *Candida albicans* HTRF results in presence of compound 409

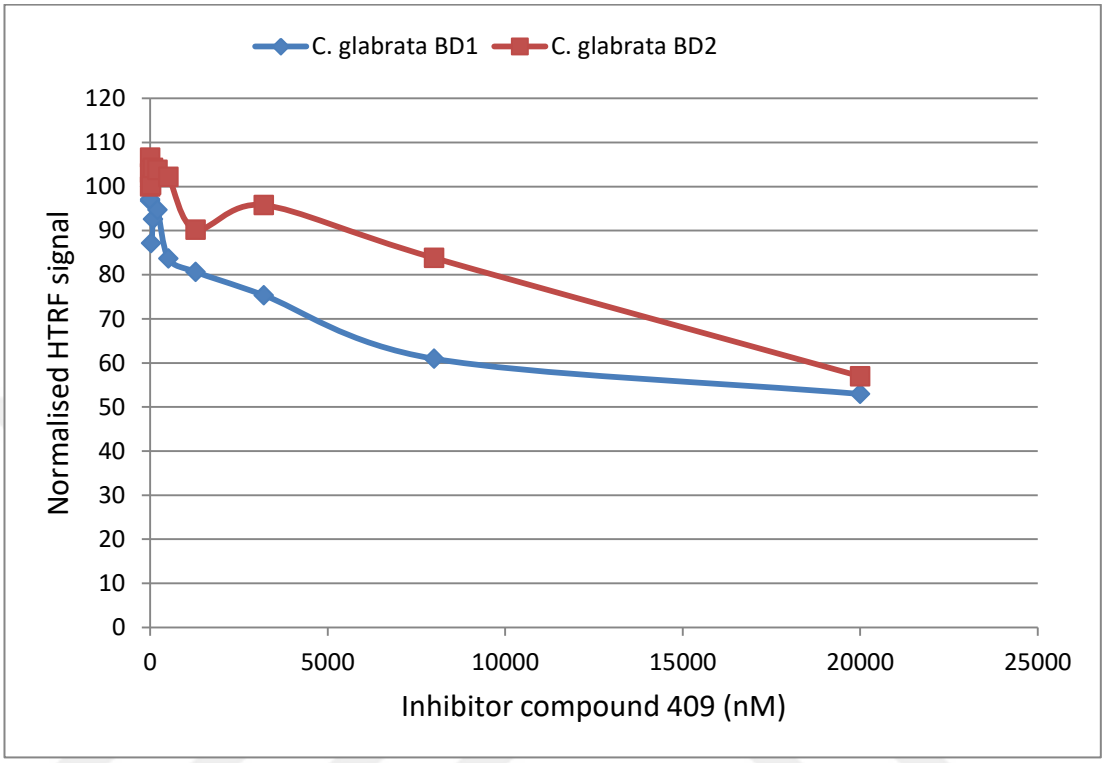

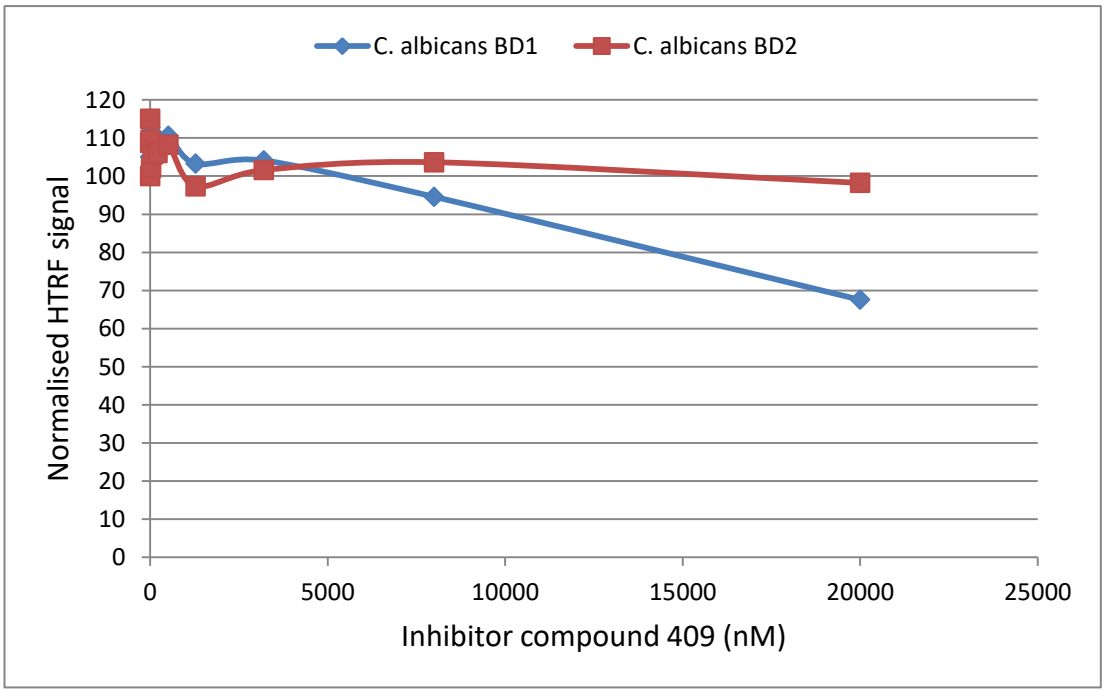

Appendix 27. HPLC profiles of synthesized histone 4 tail peptides

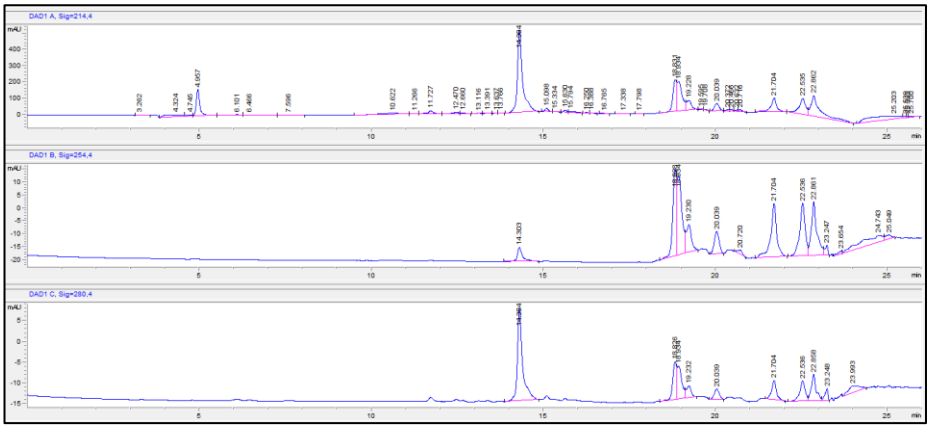

Figure 28. HPLC profile of peptide 2

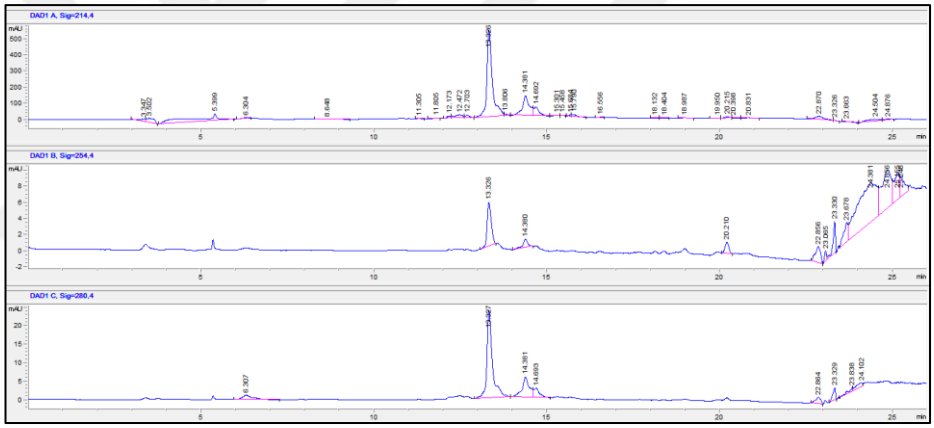

Figure 29. HPLC profile of peptide 3

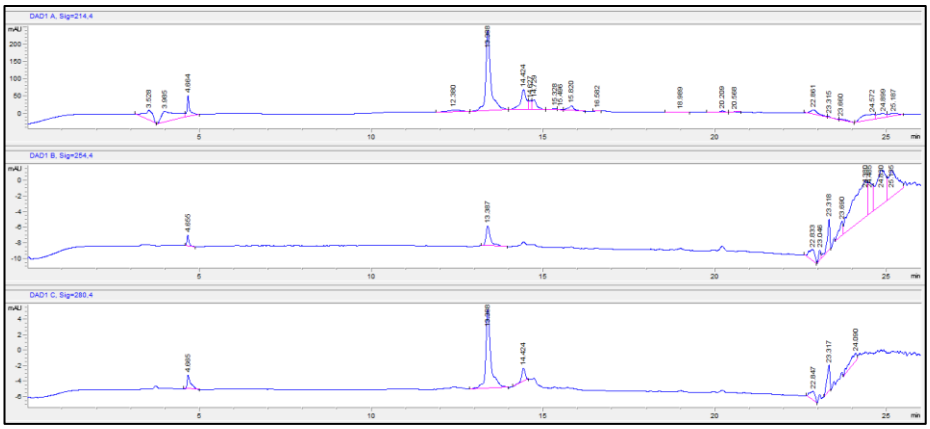

Figure 30. HPLC profile of peptide 4

Appendix 28. Mass spectrum of synthesized histone 4 tail peptides

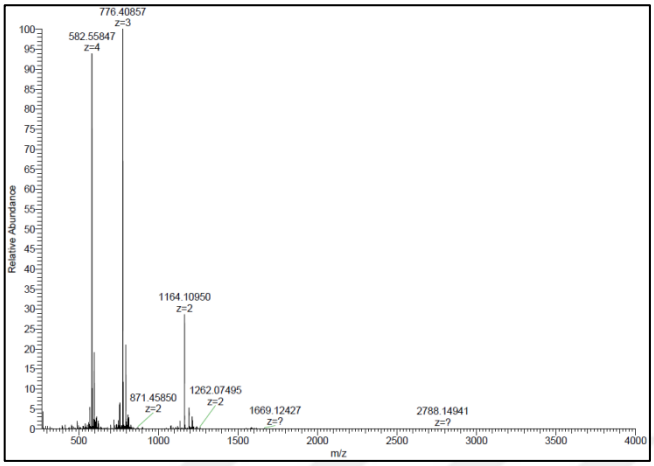

Figure 31. ESI-MS result for peptide 2

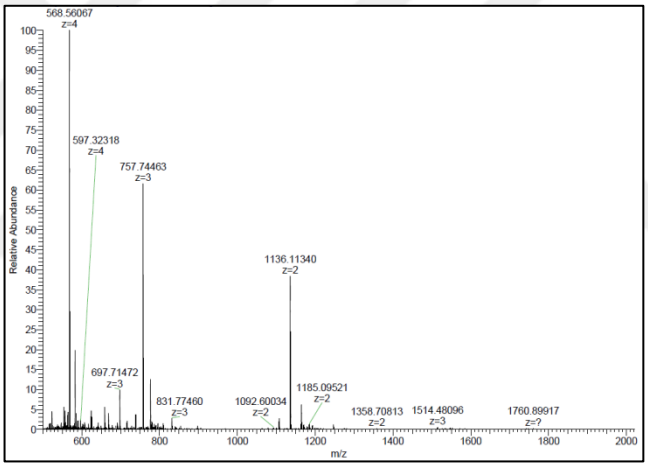

Figure 32. ESI-MS result for peptide 3

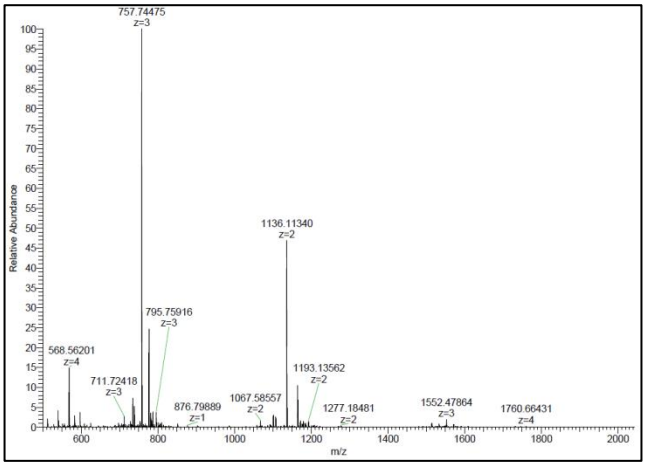

Figure 33. ESI-MS result for peptide 4

8. CURRICULUM VITAE